APPLICATIONS OF NONLINEAR DYNAMICS IN ATOMIC AND MOLECULAR SYSTEMS

A Thesis
Presented to
The Academic Faculty

by

Ji Il Choi

In Partial Fulfillment
of the Requirements for the Degree
Doctor of Philosophy in the
School of Physics

Georgia Institute of Technology
August 2007

APPLICATIONS OF NONLINEAR DYNAMICS IN ATOMIC AND MOLECULAR SYSTEMS

Approved by:

Professor Turgay Uzer, Advisor
School of Physics
Georgia Institute of Technology

Professor Dragomir Davidovic
School of Physics
Georgia Institute of Technology

Professor M. Raymond Flannery
School of Physics
Georgia Institute of Technology

Professor Chongchun Zeng
School of Mathematics
Georgia Institute of Technology

Professor Chandra Raman
School of Physics
Georgia Institute of Technology

Date Approved: 27. June. 2007

To my parents.

ACKNOWLEDGEMENTS

I would first like to thank my advisor, Professor Turgay Uzer who gave me an opportunity to study the most interesting theoretical physics to me and provided an environment where I could succeed. His patient and encouragement kept me motivated. I am fortunate to work closely with Shu Huang who joined the research area after me. I would like to thank Dongjoo Lee, Seil Lee, Dr. Bokwon Yoon, Namtae Jo, and Domenico Lippolis for their encouragement.

TABLE OF CONTENTS

LIST OF TABLES

LIST OF FIGURES

SUMMARY

In this thesis we investigate what modern nonlinear-dynamical methods can tell us about some longstanding problems in atomic physics. There are two components to this thesis: One of them is an classical-mechanical investigation of the ionization of a highly excited two-electron atom in which we look for a Horseshoe Construction in the dynamics of this problem. The bulk of the thesis is devoted to atomic systems which contain large Coriolis-like interactions $\vec{r} \times \vec{p}$, where ($\vec{r}$,$\vec{p}$) are conjugate variables. These interactions may arise quite straightforwardly as paramagnetic terms for an atomic electron which interacts with a constant magnetic field, or more subtly, from viewing the atomic problem from a rotating frame. Generally the effect of this term on spectra is treated by perturbation theory. However, this thesis is devoted to understanding the effect of Coriolis terms that are too large to be treated by perturbation theory. The full treatment of Coriolis terms by classical mechanics forces one to go beyond well-established notions of stability at a potential minimum. Indeed, by mixing coordinates and momenta in a bilinear fashion, the Coriolis term makes the definition of a conventional potential impossible.

In celestial mechanics, where large Coriolis terms are the norm rather than the exception, there is a well-established way of taking them into account as we will show in this thesis. In the context of atomic physics, we will go one step further and explore the quantum mechanics of wave packets in such systems: How they are formed, how stable they are, and how they can be manipulated. Tailoring and manipulating electronic wave packets is currently one of the most active and challenging research subjects in the broad area of quantum control.

It is well-known that it is very difficult to prevent electronic wavepackets from

spreading, and that is where we bring in coherent states. We evaluate two strategies for forming coherent states in atomic physics problems with large Coriolis interactions : One involves the use of the "Cranked Oscillator" model to construct nondispersive wavepackets. We show that it is possible to keep the wavepackets from spreading while manipulating them with dipole fields with arbitrary time profiles. The second strategy involves using additional external fields to create a stable outer minimum far from the core. Whenever this minimum approximates a harmonic well it has its own subset of near-harmonic eigenstates and nearly-coherent states can be constructed. As examples of this strategy we study two-particle ion pair systems in a applied homogeneous magnetic field, and a weakly bound heavy-ion pair ($H^+ - H^-$), where the nonspreading wavepacket corresponds to the motion of the drifting electron-ion or heavy ion pair in relative coordinates.

CHAPTER I

INTRODUCTION

Tailoring and manipulating electronic wave packets [1] is currently one of the most active and challenging research subjects in the broad area of quantum control [2, 3]. Physicists, electrical engineers and mathematicians have joined forces in an effort to keep the wave packet representing the electron from spreading in uncontrollable ways. It is well known that it is quite difficult to prevent the spreading of such an electronic wave packet.

In this thesis we investigate what modern nonlinear-dynamical methods can tell us about reducing the spreading of wavepackets in atomic physics. The use of classical-mechanical methods has proved fruitful in atomic physics research as long as the problems are chosen in the so-called semiclassical regime where the Correspondence Principle predicts the emergence of classical properties from quantum mechanical ones. It is well-established that so-called Rydberg atoms [4], i.e., atoms with one highly excited electron [5], are in this regime and our investigations take them as subjects.

There are two components to this thesis: One of them is an classical-mechanical investigation of the ionization of a highly excited atom [6]. It involves the phenomenon of chaotic scattering which can be recognized by hierarchical structure of a scattering function. The singularity structure of the scattering function is the same as the pattern resulting from the intersection of the stable manifolds with the local segment of the unstable manifold. Finding the invariant manifold and constructing the hierarchy level of the scattering function is a useful way of understanding chaotic scattering in semiclassical treatment. The bulk of the thesis is devoted to atomic

systems which contain large Coriolis-like interactions, $\vec{r} \times \vec{p}$ where ($\vec{r}$,$\vec{p}$) are conjugate variables. These may arise quite straightforwardly as a paramagnetic term for an atomic electron which interacts with a constant magnetic field, or more subtly, from viewing the atomic problem from a rotating frame. In rotating molecules, the vibrational modes may be coupled through such a term which is known as the vibrational angular momentum [8]. There, the effect of this term on spectra is generally treated by perturbation theory. However, this thesis is devoted to understanding the effect of Coriolis terms that are too large to be treated by perturbation theory.

The treatment of Coriolis terms by classical mechanics forces one to go beyond well-established notions of stability at a potential minimum. Indeed, by mixing coordinates and momenta in a bilinear fashion, the Coriolis term makes the the definition of a conventional potential impossible. For, if the term were to be treated as part of the potential, that potential would become momentum dependent; whereas regarding it as a part of the kinetic energy could make the kinetic energy negative! In problems involving the magnetic field, the potential becomes gauge dependent if one does not treat the Coriolis term properly.

In celestial mechanics, where large Coriolis terms are the norm rather than the exception, there is a well-established way of taking into account these subtleties as we will show in this section. We will go beyond classical mechanics and explore the quantum mechanics of wave packets in such systems: How they are formed, how they can be stabilized, and how they can be manipulated.

In this work, we are guided by the work rotating systems in nuclear physics where they are known under the name of "Cranked Oscillator" model which will be summarized here first.

1.1 The Cranked Oscillator Model in Nuclear Physics

In nuclear physics, a good initial model for describing the nucleus is the Liquid Drop Model (LDM) [7, 9] which assumes that the nucleus has properties similar to a liquid drop. The main analogies were the well-defined surface and the short-range forces, an attractive force holding the nucleons together, and a repulsive force stopping the nucleons from collapsing in. In the model, nucleons are assumed to interact strongly with each other so that collective motions are possible and the individual quantum properties of nucleons can be completely ignored. The collective motion of nucleons associated with a deformation in nuclear shape may be approximated by introducing a nonspherical distortion into the zero-order wave functions of the shell model [10].

The LDM can be used to explain some important physical phenomena. For example, nuclear fission can be described in terms of free vibrations of a liquid drop. However, quadrupole moments, in some cases, are too large to be accounted for by motion of a small number of nucleons and experimental evidence shows discrepancies. A fine structure was observed with magic numbers (or = 2, 8, 20, 28, 50, 82 and 126) where these nuclei were more tightly bound than the LDM predicted. Mayer [11] and Haxel *et al* [12] accounted for the magic numbers by (jj) coupling shell model on the assumptions that the nucleons move in a spherically symmetric potential with large spin-orbit coupling. Introduction of a nonspherical core by Rainwater [13] and Bohr [7] showed impressive success in accounting for the large quadrupole moments and suggested that the degree of freedom permitting distortion of the core is important to the external features of most nuclei without radically modifying the internal coupling of the nucleons as calculated in the original (jj) coupling scheme.

The distortion or deformation is assumed to arise from the pressure exerted from within the nucleus on the surface of a bag of liquid representing the core by the nucleons both belonging to closed shells. The existence of a deformation, by which

is implied a feature of anisotropy, is a common feature of systems that have rotational spectra. In a molecule, as in a solid body, the deformation reflects the highly anisotropic mass distribution, as viewed from the intrinsic coordinate frame defined by the equilibrium positions of the nuclei. In the nucleus, the rotational degrees of freedom are associated with the deformation in the nuclear equilibrium shape that results from the shell structure [14].

The deformation causes deviations in the nuclear rotational spectra and a number of efforts have been directed at understanding the deviations and making corrections by Inglis [10], Mottelson and Valatin [15], Udagawa and Sheline [16], Chan and Valatin [17], Bes and Landowne [18], Krumlinde [19] and Marshalek [20]. Of these treatments Inglis [10] suggested as so called "Cranked Model"; corrections arise from taking into account the centrifugal stretching and Coriolis-antipairing effect suggested by Mottelson and Valatin [15]. The cranking model analyzes the collective rotational motion of the deformed state in a semiclassical way since it assumes that the nuclear field is cranked externally with constant angular velocity about one of the principal axes of the nucleus.

The deformed state has a classical nature and can be represented by a wave packet expanded in terms of the angular momentum eigenstates. In the cranking model, the classical rotations are applied to this wave packet, and thereby the broken rotational symmetry is partially restored since the angular momentum is quantized semiclassically by the Bohr-Sommerfeld condition. The nuclear moments of inertia can be analyzed by considering the motion of the nucleons in the rotating nuclear potential. The Coriolis and centrifugal forces are included in the equations of motion for the system moving in the rotating potential. The forces acting in the rotating body-fixed system give rise to an increase in the energy of the nucleonic motion, which can be identified with the rotational energy.

1.1.1 The Cranking Model

The cranking model is one of the most intuitive methods to describe properties of collective rotations microscopically. In this method the nucleus is cranked externally around one of its principal axes and the response of the nuclear field is calculated either in perturbation or in Hartree-Fock theory [21]. However, because of their numerical complexity, such calculations have been restricted for heavy nuclei. This restriction is mainly due to the effects of the cranking perturbations of very large dimensions of a static states at high rotational frequencies. The much simpler case of a cranked anisotropic harmonic oscillator potential can, however, be treated analytically. Most successful models used extensively to account for collective nuclear rotation microscopically is that suggested by Inglis [10, 22]. Cranking introduces, for an asymmetric field, an explicit time dependence into the Schrödinger equation governing the system. However, by transforming to the rotating frame, this equation may be reduced to an stationary one which may be used to calculate the response of the nuclear field to rotation. The case of a cranked anisotropic harmonic oscillator potential was found to lend itself easily to analytical treatments [14, 23, 24, 25]. Glas *et al* [26] succeeded by using canonical transformations in obtaining an exact solution for the wavefunctions of this problem in coordinate space. Such wave functions have proved to be useful in nuclear structure calculations of nuclear currents and velocity fields. Due to this increase of interest in the cranked harmonic oscillator model as a theoretical tool for investigating nuclear rotations, it becomes interesting to investigate other aspects of the model which have not been dealt with.

Collective semiclassical aspects occupy a major place in this respect. In this connection, the concept of coherent states, defined originally by Schrödinger [27] and developed further by Glauber [28], were introduced for the ordinary harmonic oscillator in this spirit. Thus, a coherent state was defined as a quantum mechanical state

manifesting the oscillatory character of the amplitude of a classical harmonic oscillator. Such coherent states have provided a natural framework for the semi-classical description of a variety of collective phenomena in physics such as the radiation fields of lasers by Lax and Louisell [29], superconductivity and superfluidity (Cumming and Johnston [30], Martin [31]), phonons in crystals (Carruthers and Dy [32]), and large-amplitude nuclear collective motion by Rowe and Bassermann [33]. More relevant to our work are more recent interesting applications of the harmonic oscillator coherent states in nuclear physics by Ghosh [34] to introduce the concepts of the single-particle Schrödinger fluid and viscosity for nuclei.

For a single nucleon, the motion with respect to the potential rotating with frequency ω is described by the Hamiltonian

$$H = H_0 - \vec{\omega} \cdot \vec{l} \tag{1.1}$$

where H_0 describes the motion in the absence of the rotation. The $\vec{l}$ is the angular momentum operator and $\vec{\omega}$ is the rotation vector. It is assumed that the rotation is taking place about the axis with constant angular velocity. If the system is rotating around z-axis, the Hamiltonian can be written as

$$H = \frac{p_x^2 + p_y^2}{2} + \frac{1}{2}(\omega_x x^2 + \omega_y y^2) - \omega(xp_y - yp_x). \tag{1.2}$$

Before studying the solution of this model, we introduce another system which will be key for this thesis, and it comes from celestial mechanics.

1.2 The Restricted Three-Body Problem as a Cranked Oscillator

The Restricted Three-Body Problem of celestial mechanics is a variant of the famous Three-Body Problem in which the relative motion of two bodies of finite mass (the "primaries", for concreteness, the Sun and Jupiter) move along a circular orbit while

a third body (for concreteness, "asteroid") of negligible mass is taken to move in their common field. The origin is chosen to be the center of mass of the two primaries with the x-axis being the axis connecting the primaries. The y-axis is in the plane of the primaries' motion. So, the original eighteen-dimensional problem becomes twelve-dimensional when we move to the center-of-mass coordinates. By restricting the planets to a plane, the planar three-body problem is restricted to eight dimensions. In the nonrotating frame Jupiter is assumed to follow an orbit parametrized as

$$\begin{aligned} x &= r\,\cos\omega t \\ y &= r\,\sin\omega t \end{aligned}$$

where r is the radius of the circular orbit: the eccentricity of Jupiter's orbit is set to zero. The time dependence can be eliminated by moving to a rotating coordinate system whose axes rotate at the constant frequency ω around z-axis; the unit of time is chosen so that ω=1. Let the unit of mass be the sum of the masses of the two primaries. If the Jupiter has mass μ, the mass of the Sun will be $1-\mu$ where by convention $0 < \mu \leq 0.5$. Finally, the unit of distance is so that the distance between the two primaries is unity. In a frame rotating with the frequency ω, the location of the two primaries will be fixed at x_1 and x_2 at the plane of the motion. The distances of the third body from the two primaries, r_1 and r_2 respectively, are given by the following expressions:

$$\begin{aligned} r_1 &= \sqrt{(x-x_1)^2+y^2+z^2} \\ r_2 &= \sqrt{(x-x_2)^2+y^2+z^2} \end{aligned} \tag{1.3}$$

If the third body is at position (x, y, z) then the Hamiltonian governing its subsequent dynamics in the rotating frame is

$$K = \frac{p_x^2+p_y^2+p_z^2}{2} - \frac{1-\mu}{r_1} - \frac{\mu}{r_2} - (xp_y - yp_x) \tag{1.4}$$

where the explicit dependence on m, the third body's mass, has been scaled out of the problem in the usual manner. The energy K is a constant which is generally referred

to as *Jacobi's integral* [35] or the *Jacobi constant*. The last term "$-(xp_y - yp_x)$" is the Coriolis interaction which arises from going to the rotating frame. This Coriolis interaction prevents the direct separation of the potential terms from the Hamiltonian. However, the equilibrium points can still be determined by using zero-velocity surface which was invented by Hill [36] to study the Sun-Earth-Moon system. In fact the stable equilibrium points L_4 and L_5 in the RTBP will find direct analogs in the Trojan wavepackets investigated here. The Lagrange points mentions above, L_4 and L_5, are termed as possible equilibrium points of the third body of mass m in the rotating reference frame. In the rotating frame, the third mass m would remain at rest if placed at one of the Lagrange points. These points are fixed in the rotating frame. Conversely, in the inertial frame of reference, the Lagrange points rotate about the center of mass with angular velocity ω, and the mass m would consequently also rotate about the center of mass with same angular velocity if placed at one of these points (with the appropriate velocity). The canonical form [37, 38, 39] of the RTBP can be rewritten as

$$H = \frac{1}{2}(p_x^2 + p_y^2) - (xp_y - yp_x) - \frac{1-\mu}{\rho_1} - \frac{\mu}{\rho_2} \tag{1.5}$$

with

$$\begin{aligned} \rho_1 &= \sqrt{(x+\mu)^2 + y^2} \\ \rho_2 &= \sqrt{(x+\mu-1)^2 + y^2}. \end{aligned} \tag{1.6}$$

Restriction to the configuration plane (xy) displaces the synodical coordinate system from the center of mass to the Lagrange point L_4. The stability of motion at the equilibria is solved generally by shifting the origin of the initial coordinate system based on the center of mass to another, synodical coordinate system centered around the Lagrangian point L_4 given by

$$x = \frac{\gamma}{2};\ y = \frac{\sqrt{3}}{2};\ p_x = \frac{\sqrt{3}}{2};\ p_y = -\frac{\gamma}{2} \tag{1.7}$$

For convenience, the γ is defined by

$$\gamma = 1 - 2\mu. \tag{1.8}$$

Translation to the L_4 is a conservative, completely canonical diffeomorphism.

$$\begin{aligned} x &= \frac{\gamma}{2} + \xi, \qquad p_x = \frac{\sqrt{3}}{2} + p_\xi \\ y &= \frac{\sqrt{3}}{2} + \eta, \qquad p_y = -\frac{\gamma}{2} + p_\eta, \end{aligned} \tag{1.9}$$

The RTBP Hamiltonian is thereby converted to

$$H = \frac{1}{2}(p_\xi^2 + p_\eta^2) - (\xi p_\eta - \eta p_\xi) - \Omega \tag{1.10}$$

where

$$\Omega = \frac{1}{2}\gamma\xi + \frac{\sqrt{3}}{2}\eta + \frac{1}{2}\left(\frac{1+\gamma}{\rho_1} + \frac{1-\gamma}{\rho_2}\right). \tag{1.11}$$

In the transformation from (1.5) to (1.11), a additive constant $-(3+\gamma^2)/8$ was neglected. When this last quantity (Ω) is expanded around the equilibrium point, a cranked oscillator is obtained.

1.2.1 The Zero-Velocity Surface

The stable positions of the Hamiltonian (1.4) can be found from following equations,

$$\dot{x} = \frac{\partial K}{\partial p_x} = \dot{y} = \frac{\partial K}{\partial p_y} = \dot{z} = \frac{\partial K}{\partial p_z} = 0 \tag{1.12}$$

and

$$\dot{p_x} = -\frac{\partial K}{\partial x} = \dot{p_y} = -\frac{\partial K}{\partial y} = \dot{p_z} = -\frac{\partial K}{\partial z} = 0. \tag{1.13}$$

These equations do not provide a clear physical picture of the dynamics. That is why the zero-velocity surface is remarkably helpful. The zero-velocity surface is constructed as follows. Consider the mechanical velocities expressed as

$$\begin{aligned} \dot{x} &= p_x + y \\ \dot{y} &= p_y - x \\ \dot{z} &= p_z. \end{aligned} \tag{1.14}$$

The momenta can be expressed as functions of the velocities and the Hamiltonian (1.4) results in:

$$K = \frac{\dot{x}^2 + \dot{y}^2 + \dot{z}^2}{2} - \frac{1-\mu}{r_1} - \frac{\mu}{r_2} - \frac{1}{2}(x^2 + y^2). \tag{1.15}$$

This is still equal to Jacobi's constant, but now this Hamiltonian is separable into the mechanical velocities and the coordinates:

$$K = K_0 + V(x, y, z), \tag{1.16}$$

where K_0 is a positive definite quadratic form in the velocities while $V(x, y, z)$ depends only on the coordinates. If the third body has the Jacobi integral, and lies on the surface specified in $V(x, y, z)$, then it must have zero velocity. Hence, such a surface is termed a zero-velocity surface. The surfaces form the boundary of regions from which the third body is dynamically excluded. In the RTBP and restricting the motion to the xy plane, i.e., z=0, the zero-velocity surface is a topological map of the function

$$V(x, y, z) = -\frac{1-\mu}{r_1} - \frac{\mu}{r_2} - \frac{1}{2}(x^2 + y^2). \tag{1.17}$$

Figure 1.2.1(a) shows both an isometric and a contour plot of V for parameters x_1=-0.1, x_2=0.9 and μ=1/10. There are 5 equilibrium points marked in the Figure 1.2.1(b) as L_1,...,L_5 and these are the 5 equilibrium points discovered by Lagrange in 1772. L_1, L_2 and L_3 are saddle points, while L_4 and L_5 are maxima. In the

RTBP defined by the Sun-Jupiter system, L_4 and L_5 are stable equilibrium points and they correspond exactly to the locations of the two groups of Trojan asteroids. In this dissertation much of the analysis done for the RTBP is carried over directly to the realm of atomic physics. Specifically, the hydrogen atom in microwave electric fields is atomic-physics analog of the RTBP [40, 41, 42]. In particular the stability of suitable quantum mechanical wave packets, representing the hydrogen atom's electron positioned at locations which are analogs of the stable L_4 and L_5 will be analyzed. It is found that, given the right combinations of fields, the wave packets indeed constitute nonspreading, nondispersive quantum objects [43, 44].

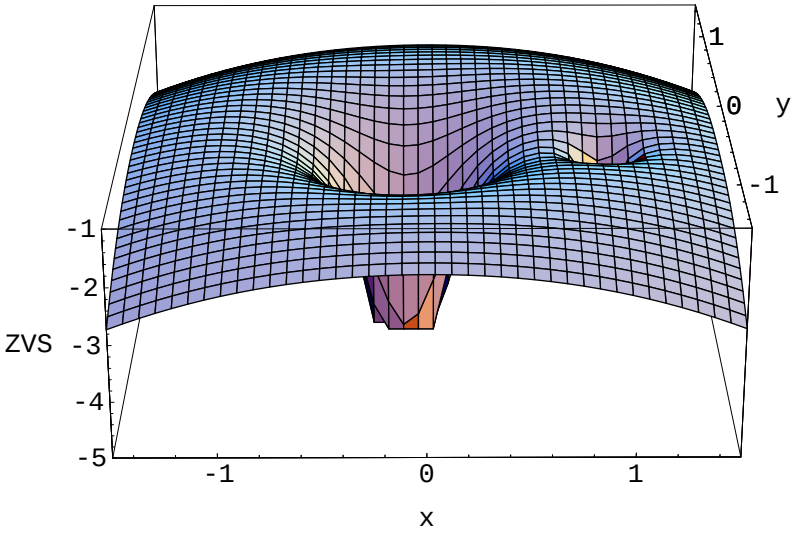

(a)

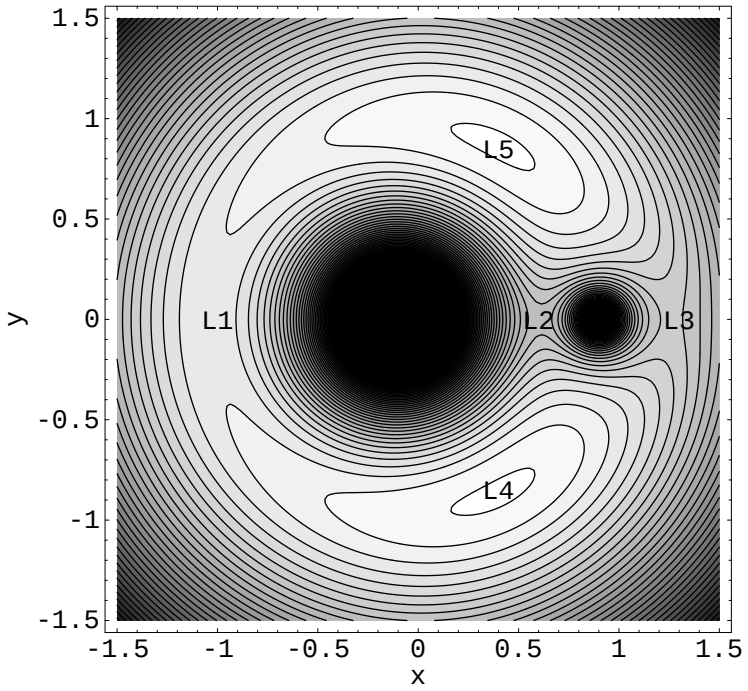

(b)

Figure 1: (a) Isometric and (b) contour plot of the zero-velocity surface for the arbitrary parameters x_1 = -0.1, x_2 = 0.9, and μ = 0.1

CHAPTER II

THE CRANKED OSCILLATOR IN ATOMIC PHYSICS: RYDBERG ATOMS IN EXTERNAL FIELDS

2.1 Introduction

Rydberg atoms [4] are atoms in which an electron has been promoted to a state with a high principal quantum number, n. In such a state the outermost electron feels an almost hydrogenic, Coulomb potential. Quantum mechanically, a state of high n refers to an atom in which the valence electron have been excited into a formerly unpopulated electron orbital with higher energy and lower binding energy. However, Rydberg states have long lifetime and the lifetimes can be explained in terms of the overlapping of wavefunctions which have very little overlap with the wavefunctions of the inner electrons. The Bohr atom encapsulates many of the fundamental properties of Rydberg atoms which make such atoms of considerable interest [4]. What distinguishes the Bohr atom from the classical Kepler problem is the quantized angular momentum, giving off radiation only when making transitions between certain quantized states of well-defined energy.

At very large n, the electron of the Bohr atom revolves around the nucleus in an orbit at the extreme outer edge of the atom and the difference in energy from one orbit to the next nearly disappears, becoming virtually continuous. Therefore, for very large n, both quantum and classical theory give the same answer. Generally, a classical study is easier to implement than the corresponding quantum mechanical study and can often provide vital insight into dynamical behavior that may be difficult to obtain from quantum mechanical calculations alone. A modern interpretation of what constitutes a classical atom can be summarized as follows: (1) A wavepacket

representing an electron will neither spread nor disperse as its center moves along a Kepler orbit [45], (2) the classical orbit that contains the electron is confined to a single plane in space. Such configuration would correspond physically to a rotating giant dipole [46]. Recent studies of "the classical limit of an atom" that have tried to implement the definitions have emphasized the creation of nondispersive electronic wavepackets in Rydberg atoms. The wavepacket is also known as a nondispersive coherent wavepacket [4, 47].

In the context of a Rydberg atom in crossed electric and magnetic fields, denoted throughout as the $E \times B$ system [48, 46], a number of workers have postulated the existence of an outer well in the atomic potential [49, 50, 51, 52]. In this field configuration a Coriolis-like term, the linear Zeeman or paramagnetic term, which is proportional to the component of electronic angular momentum along the magnetic-field direction is not conserved and can, therefore, be thought of as a velocity-dependent perturbation that mixes coordinates and momenta. The difficulty in treating such a term has led to a number of analyses that essentially ignore the paramagnetic term because its presence prevents the separation of the Hamiltonian into kinetic and potential parts. In the absence of the paramagnetic contribution, under certain conditions, the potential in the $E \times B$ system may display an outer well [49, 50, 51, 52].

Despite the uncontrolled approximations involved, these studies have engendered experimental research directed to observing the unusually large atomic dipoles that might be expected to result from such a well [46]. Unfortunately, simply ignoring the paramagnetic term is a rather poor approximation and the approximation results in an unphysical, i.e., gauge-dependent potential [46]. Cederbaum and co-workers [53] have demonstrated that an outer minimum can be created in the atomic $E \times B$ problem if the finite mass of the nucleus is taken into account, but the remoteness from the nucleus of the resulting, relatively shallow, well makes it unclear how easy it would be to observe the consequences of this well in an experiment. In this thesis, the gauge

invariant and the concept of a zero-velocity surface (ZVS) are being used to handle the paramagnetic term. In the $E \times B$ system it is easy to demonstrate that an outer well cannot exist in the effective potential in the infinite nuclear mass approximation, but, for the combined magnetic and CP fields, global equilibria corresponding to maxima or minima can be readily produced and visualized using the ZVS. In the rotating frame, therefore, all of the suggestions put forward as to the possible consequences of an outer potential well in the $E \times B$ system apply to this system, with the significant additional merits that such a well is not only (a) expected to exist theoretically, but (b) is also expected to be experimentally realizable.

The hydrogen atom, even in the ground state, is a special case of a Rydberg atom. In this chapter we will show how to construct nonstationary, nondispersive electronic wave packets in the hydrogen atom, especially, hydrogen atom in particular combinations of external electromagnetic fields - circularly polarized (CP) microwave fields. These fields produce equilibrium points at which the coherent states can be constructed and the nature of the hydrogen atom is very similar to those of RTBP outlined in the previous chapter. They are energy maxima that result from the interplay of Coriolis and Coulombic forces. However, one cannot identify separate kinetic and potential parts of the Hamiltonian because of the paramagnetic term. Additionally, the paramagnetic term complicates the computation of the frequencies associated with the coherent state, since this bilinear perturbation must first be diagonalized. Therefore, the stability of any equilibrium points must, in principle, be calculated explicitly. Appropriate frequencies at either a maximum or a minimum in the presence of the paramagnetic term will be computed. A Hamiltonian of the hydrogen atom expanded around the equilibrium points reduces to the cranked harmonic oscillator model. The possibility of classical equilibrium points in the dynamics of the hydrogen atom in CP fields leads to the question of whether a wave packet placed at such a point will be stable quantum mechanically. In what follows, we show the creation of

the equilibrium points, test of their stability and show the building of wavepacket for the cranked harmonic oscillator. Stable coherent wave packets can be launched at a equilibrium position and they are supported quantum mechanically.

2.2 The Classical Hamiltonian and The Zero-Velocity Surface

2.2.1 Classical Hamiltonian

In deriving the classical Hamiltonian, we will follow the work of the Ref. [54]. The classical study of the dynamical behavior of the Rydberg electron begins with the description of the structure of a hydrogen atom simultaneously subjected to a circularly polarized (CP) microwave and an orthogonal magnetic field. Circularly polarized light is the result of two spatially orthogonal waves being 90^o out of phase. In the dipole approximation [1], the field is time-dependent and is given by

$$F(x\cos\omega_f t + y\sin\omega_f t) \tag{2.1}$$

where F is the field strength and ω_f is the frequency. The sign of F is not a crucial point. The effect of a magnetic field in the symmetric gauge on a permanent magnetic dipole μ is to cause the angular momentum (L) and magnetic momentum to process uniformly. The precession angular velocity is known as the Larmor frequency, ω_L. For electrons, the Larmor frequency is counterclockwise around the direction of the magnetic field. The interaction energy between a magnetic dipole and an external magnetic field in the xy-plane is

$$\begin{aligned} \mathbf{v}\cdot\mathbf{A}(\mathbf{r}) &= \frac{1}{2}\mathbf{v}\cdot(\mathbf{B}\times\mathbf{r}) \\ &= \frac{1}{2}\omega_c(x\dot{y}-y\dot{x}) \end{aligned} \tag{2.2}$$

[1] The electric dipole approximation is based on the fact that the wavelength of the radiation field is far longer than atomic dimensions.

where ω_c is the cyclotron frequency (sometimes denoted as the reduced magnetic field strength, γ, where, $\gamma = B/2.35 \times 10^5 T$ in atomic units) and the choice of sign is determined by the direction of the magnetic field in the case of the paramagnetic term. Thus, the Lagrangian for a hydrogen atom (in atomic units $a_0 = \hbar = e = \mu = 1$ and assuming an infinite nuclear mass) subjected simultaneously to a CP microwave field (field strength F and frequency ω_f) and a static magnetic field perpendicular to the plane of polarization of the CP field is

$$\mathcal{L} = \frac{\dot{x}^2 + \dot{y}^2 + \dot{z}^2}{2} + \frac{1}{r} - \frac{\pm\omega_c}{2}(x\dot{y} - y\dot{x}) \pm F(x\cos\omega_f t + y\sin\omega_f t) \tag{2.3}$$

The sign of F is immaterial but our convention, consistent with Ref.[42], is to choose this sign such that global equilibria corresponding to maxima or minima will turn out to lie along the positive x-axis. The Hamiltonian corresponding to eq. (2.3) is obtained in the standard way using

$$H(q, p, t) = \sum_{i=1}^{n} \dot{q}_i p_i - L(q_i, \dot{q}_i, t) \tag{2.4}$$

where $\dot{q} = dq/dt$, H is the Hamiltonian and q_i and $\dot{q}_i$ are generalized coordinates and velocities respectively. p_i is the generalized momentum conjugate to q_i

$$p_i = \frac{\partial L}{\partial \dot{q}_i}. \tag{2.5}$$

The resulting Hamiltonian is

$$H = \frac{p_x^2 + p_y^2 + p_z^2}{2} - \frac{1}{r} + \omega_c(xp_y - yp_x) + \frac{\omega_c^2}{8}(x^2 + y^2) \pm F(x\cos\omega_f t + y\sin\omega_f t). \tag{2.6}$$

This Hamiltonian includes time dependent terms with a paramagnetic term. The presence of a nonconserved velocity dependent paramagnetic term in the Hamiltonian prevents the separation of H into a positive-definite quadratic form in momenta and a potential energy term. Nevertheless, a type of potential - a zero-velocity surface - can be constructed and provides an excellent starting point for studying the dynamics [36, 55]. Furthermore, the paramagnetic term can be eliminated by proper

transformations.

2.2.2 Equilibrium Points and Energy Maximum Configuration

Due to Cauchy's uniqueness theorem, a particle starting out in the plane of polarization, with an initial velocity contained in that plane, will never leave the plane [56]. This reduces the degrees of freedom and makes the system amenable to analysis. The time dependence in eq. (2.3) may be eliminated by going to a frame that rotates at the constant angular velocity ω_f [57]. The new coordinates (primed coordinates) are defined by

$$\begin{aligned} x &= x' \cos \omega_f t - y' \sin \omega_f t \\ y &= x' \sin \omega_f t + y' \cos \omega_f t \\ z &= z'. \end{aligned} \tag{2.7}$$

Direct substitution of the relations into the eq. (2.6) yields the time independent Hamiltonian at the transformed coordinates. Thus, the Hamiltonian in the rotating frame, after dropping the primes, is:

$$H = K = \frac{p_x^2 + p_y^2 + p_z^2}{2} - \frac{1}{r} - \omega(xp_y - yp_x) \mp Fx + \frac{\omega_c^2}{8}(x^2 + y^2), \tag{2.8}$$

with

$$\omega = \omega_f \mp \omega_c/2, \tag{2.9}$$

where K is analogous to the Jacobi constant in the restricted three-body problem (RTBP) [37]. The sign $\mp$ in the frequency ω depends on the direction of the magnetic field. It controls the nature of the stable equilibrium point: a "+" sign causes it to be an energy *maximum*, while a "-" sign results in an equilibrium point that is an energy *minimum*.

As was explained in the previous chapter, when the Hamiltonian contains a non-conserved paramagnetic term zero-velocity surface can be constructed and provides

an excellent guide to the dynamics [37]. In analogy with the RTBP of the previous chapter, the ZVS is given by re-writing the Hamiltonian in terms of velocities of momenta,

$$H = \frac{\dot{x}^2 + \dot{y}^2 + \dot{z}^2}{2} - \frac{1}{r} \mp Fx - \frac{\omega_f(\omega_f \mp \omega_c)}{2}(x^2 + y^2). \tag{2.10}$$

The kinetic part is positive definite in momenta, and ZVS is defined

$$\begin{aligned} V &= H - \frac{\dot{x}^2 + \dot{y}^2 + \dot{z}^2}{2} \\ &= -\frac{1}{r} \mp Fx - \frac{\omega_f(\omega_f \mp \omega_c)}{2}(x^2 + y^2). \end{aligned} \tag{2.11}$$

The equilibrium points of the ZVS are found to lie long the x-axis at $y = 0$ and $z = 0$ by simultaneously solving the following set of equations:

$$\begin{aligned} \dot{x} = \frac{\partial K}{\partial p_x} = \dot{y} = \frac{\partial K}{\partial p_y} = \dot{z} = \frac{\partial K}{\partial p_z} = 0 \\ \dot{p_x} = -\frac{\partial K}{\partial x} = \dot{p_y} = -\frac{\partial K}{\partial y} = \dot{p_z} = -\frac{\partial K}{\partial z} = 0. \end{aligned} \tag{2.12}$$

Level curves of the ZVS of Figure 2 may be used to provide information on the location and nature of equilibrium points and the locations of classically allowed and forbidden regions, unlike a potential-energy surface, such level curves provide no information on the linear stability of equilibrium points, unless those equilibria are saddles. The equilibrium points occur in pairs: either a saddle and a maximum or a saddle and a minimum depending on the sign chosen in eq. (2.11) (the direction of the magnetic field). The stability of its critical points in not always obvious. In particular, although a minimum in the zero-velocity surface will always be linearly stable and a saddle point will always be unstable, the maximum of the zero-velocity surface may be stable or unstable depending on the particulars. Stability is established by calculating the normal mode frequencies. The work presented in this chapter deals extensively with both configurations.

The maximum configuration is important because it raises the possibility of forming an atomic coherent state but also because a wave packet placed here is a direct

atomic analog of the Trojan asteroids of the Sun-Jupiter system. It also allows one to test the stabilizing effects of a magnetic field.

The minimum configuration is also important for the production of coherent states. Coherent states in various external field will be treated in the next chapter. After the maximum configurations is introduced, the Hamiltonian will be expanded about the equilibrium point and local frequencies, obtained from the potential, will be used to define a Gaussian wave packet. Just like in the harmonic oscillator the ground state is fundamentally presented here the Gaussian wave packet depends strongly on the harmonicity of the Hamiltonian in a neighborhood of the equilibrium point. The first step in uncovering the presence of stationary states for this system is to understand the nature and shape of the zero-velocity surface. When it comes to configurations, a saddle and a maximum will be referred to as maximum configuration and a minimum and a saddle will be referred to as minimum configuration.

2.2.3 The Maximum Configuration

The choice of the "+" sign in eq. (2.11) with $\omega_c \geq 0$ leads to the following zero-velocity surface:

$$V = -\frac{1}{r} + Fx - \frac{\omega_f(\omega_f + \omega_c)}{2}(x^2 + y^2) \tag{2.13}$$

with the maximum equilibrium points lying on the the x-axis as given by the solutions of the following two equations:

$$F + 1/x_{max}^2 - \omega_f(\omega_f + \omega_c)x_{max} = 0 \qquad \text{maximum} \tag{2.14}$$

$$F - 1/x_s^2 - \omega_f(\omega_f + \omega_c)x_s = 0 \qquad \text{saddle} \tag{2.15}$$

where x_{max} refers to the position of the maximum equilibrium point. Figure 2 is an isometric plot of the two dimensional ZVS with a CP field and no magnetic field showing the locations of the maximum L_M and the saddle L_S. This configuration of

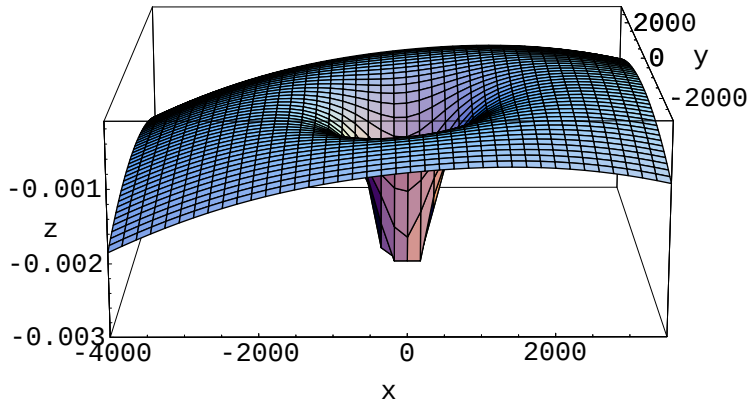

(a)

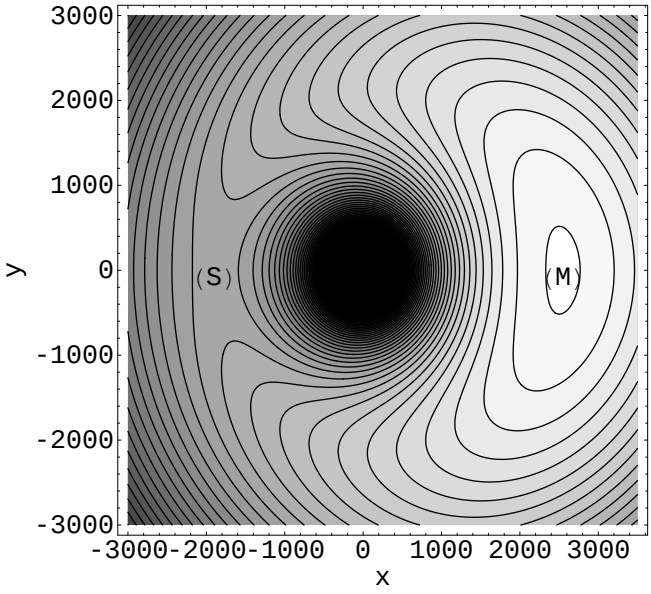

(b)

Figure 2: Isometric view of the ZVS with $F = 10^{-7}$ a.u. Figure (b) is the projection of the plot to the $x - y$ plane. It shows the saddle L_S at the position (S) from the figure and the maximum L_M at the position (M). The positions were plotted using the maximum equilibrium equations.

equilibria is preserved even on the addition of a magnetic field ($\omega_c \neq 0$), provided that the Larmor frequency and the helicity of the wave are chosen such that the plus sign emerges in eq.(2.8). Thus, it is possible to have a maximum equilibrium point either with or without a magnetic field. The stability of these points and the size of the regime supporting linear dynamics around the maximum will be influenced by the three free parameters: F, ω_f and ω_c.

2.2.4 Zero-Velocity Surface in the Neighborhood of an Equilibrium Point

The harmonic oscillator is the most ideal quantum system that can be used in the study of nondispersive nonspreading coherent states. The classical Hamiltonian for a three-dimensional harmonic oscillator is

$$H = \frac{\mathbf{p^2}}{2m} + \frac{m}{2}(\omega_x x^2 + \omega_y y^2 + \omega_z z^2). \tag{2.16}$$

It is instructive to show the two-dimensional potential energy surface at xy-plane for different values of ω_x and ω_y of the eq. (2.16) and the level curves of ZVS of the region surrounding an equilibrium point. Figure 3 is the potential shape, for example, at a maximum for the ideal harmonic oscillator and its energy contour plot (level curves) demonstrates the equal spacing between energy levels.

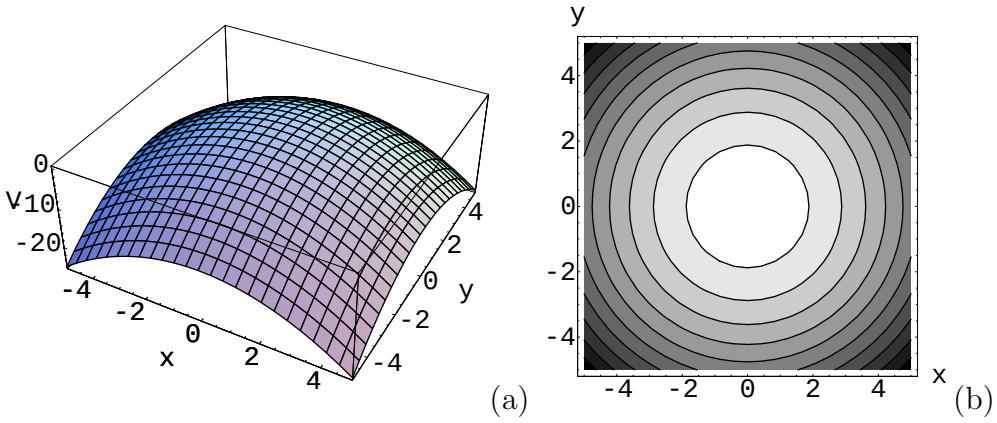

Figure 3: Contour plots of the two-dimensional harmonic oscillator at maximum; (a) potential shape for $\omega_x = \omega_y$ = -0.5, and (b) its contour plot.

It is worth to noting that in the classical dynamics the constant addition to the Hamiltonian, the eq. (2.32) can be safely neglected, and more importantly, the magnetic field can be varied to tune the frequencies "a" and "b" of the eq. (2.31). The term ω_c^2 can significantly increase the size of the frequencies with the subsequent increase of the harmonic region. For example, typically ω_c will be of the same size ω (for the cases presented here $\omega_c \sim \omega \sim 10^{-6}$ a.u.), while $x_0 \sim 10^3$. Hence, without the magnetic field $a \sim -b \sim 10^{-3}$ while in the presence of the magnetic field $a \sim -b \sim 0.25$. The stronger the frequencies, the smaller the nonlinearities will be in comparison. Figure 4 shows the energy contours of the zero-velocity surface for two distinct cases where (a) the hydrogen atom in the presence of a CP microwave field only (no magnetic field) and (b) the atom in the CP microwave field with non-zero magnetic field. In case of no magnetic field, the area surrounding the maximum has different shape with the Figure 3(b) and contains very little harmonic character and as a consequence will not support stable motion. The addition of a magnetic field perpendicular to the plane of polarization is demonstrated in Figure 4(b).

The surrounding region of the equilibrium point looks very similar to that of the harmonic oscillator. Clearly, the presence of the magnetic field can contribute to a marked increase in the size of the stability region around the equilibrium point and these region can support stable nondispersive nonspreading coherent states.

2.2.5 The minimum configuration

Selection of the negative sign in the eq.(2.11) generates this minimum configuration. It is not just change of sign but entirely different critical point topology. Zero velocity surface for this configuration is

$$V = -\frac{1}{r} - Fx - \frac{\omega_f(\omega_f - \omega_c)}{2}(x^2 + y^2). \tag{2.17}$$

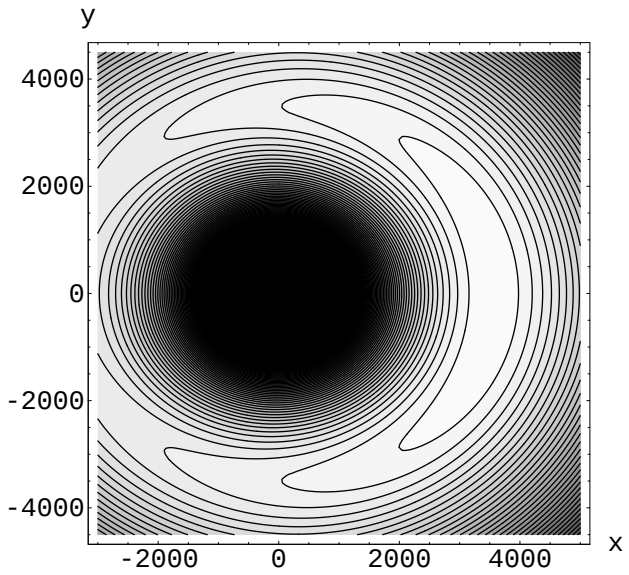

(a)

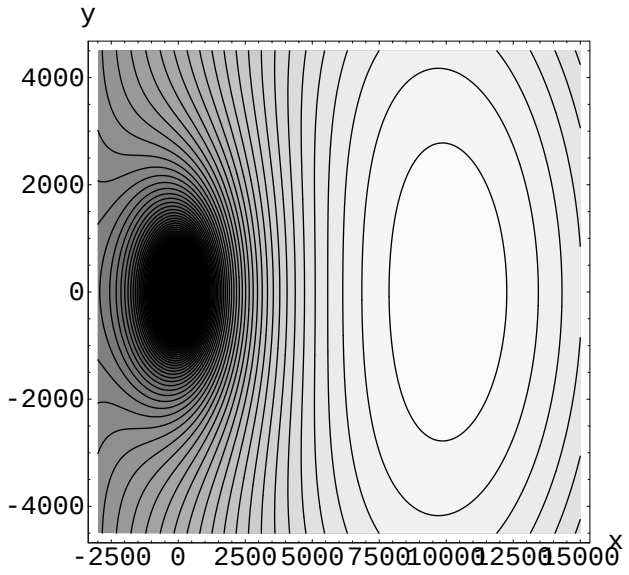

(b)

Figure 4: Contour plots of the two-dimensional zero-velocity surface at maximum; (a) without a magnetic field ($\omega_c = 0$), and (b) with the field ($\omega_c = 5 \times 10^{-5}$). Each graph has the same field strength, $F = 5 \times 10^{-9}$ a.u. and angular velocity of the external field, $\omega_f = 10^{-6}$ a.u.

Minimum configuration has one minimum and one saddle. The equilibria occur along the x axis as solutions of equations

$$F - 1/x_{min}^2 - \omega_f(\omega_f - \omega_c)x_{min} = 0 \qquad \text{minimum} \tag{2.18}$$

$$F + 1/x_s^2 - \omega_f(\omega_f - \omega_c)x_s = 0 \qquad \text{saddle} \tag{2.19}$$

Define a function $h(x_0)$,

$$h(x_0) = F \mp \frac{1}{x_0^2} - \omega_f(\omega_f - \omega_c)x_0, \tag{2.20}$$

where x_0 represents a minimum or a saddle. A critical point of F can be calculated using Eq.(2.19) and a derivative of the function $h(x_0)$, $dh/dx_0 = 0$. The critical value of F for the minimum is

$$F_c = \frac{3}{2^{2/3}}[\omega_f(\omega_f - \omega_c)]^{2/3}. \tag{2.21}$$

For $F < F_c$ the ZVS possesses no real critical points. Considering the conditions, $F > F_c$ and increasing F, the function $h(x_0)$ splits into a saddle point and a minimum. The depth of the potential well and its proximity to the nucleus depend sensitively on the field strengths. Under the conditions for the minimum configuration, Figure 5 shows a graph of the ZVS plot at the plane of $y = z = 0$ for $F = 2004\,V/cm$ and $\omega_c = 4.008T$. The minimum equilibrium point is illustrated by x_m. The x_m reaches its maximum when $\omega_f = \omega_c/2$ and the value decreases during $\omega_c > \omega_f$. For a condition, $\omega_f > \omega_c$, x_m doesn't exist. The coefficients of the in $(x^2 + y^2)$ in ZVS equation (2.13) and (2.17) can be arranged to be nonzero and positive, thus confining the electron irrespective of the size of F in the planer limit. This occurs whenever $\omega_c > \omega_f$, provided that $\omega_f \neq 0$. For a given ω_c the coefficients is maximized when $\omega_f = \omega_c/2$, i.e., the paramagnetic term of (2.8) is absent, and the ZVS becomes equivalent to a true potential energy surface.

Thus, for the frequency chosen to be $\omega_f = \omega_c/2$, such that the Larmor precession due to the external magnetic field and the precession due to the CP cancel the paramagnetic term. This result in an integrable system with an outer minimum, well away

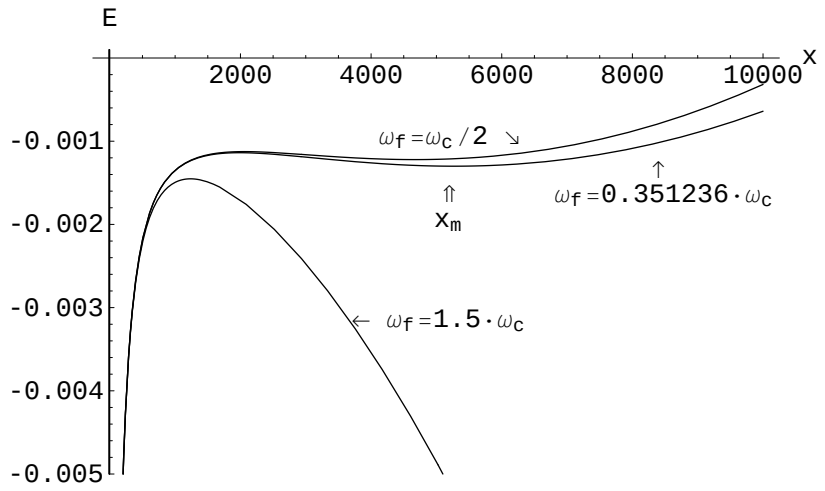

Figure 5: Plots of ZVS of minimum configurations for $\omega_f > \omega_c$, $\omega_f < \omega_c$ and $\omega_f = \omega_c/2$ ($F = 2004\,V/cm$ and $\omega_c = 4.008T$). All axes are in atomic units.

from the nucleus, which is locally harmonic [58, 54]. Consequently, its ground state can be a coherent state which represents a wave packet corresponding to an electron revolving around the nucleus on a large circular orbit without spreading - much like a classical electron traveling on the circular orbit of the planetary atom. The following section derives the nondispreading wavepacket.

2.3 The Cranked Harmonic Oscillator and Nondispersive Wavepackets

So far equilibrium points have been identified in the zero-velocity surface. It is important to analyze factors affecting the stability of these points. For conciseness, x_0 is used to refer simply to an equilibrium point. Usually, stable motion at an equilibrium point in a Hamiltonian system can occur only at a potential-energy minimum. In many experimentally important problems the Hamiltonian can be separated into a sum of a positive-definite kinetic term depending quadratically on momenta and a potential part depending exclusively on coordinates, which prevents stable motion from occurring other than at a minimum [59].

While the most common situation in atomic physics is the stable motion at a potential energy minimum, the problem in hand does not meet this criterion because of the presence of the paramagnetic term, *i.e.*, one cannot identify separate kinetic and potential parts of the Hamiltonian. A key point of the configuration of fields is the latitude it provides to vary or even eliminate the paramagnetic term by proper transformations. When it is allowed to be present, the paramagnetic term complicates the computation of the frequencies associated with the coherent state since there is no "potential" about which to expand. Thus, the basic idea for the elimination of the paramagnetic term presented here is to expand the Hamiltonian in a Taylor series at a global equilibrium point. After the expansion, canonical transformations will be followed by the redefinition of the Hamiltonian to a form of the harmonic oscillator function.

If the expansion is locally harmonic, then a coherent state (defined by the local frequencies) can be prepared provided that the equilibrium point is linearly stable. Such a coherent state in the rotating frame will neither spread nor disperse as it executes motion along a Kepler orbit (the Kepler frequency of the electron is in a 1:1 resonance with the microwave frequency), although it might decay by tunneling. In general, more significant source of dispersion will arise if the tails of the wave packet penetrate appreciably into nonlinear or chaotic parts of phase space. This is expected to be a bigger problem at the maximum than at the minimum. In the laboratory frame, if these dispersive factors can be minimized, the electronic wave packet will travel along a circular Kepler orbit while remaining localized radially and angularly for a finite number of Kepler periods.

For the maximum configuration, the strategy to be described is used to compute frequencies of the initial coherent state. The steps involved are (a) a transformation to a barycentric system of Cartesian coordinates at the equilibrium, (b) expansion of the ZVS in a power series to second order, thereby producing a cranked oscillator, which

is separable and harmonic at once, albeit in rotated coordinates (c) determination of the locally harmonic frequencies of these oscillators, and (d) computation of the vacuum state of the cranked oscillator. For future references, the derivation of the initial wave packet will be given in some detail since phase factors are essential in obtaining fully coherent wave packets.

2.3.1 Taylor Expansion and Cranked Harmonic Oscillator

The harmonic approximation in the neighborhood of the equilibrium point makes it possible to determine the ground state energy and frequencies of the coherent state for the Hamiltonian,

$$H = \frac{p_x^2 + p_y^2 + p_z^2}{2} - \frac{1}{r} - \omega(xp_y - yp_x) \mp Fx + \frac{\omega_c^2}{8}(x^2 + y^2). \tag{2.22}$$

The mapping begins with the Taylor expansion of the ZVS around the equilibrium point (x_0, y_0, z_0). The first term of the Taylor series is linear and the process of dropping the remaining terms is called linearization [60]. The process of linearization is important since linear systems are the only large class of differential equations for which there exists a definite theory [60]. Expansion of the ZVS in the neighborhood of the equilibrium point involves a canonical transformation from the original rotating center of mass coordinates to the equilibrium configuration [38]. This shifts the center from the origin to the equilibrium point. The new coordinates are derived from the equilibrium point of the Hamiltonian. The equilibrium points can be obtained by solving

$$\begin{aligned} \dot{q} &= \left(\frac{\partial H}{\partial p_q}\right)_{q_0} = 0 \\ \dot{p}_q &= -\left(\frac{\partial H}{\partial q}\right)_{q_0} = 0. \end{aligned} \tag{2.23}$$

where $q = x,\ y,\ z$. These equations lead to following equations

$$\begin{aligned} y_0 &= z_0 = 0 \\ p_{x_0} &= p_{z_0} = 0,\ p_{y_0} = \omega x_0. \end{aligned} \tag{2.24}$$

where

$$x_0 = \mp \frac{4r_0^3 F}{4\omega^2 r_0^3 - \omega_c^2 r_0^3 - 4} \tag{2.25}$$

with $r_0 = (x_0^2 + y_0^2 + z_0^2)^{1/2}$. Thus, the transformation from the original rotating center of mass coordinates to the equilibrium configuration is accomplished through the canonical transformation

$$\begin{aligned} x &= x_0 + \xi\,, \quad p_x = p_\xi \\ y &= \eta\,, \qquad\quad p_y = \omega x_0 + p_\eta \\ z &= \zeta\,, \qquad\quad p_z = p_\zeta \end{aligned} \tag{2.26}$$

which transforms the Hamiltonian (2.22) into the form of cranking model mentioned at the chapter 1,

$$H = \frac{p_\xi^2 + p_\eta^2 + p_\zeta^2}{2} - \omega(\xi p_\eta - \eta p_\xi) \mp F\xi + \Theta \tag{2.27}$$

where the "force function"[38] is given by

$$\Theta = -\frac{1}{r} \mp F x_0 + \frac{\omega_c^2}{8}(\xi^2 + \eta^2) - \frac{1}{2}\omega^2 x_0^2 + \frac{1}{8}\omega_c^2 x_0^2 + (\frac{\omega_c^2}{4} - \omega^2) x_0 \xi \tag{2.28}$$

and

$$r = (\xi^2 + \eta^2 + \zeta^2 + 2\xi x_0 + x_0^2)^{1/2} \tag{2.29}$$

which may be expanded around (ξ,η,ζ)=(0,0,0) the the second-order in (ξ,η,ζ) to produce an approximate Hamiltonian describing librations around the equilibrium point. The expansion results in

$$H = \frac{p_\xi^2 + p_\eta^2 + p_\zeta^2}{2} + \frac{\omega^2}{2}(a\xi^2 + b\eta^2 + c\zeta^2) - \omega(\xi p_\eta - \eta p_\xi) + \Theta_0 \tag{2.30}$$

with,

$$
\begin{aligned}
a &= \frac{1}{\omega^2}(\frac{\omega_c^2}{4} - \frac{2}{x_0^3}), \\
b &= \frac{1}{\omega^2}(\frac{\omega_c^2}{4} + \frac{1}{x_0^3}), \\
c &= \frac{1}{\omega^2 x_0^3}
\end{aligned}
\tag{2.31}
$$

and the part of the Hamiltonian containing only constant terms is given by

$$
\Theta_0 = -\frac{1}{2}\omega^2 x_0^2 \mp F x_0 + \frac{1}{8}\omega_c^2 x_0^2 - \frac{1}{x_0}. \tag{2.32}
$$

In the classical calculations H_c is ignored, although it provides a useful energy calibration in the quantum computations to be reported elsewhere [61]. From Cauchy's uniqueness theorem it follows that a particle starting out in the plane of polarization, with an initial velocity contained in that plane, will never leave the plane [56].

The linear stability at the equilibrium point (for both the maximum and minimum) was derived in detail in a paper [42]. Briefly, the approximation to the Hamiltonian describing librations around the equilibrium point shows the motion in the z (or ζ)-direction to be stable, harmonic, and decoupled from the planar motion. The Hamiltonian H is identical in form to the cranked oscillator [14, 26, 62, 63]. More recently, this problem has also been addressed (based on the Bogoliubov-Tyablikov transformation) in molecular physics to simplify rotational-vibrational Hamiltonians [64, 65, 66, 67].

Any eigenstate for eq. (2.30) can be written as

$$
\Psi(\xi, \eta, \zeta) = \psi(\xi, \eta)\phi(\zeta), \tag{2.33}
$$

where $\phi(\zeta)$ is the harmonic oscillator eigenfunction along the ζ-direction. To find the eigenstates of $\psi(\xi, \eta)$ is straightforward because the corresponding Hamiltonian can be rewritten in the form of two uncoupled harmonic oscillator after an appropriate canonical transformation. Therefore, for the initial conditions in the $\xi\eta$ plane, the

motion can be treated as being restricted to that plane, and the Hamiltonian in the plane is

$$H = \frac{p_\xi^2 + p_\eta^2}{2} + \frac{\omega^2}{2}(a\xi^2 + b\eta^2) - \omega(\xi p_\eta - \eta p_\xi). \tag{2.34}$$

The Hamiltonian (2.34) is the cranked anisotropic oscillator model referred on the Chapter 1.

2.3.2 Nondispersive Wavepackets

The ground-state energy and spatial distribution of the coherent state can be calculated using the cranked harmonic oscillator method. The motion in the z (or ζ)-direction was stable, harmonic and as a result the Hamiltonian is separable. Review the cranked harmonic oscillator from Eq. (2.34):

$$H = \frac{p_1^2 + p_2^2}{2} + \frac{1}{2}(\omega_1 x_1^2 + \omega_2 x_2^2) - \omega(x_1 p_2 - x_2 p_1). \tag{2.35}$$

where, for convenience, ξ and η were replaced by x_1 and x_2 respectively, and conjugate momenta by p_1, p_2. The eigenvalues of the cranked harmonic oscillator are found by diagonalizing Hamiltonian eq. (2.35) analytically. A suitable transformation of the coordinates and their conjugate momenta to new primed coordinates x_i' and momenta p_i' will make the Hamiltonian uncoupled harmonic oscillator. The transformations are given by

$$\begin{aligned} x_i' &= Ax_i + Bp_j \\ p_i' &= p_i + Cx_j, \end{aligned} \tag{2.36}$$

where $i, j = 1, 2,\ i \neq j$. The primed and unprimed coordinates are connected by a unitary transformation, which requires the commutation relation between coordinates and momenta to be preserved. This requirement is fulfilled when $A - BC = 1$, with

the primed operators should be real. Their inverse transformations are

$$\begin{aligned} x_i &= x_i' - Bp_j' \\ p_i &= Ap_i' - Cx_j'. \end{aligned} \tag{2.37}$$

Applying these inverse transformations to the Hamiltonian (2.35) leads to a new Hamiltonian with bilinear terms, which can be eliminated by setting their coefficients zero and thereby produces equations for A, B and C. The property of unitary of transformation with the equations lead to three equations for the three coefficients whose solutions are

$$\begin{aligned} A &= \frac{1}{2}\left(1 + \frac{\omega_2^2 - \omega_1^2}{S}\right) \\ B &= \frac{2\omega}{S} \\ C &= \frac{1}{4\omega}\left(\omega_2^2 - \omega_1^2 - S\right) \end{aligned} \tag{2.38}$$

with

$$S = sign(\omega_2 - \omega_1)\sqrt{\left(\omega_2^2 - \omega_1^2\right)^2 + 8\omega^2(\omega_2^2 + \omega_1^2)}.$$

The parameters A, B and C are real for all values of ω_1, ω_2 and ω, thus the primed operators, x_i', p_j', are hermitian. The sign of S is chosen such that in the limit $\omega \to 0$ the transformation goes over continuously into the identity transformation, i.e. $A \to 0$, $B \to 0$ and $C \to 0$ whereas for the opposite choice the transformation becomes singular for $\omega \to 0$. Under the transformation (2.37) and with the above definitions, the resulting rotated Hamiltonian can be written in the form

$$\mathcal{H} = \frac{p_1'^2}{2m_1} + \frac{p_2'^2}{2m_2} + \frac{1}{2}m_1\Omega_1^2 x_1'^2 + \frac{1}{2}m_2\Omega_2^2 x_2'^2. \tag{2.39}$$

The new frequencies and effective masses are defined by

$$\begin{aligned}
\Omega_1^2 &= \frac{1}{2}\left(\omega_1^2+\omega_2^2\right)+\omega^2-\frac{1}{2}S \\
\Omega_2^2 &= \frac{1}{2}\left(\omega_1^2+\omega_2^2\right)+\omega^2+\frac{1}{2}S \\
m_1 &= \frac{\Omega_1^2-\Omega_2^2}{\Omega_1^2-\omega_2^2+\omega^2} \\
m_2 &= \frac{\Omega_2^2-\Omega_1^2}{\Omega_2^2-\omega_1^2+\omega^2}.
\end{aligned} \tag{2.40}$$

The masses approach the particle's mass[2] m in the limit $\omega \to 0$ and $\Omega_i \to \omega_i$. Because the masses depend on the frequencies, they may be positive or negative. The eigenvalues of the Hamiltonian $\mathcal{H}$ are real and this imposes the restriction $\Omega_i^2 > 0$ $(i = 1, 2)$ on the solution which is fulfilled for:

$$\omega < min(\omega_1, \omega_2) \qquad \text{or} \qquad \omega < max(\omega_1, \omega_2). \tag{2.41}$$

In the low frequency range $\omega < min(\omega_1, \omega_2)$ both masses are positive whereas for $\omega > max(\omega_1, \omega_2)$ one of them is negative and the energy spectrum E has no lower bound. In the case of stable motion at a maximum, the masses have opposite signs. The intermediate range must be excluded. In these two allowed regions the energy eigenvalues of Hamiltonian (2.35) are given by

$$\begin{aligned}
E_0 &= \text{sign}(m_1)\left(n_1+\frac{1}{2}\right)\hbar|\Omega_1| + \text{sign}(m_2)\left(n_2+\frac{1}{2}\right)\hbar|\Omega_2| \\
&= \hbar\Omega_0
\end{aligned} \tag{2.42}$$

with n_1 and n_2 being non-negative integers. In the following, the frequencies Ω_i will be assumed to be positive. The ground state ($n_1 = n_2 = 0$) eigenfunction can be found by solving the differential equation for the eigenfunction of the rotating harmonic oscillator with known eigenvalue E_0 of eq. (2.42). The eigenfunctions can

[2]The Lagrangian and Hamiltonian in this paper use atomic units. The particle's mass is in unscaled units.

be expressed as follows in terms of the original coordinates at the x_1x_2-plane:

$$\psi(x_1, x_2) = N\exp\left(-\frac{\alpha}{2}x_1^2 - \frac{\beta}{2}x_2^2 - i\gamma x_1 x_2\right) \tag{2.43}$$

where the parameters α, β and γ are found as:

$$\begin{aligned}
\alpha &= \frac{\Omega_0(1+Q)}{\hbar} \\
\beta &= \frac{\Omega_0(1-Q)}{\hbar} \\
\gamma &= \frac{\omega Q}{\hbar} \\
\text{with } Q &= \frac{(a-b)\omega^2}{4(\Omega_0^2 - \omega^2)}.
\end{aligned} \tag{2.44}$$

In atomic units, $\hbar = 1$. Here the normalization constant is given by

$$|N|^2 = \frac{\sqrt{\alpha\beta}}{\pi}. \tag{2.45}$$

α and β are positive in the allowed regions $\omega < \omega_<$ and $\omega > \omega_>$. The spatial distribution of the coherent state is given by $|\psi(x_1, x_2)\psi(x_3)|^2$. The phase $i\gamma x_1 x_2$ has no classical consequence, and this term will be cancelled when the spatial distribution in considered [3]. Figure 6(a) shows the harmonic approximation and the corresponding ground-state wavefunction of the effective potential surrounding a minimum equilibrium point. Note how well the harmonic approximation fits and is therefore an excellent estimation of the effective potential. Figure 6(b) shows the iso-energy contours of the zero velocity surface (in the plane $z = 0$) together with a contour plot of a ground state for the potential well.

This procedure is valid both at the maximum and minimum, although it is unnecessary at the minimum for the special case of $\omega_f = \omega_c/2$, paramagnetic term is eliminated and the Hamiltonian reduces to a harmonic oscillator and the the coherent states can be calculated directly. Even with coupling terms, same calculations can

[3] If the position is shifted along x_1-axis, it will introduces an additional phase into the ground sate wavefunction [61], which cannot be ignored when performing quantum mechanical calculations.

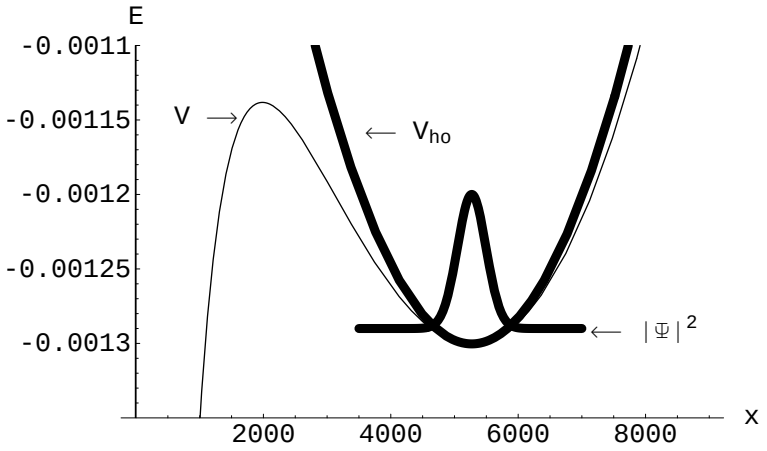

(a)

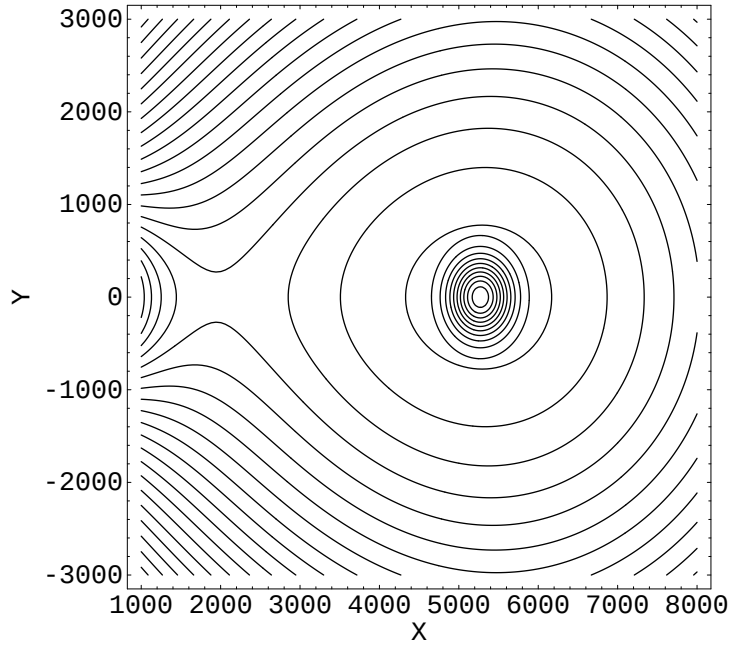

(b)

Figure 6: (a) Zero velocity surface for the minimum configuration with $\omega_c = 4.00813$ T, $\omega_f = 39.7$ GHz and $F = 2004.09$ V/cm. A section ($y = z = 0$) through the potential is shown. The harmonic approximation to the potential V_{ho} and the Gaussian probability density of the ground-state $|\Psi|^2$ are also plotted. (b) Level curves of the Zero Velocity Surface together with contours of the ground states as obtained by Taylor expansion about the minimum. The parameters are the same as in (a).

be done. The following chapter introduces two additional couplings to the cranked harmonic oscillator.

CHAPTER III

COHERENT STATES OF THE CRANKED HARMONIC OSCILLATOR WITH COUPLINGS

3.1 Introduction

Tailoring and manipulating electronic wave packets [1] is currently one of the most active and challenging research subjects in the broad area of quantum control [2, 3]. Physicists, electrical engineers and mathematicians have joined forces in an effort to keep the wave packet representing the electron from spreading in uncontrollable ways. It is well known that it is quite difficult to prevent the spreading of such an electronic wave packet-and that's where the concept of a coherent state enters [68].

The coherent state concept was first proposed by Schrödinger [27] for the harmonic oscillator and developed further by Glauber [28]. These states also can be defined in several equivalent ways, for example, Gaussian wave packets evolving without spreading. For the one-dimensional harmonic oscillator it is well known that the minimum uncertainty state gives the corresponding classical behavior for the expectation values of the position and momentum operators. Coherent states have provided a natural framework for the semi-classical description of a variety of collective phenomena in physics such as the radiation fields of lasers [29], and large amplitude nuclear collective motion [34], and interesting application of the harmonic oscillator coherent states in nuclear physics by Ghosh [34].

The construction of exact coherent states for quantum mechanical systems can facilitate the investigation of the collective aspects of these systems in a semiclassical fashion. With this motivation, a number of investigators have succeeded in constructing coherent states for the rotation groups and the asymmetric top [72] and for

potentials more general than the harmonic oscillator [73], and for the time-dependent harmonic oscillator [74]. The hydrogen atom, however, has been the most problematic system in which to look for coherent states [75] ever since Schrödinger failed to repeat his previous success with the harmonic oscillator [76], *i.e.*, to superpose stationary states of the hydrogen atom into nondispersing wave packets which moved on the elliptic orbits generic to the Kepler/Coulomb problem [45]. Today, it is certainly possible, both theoretically [77, 78, 79, 80, 81] and experimentally [82, 83] to construct an electronic wave packet which rides on an elliptic Kepler orbit [78, 79] as well as on circular orbits that correspond to maximal orbital angular momentum [84, 85, 86]. While this wave packet can be localized on the orbital plane and, within that plane, in the radial direction, it cannot be localized angularly [45].

It is useful to review briefly how nonspreading coherent wave packets might be prepared in an atom or molecule. Naturally the harmonic oscillator is the ideal quantum system in which to carry out studies on truly non-dispersive coherent wave packets due to the constant energy level spacings. Thus the question arises as to whether it might be possible to prepare locally harmonic regimes in atoms thereby allowing the creation of almost completely non-dispersive coherent atomic states that are identical to the coherent states of the harmonic oscillator. The energy level spacings of a hydrogen atom are clearly not constant but be made to be almost so with the use of a perturbation such as an external static electric field (the Stark Effect). From perturbation theory, the energy levels of the hydrogen atom in static electric field are given to first order by

$$E_{nk} \simeq -\frac{1}{2n^2} + \frac{3}{2}Fnk \tag{3.1}$$

where n is the principal quantum number and k is parabolic quantum number (the stark effect separates in parabolic coordinates). The electric field thus splits the states of a given principal quantum number manifold into equally spaced (locally almost harmonic) Stark states.

Empirically, the symmetry breaking by crossed electric magnetic fields must be used in order to achieve complete localization [87], but even under favorable circumstances, this full localization (planar, radial and angular) is short-lived - a brief encounter with the core is sufficient to undo it [87]. This bleak outlook for full localization was improved by the recent discovery of localized "Trojan" wave packets in Rydberg atoms in a circularly polarized microwave field (CPM) by Bialynicki-Birula et al. (BKE) [40, 88, 89, 90] using the analogy to the famous Restricted Three-Body Problem (RTBP) of classical mechanics in the previous chapter. Their treatment maps the CP problem onto an anisotropic cranked oscillator which lends itself easily to analytical treatments [24, 25].

The construction of nondispersive wave packets in periodically driven quantum systems has been reviewed thoroughly [92] and realized recently [93]. The addition of a magnetic field perpendicular to the plane of polarization of the CPM field in the crossed fields configuration can not only stabilize the localized states of this system, but more strikingly, create a stable outer potential [58, 54, 61, 94, 95]. This well is locally harmonic in a region of space that also excludes the nucleus, thereby allowing the wave packet to circle the nucleus clear of the core and safe from its detrimental influence on the localization [58, 61]. Because the potential is locally harmonic to an excellent approximation [96], its vacuum state is a coherent state in the sense of Schrödinger to the same excellent approximation and therefore does not spread. If the potential supporting the coherent state were perfectly harmonic, that state would be merely one of an infinite set of coherent states supported by the field configuration. These states correspond to tightly localized electron performing classical motion in the atom. If $[x_{c1},\ x_{c2}]$ denotes the classical trajectory of the electron in the orbital plane of the motion, the probability density of such a coherent state $\psi_{\alpha_1\alpha_2}(x_1, x_2)$ is given in terms of the classical trajectory as the double Gaussian (where the α's are

coherent state arguments)

$$|\psi_{\alpha_1\alpha_2}(x_1,x_2)|^2 = \mathcal{N}^2 \exp\left\{-\frac{D}{b_1^2}(x_1 - x_{c1}(t))^2\right\} \cdot \exp\left\{-\frac{D}{b_2^2}(x_2 - x_{c2}(t))^2\right\}.$$

The $\psi_{\alpha_1\alpha_2}(x_1,x_2)$ is not minimum uncertainty state and involves many intricate phase factors. But remarkably, it does not spread in time [62].

This chapter will go one step further by asking if the motion of the electron, represented by a non-spreading (or slowly-spreading) wave packet can be controlled using external fields, such as a dipole field. The ultimate aim is to make wave packets move in a prescribed way before they can spread appreciably. As a first step to this ultimate goal, the behavior of cranked oscillator coherent states in a dipole field will be presented: we find that they indeed can move in a way prescribed by the dipole field, constructing near-coherent states for specific atomic potentials and investigation of their properties in the field configuration will be followed by, where Glauber-type coherent states [28] are defined in the usual manner.

3.2 Coherent States of a Harmonic Oscillator

The first modern, specific modifications to the coherent states since Schrödinger's works were made by Glauber [28] and Sudarshan [97]. Glauber constructed the eigenstates of the annihilation operator of the harmonic oscillator in order to study the electromagnetic correlation functions. As emphasized by Glauber, there are three equivalent ways to construct the coherent states. The first is to define them as eigenstates of the annihilation operator. The second is to define them by the application of a "displacement" operator on the vacuum state. The comes from the consideration of the coherent states as quantum states with a minimum uncertainty relationship. These definitions are applied to a expanded Hilbert space to generate the Glauber-type coherent states. To begin with the construction of coherent states, Glauber's definitions of the coherent states will be introduced. Next, It will be shown that

coherent states can be constructed from the classical quantities of coordinates and momenta calculated from cranked harmonic oscillator with or without the coupling terms. Remaining of this chapter shows a method to find coordinates representations of the coherent states and probability distribution to investigate the classical behavior.

According to Glauber [28], the coherent states can be constructed by three different definitions for the harmonic oscillator in no external field.

(a) The coherent states are eigenstates ($|\alpha\rangle$)of the harmonic oscillator annihilation operator a,

$$a|\alpha\rangle = \alpha|\alpha\rangle, \tag{3.2}$$

where α is complex number.

(b) The coherent states can be obtained by applying a displacement operator to the ground state of the oscillator, $D(\alpha)$.

$$|\alpha\rangle = D(\alpha)|0\rangle, \tag{3.3}$$

where the displacement operator is defined as

$$D(\alpha) = e^{\alpha a^\dagger - \alpha^* a}. \tag{3.4}$$

and $[a, a^\dagger] = 1$ as usual.

(c) The coherent states are quantum states with minimum-uncertainty relationship.

$$(\Delta q)^2(\Delta p)^2 = \left(\frac{\hbar}{2}\right)^2 \tag{3.5}$$

where the coordinates and momentum operators are defined,

$$\begin{aligned} \hat{q} &= \frac{b}{\sqrt{2}}(a^\dagger + a) \\ \hat{p} &= \frac{i\hbar}{\sqrt{2}b}(a^\dagger - a). \end{aligned} \tag{3.6}$$

where $b = \sqrt{\hbar/m\omega}$. Time-dependent expectation values of the operators are straightforwardly evaluated for the state $|\alpha\rangle$ using Heisenberg picture for the operators and also they retain the property of being a minimum uncertainty state for all times. The third definition is by no means unique because the uncertainty relationship does not provide unique solution for the set of (Δq, Δp). Expansion in a Hilbert space may be performed in a number of ways. For following calculations, consider the expansion in terms of the eigenstates of the Fock states:

$$\begin{aligned} |\alpha\rangle &= D(\alpha)|0\rangle \\ &= e^{-\alpha^*\alpha/2} \sum_{n=0}^{\infty} \alpha^n (n!)^{-1/2} |n\rangle. \end{aligned} \tag{3.7}$$

Here $|n\rangle$, $n = 0, 1, 2, \cdots$, denote normalized eigenstates of the number operator N, $N|n\rangle = n|n\rangle$, which may be identified with the eigenstates of the harmonic oscillator Hamiltonian $H_0 = (N+1/2)\hbar\Omega_0$. The time evolution of the coherent states is given by

$$\begin{aligned} |\alpha(t)\rangle &= e^{-iH_0 t/\hbar}|\alpha\rangle \\ &= e^{-\alpha^*\alpha/2} \sum_{n=0}^{\infty} \frac{1}{\sqrt{n!}} \alpha^n e^{-in\Omega_0 t - i\Omega_0 t/2} |n\rangle \\ &= e^{-i\Omega_0 t/2} |\alpha e^{-i\Omega_0 t}\rangle. \end{aligned} \tag{3.8}$$

Thus the time evolution shows that any coherent states of a harmonic oscillator remains within the family of coherent states, which is referred as *temporal stability* under H_0 [80]. By calculating the expectation values of the position and momentum operators of the harmonic oscillator, following relations are obtained,

$$\begin{aligned} < \hat{q}(t) > &= \sqrt{2} b \ \mathrm{Re}\{\alpha(t)\} \\ < \hat{p}(t) > &= \frac{\sqrt{2}\hbar}{b} \ \mathrm{Im}\{\alpha(t)\} \end{aligned} \tag{3.9}$$

Therefore the coherent states $|\alpha(t)\rangle$ are minimum uncertainty quantum states $\{q(t)$, $p(t)\ \}$, which follow the classical motion of a harmonic oscillator. $\alpha(t)$ can be written

as

$$\alpha(t) = \frac{1}{\sqrt{2}b}\left(q(t) + i\frac{b^2}{\hbar}p(t)\right) \tag{3.10}$$

and the classical motion can be described by

$$\begin{aligned} q(t) &= \sqrt{2}b\ \mathrm{Re}\{\alpha(t)\} = \ \mathrm{Re}\left\{\left(q(0) + i\frac{b^2}{\hbar}p(0)\right)e^{-i\Omega_0 t}\right\} \\ p(t) &= \frac{\sqrt{2}\hbar}{b}\ \mathrm{Im}\{\alpha(t)\} = \frac{\hbar}{b^2}\ \mathrm{Im}\left\{\left(q(0) + i\frac{b^2}{\hbar}p(0)\right)e^{-i\Omega_0 t}\right\}. \end{aligned} \tag{3.11}$$

The above relations will be used in the next section to find the coherent states of the cranked harmonic oscillator in an external field. The coherent states are continuous in their label $\alpha = \alpha^R + i\alpha^I$ and admit a resolution of unity given by

$$\mathbf{1} = \frac{1}{\pi}\int\int |\alpha\rangle\langle\alpha| d^2\alpha. \tag{3.12}$$

Continuity in the labels plus a resolution of unity establish that the set $|\alpha\rangle$ is a set of coherent states in the modern sense of the term [99].

3.3 Coherent States of a Cranked Harmonic Oscillator

The Glauber definition of the coherent states can be applied to construct coherent states for the cranked harmonic oscillator which was introduced to the previous chapter. In Chapter 2, the Hamiltonian of a hydrogen atom subjected to a CP microwave and static magnetic field was transformed to a cranked harmonic oscillator by Taylor expansion of the ZVS around its equilibrium point. It was also shown that the nondispersive nonspreading wavepackets could be constructed from the cranked harmonic oscillator. This section shows that the coherent states can be constructed from the classical quantities of coordinates and momenta calculated from cranked harmonic oscillator using Glauber definitions. As an extension of the discussion, this section introduces various dipole couplings into the cranked harmonic oscillator and shows that the coherent states can be constructed.

3.3.1 The Cranked Harmonic Oscillator with Time-Independent Couplings

With time-independent dipole couplings, the Hamiltonian can be reduced to a separable form directly by suitable transformation, where $l_z = x_1 p_2 - x_2 p_1$, and d_1, d_2 are couplings. We will consider two different cases where the dipole couplings are (A) time-independent and (B) time-dependent. The Hamiltonian for a spinless particle moving in dipole fields at xy-plane can be obtained by adding the field into the eq. (2.34).

$$H = \frac{1}{2}\left(p_1^2 + p_2^2\right) + \frac{1}{2}\left(\omega_1^2 x_1^2 + \omega_2^2 x_2^2\right) - \omega l_z + d_1 x_1 + d_2 x_2 \tag{3.13}$$

Using the same unitary transformation eq. (2.37), the Hamiltonian can be converted to two decoupled harmonic oscillators with new frequencies and masses in the primed coordinates as

$$\begin{aligned} H' = &\frac{1}{2m_1}\left(p_1' - Bm_1 d_2\right)^2 + \frac{1}{2}m_1\Omega_1^2\left(x_1' + \frac{d_1}{m_1\Omega_1^2}\right)^2 \\ &+ \frac{1}{2m_2}\left(p_2' - Bm_2 d_1\right)^2 + \frac{1}{2}m_2\Omega_2^2\left(x_2' + \frac{d_2}{m_2\Omega_2^2}\right)^2 + H'_{shift} \end{aligned} \tag{3.14}$$

where the frequencies and masses are given by eq. (2.40). The masses m_1 and m_2 depend on new frequencies. As was explained before, they approach the particle's mass as $\omega \to 0$. The frequencies and masses are same as the results from Habeeb's paper [62], which are given by eq. (2.40). However, the coordinates and momenta are shifted because of the dipole couplings. The energy shift is given by

$$H'_{shift} = \sum_{i,j=1,2}\left(\frac{1}{2}B^2 m_i d_j^2 + \frac{d_i^2}{2m_i\Omega_i^2}\right). \tag{3.15}$$

Define $\mathcal{H} = H' - H'_{shift}$ to reduce the Hamiltonian into a separable form:

$$\mathcal{H} = \frac{\mathcal{P}_1^2}{2m_1} + \frac{\mathcal{P}_2^2}{2m_2} + \frac{1}{2}m_1\Omega_1^2\chi_1^2 + \frac{1}{2}m_2\Omega_2^2\chi_2^2, \tag{3.16}$$

where

$$\chi_i = x_i' + \frac{d_i}{m_i\Omega_i^2} \;=\; Ax_i + Bp_j + \frac{d_i}{m_i\Omega_i^2}$$
$$\mathcal{P}_i = p_i' - Bm_i d_j \;=\; p_i + Cx_j - Bm_i d_j \tag{3.17}$$

with $i, j = 1, 2$ and $i \neq j$. Exact classical solutions $x_i(t)$, $p_i(t)$ of the equations of motion governed by the Hamiltonian (3.13) can be found by transforming the classical solutions of the harmonic oscillator (3.16) to the non-primed system using the inverse transformation (2.37) and (3.17). The results are

$$\begin{aligned} x_i(t) = {} & [Ax_i(0) + Bp_j(0) + \frac{d_i}{m_i\Omega_i^2}]\cos\Omega_i t \\ & + \frac{1}{m_i\Omega_i}[p_i(0) + Cx_j(0) - Bm_i d_j]\sin\Omega_i t \\ & - B[p_j(0) + Cx_i(0) - Bm_j d_i]\cos\Omega_j t \\ & + Bm_j\Omega_j[Ax_j(0) + Bp_i(0) + \frac{d_j}{m_j\Omega_j^2}]\sin\Omega_j t - \frac{d_i}{m_i\Omega_i^2} - B^2 m_j d_i, \end{aligned} \tag{3.18}$$

$$\begin{aligned} p_i(t) = {} & -Am_i\Omega_i[Ax_i(0) + Bp_j(0) + \frac{d_i}{m_i\Omega_i^2}]\sin\Omega_i t \\ & + A[p_i(0) + Cx_j(0) - Bm_i d_j]\cos\Omega_i t \\ & - \frac{C}{m_j\Omega_j}[p_j(0) + Cx_i(0) - Bm_j d_i]\sin\Omega_j t \\ & - C[Ax_j(0) + Bp_i(0) + \frac{d_j}{m_j\Omega_j^2}]\cos\Omega_j t + \frac{Cd_j}{m_j\Omega_j^2} - ABm_i d_j, \end{aligned} \tag{3.19}$$

where $i, j = 1, 2,\ (i \neq j)$.

3.3.2 The Cranked Harmonic Oscillator with Time-Dependent Couplings

Time dependent coupling terms arise when a polarized microwave field is applied to the cranked oscillator, which could be given by

$$d_1(t) = F_1\cos\omega_f t$$
$$d_2(t) = F_2\sin\omega_f t. \tag{3.20}$$

The d_1 and d_2 will describe the oscillating field strengths, F_1, F_2 are the amplitudes and ω_f is the frequency of the polarized field. Thus Hamiltonian (3.13) will be replaced by

$$H = \frac{1}{2}\left(p_1^2 + p_2^2\right) + \frac{1}{2}\left(\omega_1^2 x_1^2 + \omega_2^2 x_2^2\right) - \omega l_z$$
$$+ F_1 x_1 \cdot \cos\omega_f t + F_2 x_2 \cdot \sin\omega_f t. \tag{3.21}$$

Circularly and elliptically polarized microwave fields correspond to $F_1 = F_2$ and $F_1 \neq F_2$, respectively. We use following transformations to eliminate the time dependent terms of the eq. (3.21). These transformations do not change the constant frequency ω of the rotating frame and other canonical variables, but cancel out the polarized microwave field in the rotating frame of reference.

$$\begin{aligned} x_1 &= \xi + f_1(t), \qquad & x_2 &= \zeta + f_2(t) \\ p_1 &= p_\xi + g_1(t), \qquad & p_2 &= p_\zeta + g_2(t) \end{aligned} \tag{3.22}$$

where

$$\begin{aligned} f_1(t) &= \frac{d_1(t)}{\omega^2 - \omega_1^2}, \qquad & f_2(t) &= \frac{d_2(t)}{\omega^2 - \omega_2^2} \\ g_1(t) &= \frac{-\omega d_2(t)}{\omega^2 - \omega_2^2}, \qquad & g_2(t) &= \frac{\omega d_1(t)}{\omega^2 - \omega_1^2}. \end{aligned} \tag{3.23}$$

The f_i and g_i $(i = 1, 2)$ were determined to eliminate the explicit time dependent terms. The new Hamiltonian function is given by

$$H' = \frac{1}{2}(p_\xi^2 + p_\zeta^2) + \frac{1}{2}(\omega_1^2\xi^2 + \omega_2^2\zeta^2) - \omega(\xi p_\zeta - \zeta p_\xi) - \epsilon\cos\omega_f t \tag{3.24}$$

with

$$\epsilon = \frac{F_1^2/4}{\omega^2 - \omega_1^2} - \frac{F_2^2/4}{\omega^2 - \omega_2^2}.$$

The Hamiltonian turns out to be the cranked harmonic oscillator with a time dependent term. Using the canonical transformation presented at eq.(2.37),

$$\begin{aligned}
\xi &= \chi_1 - B\mathcal{P}_2 \\
\zeta &= \chi_2 - B\mathcal{P}_1 \\
p_\xi &= A\mathcal{P}_1 - C\chi_2 \\
p_\zeta &= A\mathcal{P}_2 - C\chi_1,
\end{aligned} \tag{3.25}$$

the Hamiltonian can be reduced to the separable form too:

$$\mathcal{H} = \frac{\mathcal{P}_1^2}{2m_1} + \frac{\mathcal{P}_2^2}{2m_2} + \frac{1}{2}m_1\Omega_1^2\chi_1^2 + \frac{1}{2}m_2\Omega_2^2\chi_2^2. \tag{3.26}$$

where the relations between transformed variables and initial variables are

$$\begin{aligned}
\chi_i &= Ax_i + Bp_j - Af_i(t) - Bg_j(t) \\
\mathcal{P}_i &= p_i + Cx_j - g_i(t) - Cf_j(t).
\end{aligned} \tag{3.27}$$

Hamiltonian (3.26) is identical to the Hamiltonian (3.16) transformed from the Hamiltonian with dipole couplings, and new masses and frequencies are also given by equation (2.40). This results shows that the linear time independent couplings or polarized time dependent couplings (circularly or elliptically polarized fields) produce exactly the same dynamics at the transformed coordinates. The classical solutions, $x_i(t)$ and $p_i(t)$, of the equations of motion governed by the Hamiltonian eq.(3.21) can also be calculated from (3.23) and (3.25), and they are given by

$$\begin{aligned}
x_i(t) = f_i(t) + \chi_i(0)\cos\Omega_i t + \frac{\mathcal{P}_i(0)}{m_i\Omega_i}\sin\Omega_j t \\
- B\mathcal{P}_j(0)\cos\Omega_j t + Bm_j\Omega_j\chi_j(0)\sin\Omega_j t
\end{aligned} \tag{3.28}$$

and

$$\begin{aligned}
p_i(t) = g_i(t) + A\mathcal{P}_i(0)\cos\Omega_i t - Am_i\Omega_i\chi_i(0)\sin\Omega_i t \\
- C\chi_j(0)\cos\Omega_j t - \frac{C\mathcal{P}_j(0)}{m_j\Omega_j}\sin\Omega_j t
\end{aligned} \tag{3.29}$$

with the initial values

$$\chi_i(0) = Ax_i(0) + Bp_j(0) - \frac{F_i(A+\omega B)}{\omega^2 - \omega_i^2}\delta_{i1}$$
$$\mathcal{P}_i(0) = p_i(0) + Cx_j(0) - \frac{F_i(\omega + C)}{\omega^2 - \omega_i^2}\delta_{i2} \tag{3.30}$$

where $i, j = 1, 2$, $i \neq j$ and δ is the Kronecker delta.

Therefore, the energy eigenvalues of the harmonic oscillator Hamiltonian eq.(3.26) are given by

$$E = \text{sign}(m_1)\left(n_1 + \frac{1}{2}\right)\hbar|\Omega_1| + \text{sign}(m_2)\left(n_2 + \frac{1}{2}\right)\hbar|\Omega_2|, \tag{3.31}$$

with n_1 and n_2 being non-negative integers. This result is same as eq. (2.42) because the transformed Hamiltonian is simply a harmonic oscillator. Both Hamiltonians with different couplings ended up with harmonic oscillator after suitable transformations, so it is possible to construct the coherent states using classical solutions and calculate the resultant probability density functions for each different cases in the following section.

3.3.3 Construction of the Coherent States from Classical Solutions

It has been shown that the cranked harmonic oscillator with or without the coupling terms can be transformed to uncoupled harmonic oscillators (Eq. (2.39), (3.16) and (3.26)). The classical solutions of the harmonic oscillator are easily found and thereby they can be expressed as the solutions of the equations of the original coordinates Hamiltonian. The coherent states can be constructed from these classical quantities using the relations in the equations (3.10) and (3.11). Construction of the coherent states will be performed for the cranked harmonic oscillator with dipole couplings through this section. Recalling the uncoupled harmonic oscillator in the transformed coordinates (χ_1, χ_2)

$$\mathcal{H} = \frac{\mathcal{P}_1^2}{2m_1} + \frac{\mathcal{P}_2^2}{2m_2} + \frac{1}{2}m_1\Omega_1^2\chi_1^2 + \frac{1}{2}m_2\Omega_2^2\chi_2^2, \tag{3.32}$$

define the coherent states from the representation of eq. (3.8) in terms of their stationary occupation number states, parametrized by three complex quantities α_i ($i = 1, 2, 3$)[26].

$$|\{\alpha_i\}; t\rangle = \prod_{i=1}^{3} \exp\left(-\frac{|\alpha_i|^2}{4b_i^2}\right) \sum_{n_i=0}^{\infty} \left(\frac{\alpha_i}{\sqrt{2}b_i}\right)^{n_i} \cdot \frac{1}{\sqrt{n_i!}} e^{-\mathrm{i}\Omega_i(n_i+1/2)t} |n_i\rangle \tag{3.33}$$

where $b_i = \sqrt{\frac{\hbar}{|m_i|\Omega_i}}$ ($i = 1, 2, 3$), and the α of eq. (3.10) was scaled as follows:

$$\alpha(t) = q(t) + i\frac{b^2}{\hbar} p(t). \tag{3.34}$$

In the following calculations for expectation values, the definition of coherent states (3.33) will be used. The motion in the x_3 direction will not be dealt with since it is decoupled from the motion along x_1, x_2 direction and it is not affected by the rotation. Since the coherent states defined by the equation (3.33) are by construction the ordinary coherent states for the transformed Hamiltonian of equation (3.32), it follows the standard results for expectation values still hold in the uncoupled system.

$$\begin{aligned} &< \chi_i(t) > = \alpha_i^R(t) \\ &< \mathcal{P}_i(t) > = \frac{\hbar}{b_i^2} \alpha_i^I(t) \end{aligned} \tag{3.35}$$

where $\alpha_i(t) = \alpha_i \exp(-\mathrm{i}\Omega_i t)$ ($i = 1, 2$), and the superscripts R and I stand for real and imaginary parts respectively. The classical solutions of coordinates and momenta at the initial coordinates system ($x_1 x_2$ coordinates) can be expressed by $\chi_i(t)$, $\mathcal{P}_i(t)$ using the inverse transformation, so the classical solutions $x_i(t)$ and $p_i(t)$ can be calculated easily, provided that the classical solutions at the transformed coordinates are known. For the known initial conditions, the harmonic oscillators has followings as their solutions:

$$\begin{aligned} \chi_i(t) &= \chi_i(0)\ \mathrm{cos}\Omega_i t + \frac{\mathcal{P}_i(0)}{m_i\Omega_i}\ \mathrm{sin}\Omega_i t \\ \mathcal{P}_i(t) &= -m_i\Omega_i\chi_i(0)\ \mathrm{sin}\Omega_i t + \mathcal{P}_i(0)\ \mathrm{cos}\Omega_i t, \end{aligned} \tag{3.36}$$

thereby, $x_i(t)$ and $p_i(t)$) are given by

$$\begin{aligned} x_i(t) &= \chi_i(t) + B\mathcal{P}_i(t) - \frac{d_i}{m_i\Omega_i^2} - B^2 m_j d_i \\ p_i(t) &= A\mathcal{P}_i(t) - C\chi_j(t) + \frac{Cd_j}{m_j\Omega_j^2} + ABm_i d_j \end{aligned} \tag{3.37}$$

for the Hamiltonian with dipole couplings, and for the Hamiltonian with polarized field they are described as

$$\begin{aligned} x_i(t) &= \chi_i(t) - B\mathcal{P}_j(t) + f_i(t) \\ p_i(t) &= A\mathcal{P}_i(t) - C\chi_j(t) + g_i(t). \end{aligned} \tag{3.38}$$

Furthermore, we can find the quantum mechanical expectation values, $\langle x_i \rangle$ and $\langle p_i \rangle$, in terms of $\alpha_i^R(t), \alpha_i^I(t)$ using the relation (3.35). If we identify α_i with the combined initial values of classical coordinates and momenta, the expectation values $\langle x_i \rangle$ and $\langle p_i \rangle$ are identical to the values from the classical solutions. The α_i can be found from $\alpha_i(t)$ at $t = 0$:

$$\alpha_i = \alpha_i(0) = \alpha_i^R(0) + \mathrm{i}\alpha_i^I(0), \tag{3.39}$$

and also following relations are derived:

$$\begin{aligned} x_i(0) &= \alpha_i^R(0) + B\frac{\hbar}{b_j^2}\alpha_j^I(0) - \frac{d_i}{m_i\Omega_i^2} - B^2 m_j d_i \\ p_j(0) &= A\frac{\hbar}{b_j^2}\alpha_j^I(0) - C\alpha_i^R(0) + \frac{Cd_i}{m_i\Omega_i^2} + ABm_j d_i \end{aligned} \tag{3.40}$$

for the Hamiltonian with dipole couplings, and

$$\begin{aligned} x_i(0) &= \alpha_i^R(0) - B\frac{\hbar}{b_j^2}\alpha_j^I + f_i(0) \\ p_j(0) &= A\frac{\hbar}{b_j^2}\alpha_j^I(0) - C\alpha_i^R(0) + g_j(0). \end{aligned} \tag{3.41}$$

for the Hamiltonian with polarized field, where the subscript of the momentum is switched to j. Equating two equations of eq.(3.40) or (3.41) with respect to α_i^R and

α_j^I results in α_i's for both cases:

$$\alpha_i = Ax_i(0) + Bp_j(0) + \frac{d_i}{m_i\Omega_i^2} + \mathrm{i}\frac{b_i^2}{\hbar}\left(p_i(0) + Cx_j(0) + Bm_i d_j\right) \tag{3.42}$$

for the constant dipole field, and

$$\alpha_i = Ax_i(0) + Bp_j(0) - \frac{F_i(A+\omega B)}{\omega^2 - \omega_i^2}\delta_{i1} + \mathrm{i}\frac{b_i^2}{\hbar}\left[p_i(0) + Cx_j(0) - \frac{F_i(\omega + C)}{\omega^2 - \omega_i^2}\delta_{i2}\right] \tag{3.43}$$

for the both circularly and elliptically polarized fields. $\alpha_i(t)$ can be found from $\alpha_i \exp(-\mathrm{i}\Omega_i t)$.

Thus, the coherent states constructed by the equation (3.33) may serve as the exact quantum-mechanical counterpart of a classical cranked harmonic oscillator [62]. Coherent states are known to the minimum uncertainty states for the ordinary harmonic oscillator. In the $(\chi_1\chi_2)$ coordinate representation, the uncertainty is evidently minimal:

$$\Delta\chi_i\Delta\mathcal{P}_i = \frac{\hbar}{2} \tag{3.44}$$

However, at the initial coordinates system (x_1x_2 coordinates), the uncertainty is given by

$$\Delta x_i \Delta p_i = \frac{\hbar}{2}\left(1+\delta^2\right)^{1/2} \tag{3.45}$$

where

$$\delta = \frac{\hbar AB}{b_1 b_2} + \frac{Cb_1 b_2}{\hbar} \tag{3.46}$$

for both cases. Since $\delta^2 \geqslant 0$, these coherent states do not retain the minimum uncertainty product at the unprimed coordinates unless $\delta = 0$. The condition for minimum uncertainty corresponds to $\omega \to 0$. The minimum uncertainty, however, is not a unique definition for the coherent states as mentioned earlier, and the coherent states are nondispersive states. This is simply shown by $d(\Delta x_i)/dt$ =0.

Another aspect of coherent states can be seen by investigating the classical behavior, describing the coherent states in their coordinates representation.

$$\psi_{\alpha_1\alpha_2}(x_1,x_2)=\int_{-\infty}^{\infty}\int_{-\infty}^{\infty}d\chi_1 d\chi_2 \cdot < x_1x_2|\chi_1\chi_2 >< \chi_1\chi_2|\alpha_1\alpha_2 > \tag{3.47}$$

$\phi_{\alpha_1\alpha_2}(\chi_1,\chi_2)=\langle\chi_1\chi_2|\alpha_1\alpha_2\rangle$ is a wave function in the $(\chi_1\chi_2)$ coordinate representation , which is

$$\begin{aligned}\phi_{\alpha_1\alpha_2}(\chi_1,\chi_2)=\prod_{k=1,2}\exp\left(-\frac{|\alpha_k|^2}{4b_k^2}\right)\sum_{n=0}^{\infty}\left(\frac{\alpha_k}{\sqrt{2}b_k}\right)^{n_k}\\ \cdot\frac{1}{\sqrt{n!}}\exp\left(-\mathrm{i}\Omega_k(n+1/2)t\right)\phi_n(\chi_k)\end{aligned} \tag{3.48}$$

where $\phi_n(\chi_k)$ is the well-known eigenfunction of a one-dimensional harmonic oscillator. Using the expression of the eigenfunction, $\phi_{\alpha_1\alpha_2}(\chi_1,\chi_2)$ can be written as

$$\begin{aligned}\phi_{\alpha_1\alpha_2}(\chi_1,\chi_2)=\prod_{k=1,2}\frac{1}{\pi^{1/4}\sqrt{b_k}}e^{-\mathrm{i}\Omega_k t/2}\\ \cdot\exp\left\{-\frac{1}{2b_k^2}\left(\chi_k^2-2\alpha_k(t)\chi_k+\alpha_k^R(t)\alpha_k(t)\right)\right\}.\end{aligned} \tag{3.49}$$

The generating formula for Hermite polynomials was used to drive above equation.

$$e^{-s^2+2sx}=\sum_{n=0}^{\infty}\frac{s^n}{n!}H_n(x) \tag{3.50}$$

where $H_n(x)$ are Hermite polynomials.

The integral kernel $\phi_{\chi_1\chi_2}(x_1x_2)$=$\langle x_1x_2|\chi_1\chi_2\rangle$ from the equation (3.47) is a simultaneous eigenfunction of the operator x_1 and x_2 in the (χ_1,χ_2) representation. Analogously, because of the hermitian metric of the probability amplitudes its complex conjugate is the eigenfunction of the operators χ_1,χ_2 in the (x_1,x_2) representation. Exploiting these properties, $\phi_{\chi_1\chi_2}(x_1x_2)$ can be obtained. From the transformation relations (2.36) and (3.17), the following relations can be derived:

$$\begin{aligned}\hat{p}_j\phi &\backsim \frac{1}{B}\left(\chi_i-Ax_i\right)\phi\\ \hat{\mathcal{P}}_j\phi^* &\backsim \frac{1}{B}\left(\chi_i-x_i\right)\phi^*\end{aligned} \tag{3.51}$$

where $\hat{p}_j$, $\hat{\mathcal{P}}_j$ are momentum operators and ϕ, ϕ^* are eigenfunctions in the $(\chi_1\chi_2)$, (x_1x_2) representations respectively. It leads to

$$\phi_{\chi_1\chi_2}(x_1x_2) = N_0 \exp\left\{\frac{\mathrm{i}}{\hbar B}\left(-Ax_1x_2 + \chi_1x_2 + x_1\chi_2 - \chi_1\chi_2\right)\right\}. \tag{3.52}$$

N_0 is chosen such that $\psi_{\alpha_1\alpha_2}(x_1, x_2)$ is unitary:

$$N_0 = \frac{1}{2\pi\hbar|B|}.$$

Inserting equations (3.49) and (3.52) into the equation (3.47), and performing integrations gives

$$\begin{aligned}\psi_{\alpha_1\alpha_2}(x_1x_2) &= Ne^{-\frac{\mathrm{i}}{2}(\Omega_1+\Omega_2)t} \\ &\quad \cdot \exp\left(-\gamma_1^2x_1^2 - \gamma_2^2x_2^2 + \delta_1x_1 + \delta_2x_2 + \eta x_1x_2 + \zeta\right)\end{aligned} \tag{3.53}$$

where the parameters are

$$\begin{aligned}\gamma_i^2 &= \frac{D}{2b_i^2} \\ \delta_i &= \frac{D}{b_i^2}\left(\alpha_i(t) + \frac{\mathrm{i}\hbar B\alpha_j(t)}{b_j^2}\right) \quad i,j = 1,2(j \neq i) \\ \zeta &= \frac{\hbar BD}{b_1^2b_2^2}\left[\frac{\hbar B}{2}\left(\frac{\alpha_1^2(t)}{b_1^2} + \frac{\alpha_2^2}{b_2^2}\right) - \mathrm{i}\alpha_1(t)\alpha_2(t)\right] \\ \eta &= -\frac{\mathrm{i}}{\hbar B}(A - D) \\ D &= \frac{1}{1 + \hbar^2B^2/b_1^2b_2^2}.\end{aligned} \tag{3.54}$$

N is a normalization constant of the wave function:

$$N = \left(\frac{D}{\pi b_1b_2}\right)^{1/2} \prod_{i=1,2} \exp\left(-\frac{\alpha_i^R(t)\alpha_i(t)}{2b_i^2}\right).$$

From equations (3.52) and (3.53), χ_i or x_i can be replaced by one of following relations to obtain the wave function $\psi_{\alpha_1\alpha_2}$ for each field:

$$\begin{aligned}\chi_i &\rightarrow \chi_i - \frac{d_i}{m_i\Omega_i^2} \quad \text{(for constant dipole field)} \\ x_i &\rightarrow x_i - f_i(t) \quad \text{(for polarized fields).}\end{aligned} \tag{3.55}$$

After the replacement, the probability density, modulus squared of the wave function $\psi_{\alpha_1\alpha_2}(x_1x_2)$, can be brought to the form

$$|\psi_{\alpha_1\alpha_2}(x_1x_2)|^2 = \mathcal{N}^2 \prod_{i=1,2} \exp\left\{-\frac{D}{b_i^2}(x_i - x_{ci}(t))^2\right\} \tag{3.56}$$

where

$$\mathcal{N}^2 = \left|\frac{D}{\pi b_1 b_2}\right| \tag{3.57}$$

and $x_{ci}(t)$ $(i = 1, 2)$ indicates classical trajectory given by equations (3.19) or (3.28) for each cases. The probability density is a Gaussian probability distribution whose center follows the classical trajectory for the cranked oscillator in the x_1x_2 plane. This supports the fact that $\psi_{\alpha_1\alpha_2}$ is really a coherent state for this system.

3.4 Conclusions

This chapter showed that the non-spreading wave packets could be controlled using external dipole fields while remaining nonspreading. The behavior of cranked oscillator coherent states in a dipole field was presented also. We found that they indeed could move in a way prescribed by the dipole field.

The properties in the external field configuration were investigated by Glauber-type coherent states. The coherent states constructed here for the different external fields, constant dipole field and polarized microwave field, both do not satisfy the minimum uncertainty relation unless $\omega \to 0$. However, the states show minimum uncertainty at the transformed coordinates, and they are nondispersive states. The probability densities of both cases follow their own classical trajectory in the x_1x_2 plane without spreading in time with a Gaussian distribution given by

$$|\psi_{\alpha_1\alpha_2}(x_1x_2)|^2 = \mathcal{N}^2 \prod_{i=1,2} \exp\left\{-\frac{D}{b_i^2}(x_i - x_{ci}(t))^2\right\},$$

where $x_{ci}(t)$ is the classical trajectories given by the eq. (3.19) and (3.28) for the time independent couplings and time depent couplings, respectively. Thus, the constructed

coherent states have the behavior expected of coherent state for the systems. This expression points the way to constructing nondispersive states in a system which is strongly cranked.

CHAPTER IV

INTEGRABILITY OF THE GUIDING CENTER PROBLEM

4.1 Introduction

In the previous chapter, the cranked harmonic oscillator was derived by a Taylor expansion of the potential or ZVS at an equilibrium point. It was then shown that the coherent states can be constructed for the cranked harmonic oscillator with the dipole couplings whether they are time independent or not through the previous chapter.

However, the $electron - ion$ pair, which is introduced in this chapter, can not be separated into kinetic energy and potential nor ZVS easily. It needs to be manipulated into a separable form. To investigate the possibility of separation of the system, we place the system in a strong magnetic field, which will lead to "guiding center" approximation [111, 112], and thereby reduce the Hamiltonian in dimensionality. The Lorentz force experienced by a charged particle moving in a magnetic field causes it to gyrate about an axis parallel to the local magnetic field while the center of gyration, or guiding center, undergoes various drifts. The guiding center (drift) approximation applies when the gyration radius is much smaller than the scale length of any field inhomogeneity and the gyro-frequency is much higher than any characteristic field frequency. In this approach the helical trajectory of the particle in a magnetic field is approximated by a smooth drift motion. The first two sections are devoted to find the constants of motion and test the integrability of the system under the guiding center approximation. The dynamics of the system will also be studied. The coherent state will be constructed after testing the possibility of a potential minimum in the

reduced Hamiltonian.

There has been a great deal of work on the *electron-ion* system in a strong magnetic field [112, 113, 114]. The motion of N interacting particles (in the applied external field) can be factored into the Hamiltonian with the center of mass (CM), which will be used as a fixed frame, and remaining part that describes the motion with respect to the center of mass. The separation of the CM is sufficiently useful. The Hamiltonians with the removed center of mass are easier to analyze because the potential interaction is, in many cases, a relatively compact perturbation. For example, the absorption and emission spectrum is the spectrum of the Hamiltonian with the CM removed [115] and so is more natural. However, a difficulty is that a true separation of the center of mass motion and the internal motion is rigorouly not possible. Avron, Herbst and Simon [115] found an effective separation by introducing the transverse pseudomomentum and showing that it is a constant of motion. This effective separation was applied to the hydrogen atom [53] and positronium [116] reducing them to a one-body problem. In the case of a system in magnetic field, the vector potential is fixed only up to gauge transformations. This arbitrariness enables a realization of the translation invariance of the physics in constant magnetic field, as an invariance of the Hamiltonian under a "translation group". The classical Hamiltonian, being a function of velocity and coordinate difference is invariant under the phase space translation g_α [117],

$$g_\alpha[x,p] = \left(x+\alpha, p+\frac{q}{2c}\boldsymbol{B}\times\alpha\right).$$

More precisely, consider N particles in constant magnetic field with a translation invariant potential interaction. The kinetic energy is translated with $mv{=}p-qA/c$.

The applied homogeneous magnetic field leads to a constant of motion, the pseudomomentum, which was recognized by Johnson and Lippmann [118]. It is the natural analog of the momentum for the Laplacian. In general, the constant of motion is defined when interacting particles with translation are in invariant interaction. There are three ways of looking at this constant of motion: The center of the Landau orbit

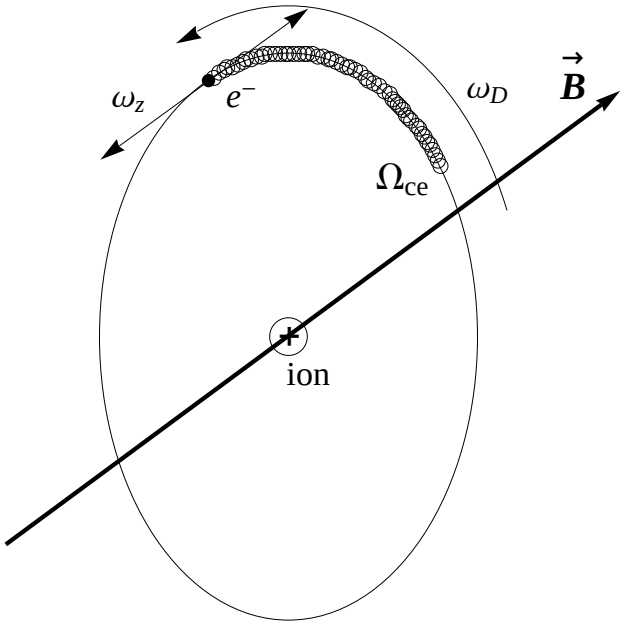

Figure 7: A circular guiding center *electron-ion* pair. The electron executes cyclotron motion with frequency Ω_{ce} and oscillates with frequency ω_z. ω_D is the frequency of $\mathbf{E}\times\mathbf{B}$ drifts [113].

(the so-called "guiding center") [118]; the generator of skewed phase space translations [117], and a pair of creation-destruction operators. In this chapter we are more interested in the guiding center motion. The elimination of a degree of freedom makes the system more accessible. The weakly bound electron-ion pair (ion with positive charge) in a strong magnetic field also will be treated by reducing the degrees of freedom through this chapter. More properly, these weakly bound and strongly magnetized systems should be referred to as guiding center drift atoms [112]. Figure 7 is a drawing of a guiding center drift atom.

The guiding center electron oscillates back and forth along the magnetic field in the Coulomb well of the ion, and more slowly $\mathbf{E}\times\mathbf{B}$ drifts around the ion. The magnetic field is sufficiently strong that the cyclotron frequency for the electron is sufficiently large and the cyclotron radius is sufficiently small that the electron dynamics can be treated by the guiding center drift theory. Thus the electron-cyclotron motion can

be averaged over a complete cycle and removed. The type of motion executed by the *electron-ion* system depends on the relative size of various dimensionless parameters. In a particularly simple limit, the guiding center for the electron oscillates back and forth, as mentioned above, *i.e.*, the pair moves across the magnetic field with the initial ion velocity like a neutral atom. In another limit, the election and ion $\mathbf{E}\times\mathbf{B}$ drift together across the magnetic field. In a third limit, the electron executes a large cyclotron orbit in the vicinity of the ion, which is effectively pinned to the magnetic field. These limits might produce restrictions in the dynamics resulting in reduction of degrees of freedom by proper approximations. To find the integrable system, constants of motion by action angle variables will be searched and then the dynamics will be investigated.

This chapter will analyze and classify the possible motions.

4.2 The Motion in a Magnetic Field and Constants of Motion

When a uniform magnetic field along $\hat{z}$-direction like $\boldsymbol{B} = B\,\hat{z}$, the vector potential of the field is defined by $\boldsymbol{A}$. Consider a specific case of the vector potential, $\boldsymbol{A} = Bx\,\hat{y}$ which has only a component along y-direction. All of vector quantities will be illustrated bold faced letter through this chapter. The external electric field is chosen to be zero, however, the electron-ion pair interact electrostatically and moves in the uniform magnetic field. If the separation between two particle is large enough, there is no governing force but magnetic field. If not, the resulting motion of a particle is governed by external magnetic field, end the electrostatic force by the ion. In general, In the magnetic field, a charged particle oscillates back and forth along the magnetic field in the Coulomb well of the ion and the equations of motion of an individual particle with mass m and charge q in electromagnetic fields $\boldsymbol{E}(\boldsymbol{r},t)$ and $\boldsymbol{B}(\boldsymbol{r},t)$, take

the form

$$\begin{aligned} \dot{\boldsymbol{r}} &= \boldsymbol{v} \\ m\,\dot{\boldsymbol{v}} &= \frac{q}{c}(\boldsymbol{v}\times\boldsymbol{B}) + q\boldsymbol{E}. \end{aligned} \tag{4.1}$$

In case of an electron, for clear definition, the charge q is equal to $-e$. The next section deals with the motion by separating the each vectors into two parts, parallel or perpendicular to the magnetic field. This is a good way to investigate the motion along or transverse to the field.

4.2.1 Motion of a Charged Particle in a Magnetic Field

The parallel component of the equation (4.1) can be represented by

$$\frac{\mathrm{d}v_{\parallel}}{\mathrm{d}t} = \frac{q}{m}\,E_{\parallel}, \tag{4.2}$$

which predicts uniform acceleration along magnetic field lines. No external electric field results in vanishing of $E_{\parallel}$, hereby,

$$v_{\parallel} = const. \tag{4.3}$$

So, the velocity parallel to the magnetic field keeps constant speed. When it is zero, the motion happens in a transverse plane, otherwise, the orbit in the transverse plane moves with constant speed along the field direction so the trajectory is a helix. The primary effect of a magnetic field is to cause the plane of the orbit of a electron to precess with a cyclotron frequency defined by

$$\Omega_{ce} = \frac{|q|B}{mc}. \tag{4.4}$$

Thus, it shows that only the transverse component interacts with $\boldsymbol{B}$, leading to a circular motion perpendicular to the $\boldsymbol{B}$. Because the Lorentz force is always perpendicular to the velocity and thus changes only its direction, but not its magnitude, the

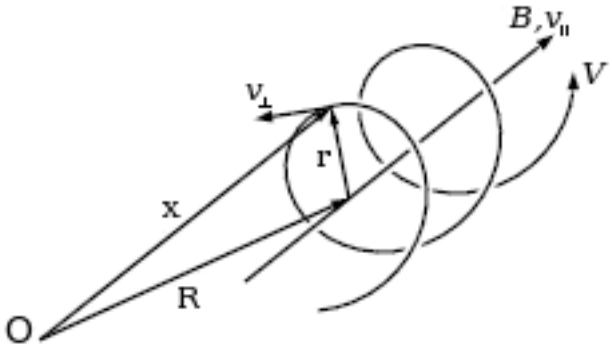

Figure 8: Guiding center coordinates and directions of the velocity vector [119].

kinetic energy of the electron remains constant resulting in reduction of the degree of freedom of the system. The velocity of the guiding center can be obtained by differentiating the guiding center position $\boldsymbol{R}$ shown in Figure 8. The figure also shows the schematic position of a guiding center $\boldsymbol{R}$, electron position $\boldsymbol{x}$ and a rotating gyration radius vector $\boldsymbol{r}$.

The particle trajectory is a helix around the guiding center magnetic field line. The electron position $\boldsymbol{x}$ can be decomposed into the guiding center position that moves with velocity $v_\parallel \hat{z}$, and the rotating gyration radius vector. The magnitude of a gyration radius r can be calculated from the fact that the centrifugal force balances the Lorentz force as follows:

$$\boldsymbol{r} = -\frac{mc}{qB^2}\boldsymbol{v} \times \boldsymbol{B}. \tag{4.5}$$

or $r = mcv_\perp/|q|B$ for the vertical part of the velocity. Using the following relations

$$(\boldsymbol{v} \times \boldsymbol{B}) \times \boldsymbol{B} = -\boldsymbol{v}_\perp B^2$$

$$\boldsymbol{v} - \boldsymbol{v}_\perp = v_\parallel \hat{z},$$

the velocity of the guiding center $\boldsymbol{v}_g$ can be obtained using eq. (4.1) [119],

$$\begin{aligned} \boldsymbol{v}_g \equiv \dot{\boldsymbol{R}} &= \dot{\boldsymbol{x}} - \dot{\boldsymbol{r}} \\ &= \boldsymbol{v} + \frac{mc}{qB^2}\dot{\boldsymbol{v}} \times \boldsymbol{B} \\ &= v_\parallel \hat{z} + \frac{c\,\boldsymbol{E} \times \boldsymbol{B}}{B^2}, \end{aligned} \tag{4.6}$$

thereby, the $\mathbf{E}\times\mathbf{B}$ drift velocity $\boldsymbol{v}_D$ is given by

$$\boldsymbol{v}_D = \frac{c\,\boldsymbol{E}\times\boldsymbol{B}}{B^2}. \tag{4.7}$$

Above equation (4.7) shows that the velocity is independent of the particle mass, type of charge. Since the electric force is in opposite directions for the electron and ion, the drift velocity does not depend on the sign of the charges or sort of particles. Therefore, they form a so-called "drifting pair"[113]. The drifting pair of the guiding center happens for the special case where the effective electric field vanishes. During the drifting motion, the electron executes very rapid cyclotron motion with a small cyclotron radius. More slowly, the ion oscillates back and forth along the magnetic field in the Coulomb well of the electron. In this limit, the pair flows in a group like a neutral atom with same velocity and there is no net current as a result of the motion.

4.2.2 The Classical Hamiltonian

When analyzing charged particle motion in uniform (or non-uniform) electromagnetic fields, somehow, it is possible to neglect the rapid, and relatively uninteresting, gyromotion, and focus, instead, on the far slower motion of the guiding center. The effect of spin will be neglected since the magnetic field is uniform and the spin-field interaction does not couple the spin and orbital dynamics [114]. The usual spin-orbit interaction, which is smaller than the electrostatic interaction by order $(v/c)^2$, is very small for the small binding energies and small velocities. In order to achieve this goal, averaging the equation of motion over gyrophase is useful to obtain a reduced equation of motion for the guiding center. Following the concept, this section will show the construction of a Hamiltonian for the guiding center model, and describe how to eliminate some degree of freedom from the Hamiltonian.

The Lagrangian for this system can be written as

$$L = \frac{m_i}{2}(\dot{x}_i^2 + \dot{y}_i^2 + \dot{z}_i^2) + \frac{m_e}{2}(\dot{x}_e^2 + \dot{y}_e^2 + \dot{z}_e^2) + \frac{eB}{c}x_i\dot{y}_i - \frac{eB}{c}x_e\dot{y}_e - V_{int} \tag{4.8}$$

where i, e indicate *ion* and *electron*, respectively. V_{int} is the interaction potential between two particles given by

$$V_{int} = -\frac{e^2}{\sqrt{(x_i - x_e)^2 + (y_i - y_e)^2 + (z_i - z_e)^2}}. \tag{4.9}$$

The Hamiltonian can be obtained from the generalized momentum associated with the coordinates q_k:

$$H = \sum p_k \dot{q}_k - L(q_k, \dot{q}_k), \tag{4.10}$$

with

$$p_k = \frac{\partial L}{\partial \dot{q}_k}. \tag{4.11}$$

This leads to

$$H = \frac{1}{2m_i}(\boldsymbol{p}_i - \frac{eB}{c}\boldsymbol{A}_i)^2 + \frac{1}{2m_i}(\boldsymbol{p}_e + \frac{eB}{c}\boldsymbol{A}_e)^2 + V_{int}, \tag{4.12}$$

where the vector potentials are chosen to be in the static symmetric gauge,

$$\boldsymbol{A} = \frac{1}{2}\boldsymbol{B} \times \boldsymbol{r}. \tag{4.13}$$

At first, consider the motion of the electron. Because of the rapid gyromotion (the gyration due to the Lorentz force) of the electron which direction is perpendicular to the uniform magnetic field, the cyclotron frequency Ω_{ce} is much larger than the drift frequency ω_D and the cyclotron frequency is constant. The action variable conjugate to the cyclotron frequency can be calculated using the transformation of action-angle variable. The kinetic energy of the electron can be separated into two parts which are transverse or parallel to the magnetic field,

$$T = T_\perp + T_\parallel. \tag{4.14}$$

Here, rewrite the transverse component of the kinetic energy of electron as follows:

$$T_\perp = \frac{p_{xe}^2}{2m_e} + \frac{1}{2}\Omega_{ce}\left(\frac{c}{eB}p_{ye} + x_e\right)^2 \tag{4.15}$$

where the cyclotron frequency is defined by

$$\Omega_{c\,e} = \frac{eB}{m_e c}. \tag{4.16}$$

Consider the following canonical transformations,

$$\begin{aligned} x_e &= \sqrt{\frac{2I_{ce}}{m_e\Omega_{ce}}}\sin\varphi_{ce} - \frac{c}{eB}p_{ye} \\ p_{xe} &= \sqrt{2m_e\Omega_{c\,e}I_{c\,e}}\cos\varphi_{ce}. \end{aligned} \tag{4.17}$$

These transform the kinetic energy $T_\perp$ into

$$T_\perp = I_{ce}\Omega_{ce}, \tag{4.18}$$

where I_{ce} is a cyclotron action. Since I_{ce} is a good adiabatic invariant and Ω_{ce} is constant (for a uniform magnetic field), the product $I_{ce}\Omega_{ce}$ is constant and does not influence the dynamics of the remaining variables. Thus the new Hamiltonian can be written as

$$H = I_{ce}\Omega_{ce} + \frac{p_{ze}^2}{2m_e} + \frac{1}{2m_i}\left(\boldsymbol{p}_i - \frac{e}{c}\boldsymbol{A}_i\right)^2 + V_{int} \tag{4.19}$$

with

$$V_{int} = -\frac{e^2}{\sqrt{\left(x_i + \frac{c}{eB}p_{ye} - \sqrt{\frac{2I_{ce}}{m_e\Omega_{ce}}}\sin\varphi_{ce}\right)^2 + (y_i - y_e)^2 + (z_i - z_e)^2}}. \tag{4.20}$$

As mentioned earlier, the rapid cyclotron motion can be averaged out in the limit of which the electron cyclotron frequency is the largest of the dynamical frequencies and the cyclotron radius is the smallest of the length scales. The next step is to expand the Hamiltonian with respect to $\sin\varphi_{ce}$. Averaging will be performed by integrating the Hamiltonian over the complete cycle of φ_{ce}. The integration produces zero for odd functions and nonzero correction terms for even functions but higher order correction terms are negligible. Thus the Hamiltonian is given by

$$\begin{aligned} H = I_{ce}\Omega_{ce} + \frac{p_{ze}^2}{2m_e} &+ \frac{1}{2m_i}\left(\boldsymbol{p}_i - \frac{e}{c}\boldsymbol{A}_i\right)^2 \\ &- \frac{e^2}{\sqrt{\left(x_i + \frac{c}{eB}p_{ye}\right)^2 + (y_i - y_e)^2 + (z_i - z_e)^2}}. \end{aligned} \tag{4.21}$$

This Hamiltonian can be derived more simply from the limit of the largest Ω_{ce} and the smallest cyclotron radius. Because the electronic motion influences the Hamiltonian dynamics only along z-axis, the constant $I_{ce}\Omega_{ce}$ does not influence the dynamics. The mechanical momentum of eq. (4.12) can be expressed by

$$m\dot{\boldsymbol{r}} = \boldsymbol{p} - \frac{q}{c}\boldsymbol{A}. \tag{4.22}$$

For the choice of vector potential $\boldsymbol{A}_e = Bx_e\hat{y}$, the mechanical momentum of the electron has effective value for z-motion,

$$\boldsymbol{p}_e + \frac{e}{c}\boldsymbol{A}_e = (0,\, 0,\, p_{ze}). \tag{4.23}$$

Thus, the canonical momentum of the electron can be described by

$$\begin{aligned} p_{xe} &= 0 \\ p_{ye} &= -\frac{eB}{c}x_e \\ p_{ze} &= p_{ze}. \end{aligned} \tag{4.24}$$

p_{xe} is removed from the system and x_e can be replaced by p_y. The position of the electron in a transverse plane is specified by

$$(x_e,\, y_e) \rightarrow (-\frac{c}{eB}p_{ye},\, y_e). \tag{4.25}$$

Therefore, (x_e, p_{xe}) are eliminated from the dynamics and this elimination of the two degrees of freedom resulted from averaging out the rapid cyclotron motion and results in a more reduced form of the Hamiltonian (4.21).

4.2.3 The Pseudomomentum and Canonical Transformation

The previous section showed that the introduction of a cyclotron action I_{ce} and a action for the field aligned bounce motion effectively averaged the Hamiltonian over the rapid cyclotron and bounce motions, removing two degrees of freedom. However,

we need more constant of the motion for the Hamiltonian to be integrable. This section introduces the pseudomomentum, constants of motion in magnetic field, and gives the nonrelativistic treatment of particles kinematics in constant fields. Using the constants of motion to a canonical transformation gives more opportunities to make the system integrable in certain limits, weak binding and strong magnetic field. Furthermore, for this guiding center system, the description of center of mass (CM) motion makes it possible to separate the CM motion from the internal degree of freedom[120].

For a single particle of charge q and mass m in constant electric and magnetic field, there are three momentumlike vectors [68],

(1) The canonical momentum $\boldsymbol{p}$, all of whose components commute or have vanishing Poisson brackets,

(2) The mechanical momentum $\boldsymbol{\Pi}$:

$$\boldsymbol{\Pi} = \boldsymbol{p} - \frac{q}{c}\boldsymbol{A}, \tag{4.26}$$

(3) The pseudomomentum $\boldsymbol{K}$:

$$\boldsymbol{K} = \boldsymbol{\Pi} + \frac{q}{c}\boldsymbol{B} \times \boldsymbol{r} - q\boldsymbol{E}t. \tag{4.27}$$

where $\boldsymbol{A}$ and c are the vector potential and the speed of light, respectively, and q is the charge of a particle. The pseudomomentum $\boldsymbol{K}$ is a constant of motion in a uniform magnetic field. It can found by taking time derivative of the mechanical momentum. For a constant magnetic field, the time derivative of $\boldsymbol{\Pi}$ is given by

$$\begin{aligned} \dot{\boldsymbol{\Pi}} &= \dot{\boldsymbol{p}} - \frac{q}{2c}\boldsymbol{B} \times \dot{\boldsymbol{r}} \\ &= \dot{\boldsymbol{p}} - \frac{1}{2}(q\boldsymbol{E} - m\ddot{\boldsymbol{r}}) \\ &= \dot{\boldsymbol{p}} - \frac{1}{2}(q\boldsymbol{E} - \dot{\boldsymbol{\Pi}}), \end{aligned} \tag{4.28}$$

and, it can be rearranged as follow

$$\frac{\mathrm{d}}{\mathrm{d}t}\boldsymbol{K} = \frac{\mathrm{d}}{\mathrm{d}t}\left(-\boldsymbol{\Pi} + 2\boldsymbol{p} - q\boldsymbol{E}t\right) = 0. \tag{4.29}$$

where

$$\begin{aligned} \boldsymbol{K} &= -\boldsymbol{\Pi} + 2\boldsymbol{p} - q\boldsymbol{E}t \\ &= \boldsymbol{\Pi} + \frac{q}{c}\boldsymbol{B} \times \boldsymbol{r} - q\boldsymbol{E}t. \end{aligned} \tag{4.30}$$

The vector constant of the motion, $\boldsymbol{K}$, is called the pseudomomentum. The pseudomomentum was derived for $E = 0$ by Johnson and Lippmann[118]. They described the pseudomomentum and its significance when only a magnetic field is present. Not all of the components of $\boldsymbol{\Pi}$, nor those of $\boldsymbol{K}$, commute with each other (unless $q = 0$ or $B = 0$). Later, the momentum was applied for combined fields by Bacry [121, 122].

For the *electron-ion* system, (1) total canonical momentum is the momentum conjugate to the center of mass and (2) the total mechanical momentum represents the total mass times the CM velocity, and (3) the total pseudomomentum is a constant of the motion which is important in separating the center of mass and internal degrees of freedom. Whether or not an electric field is present, it is possible to eliminate (at least some of the) CM degrees of freedom by diagonalizing components of the total pseudomomentum ([123]-[130]). Thus, this pseudomomentum will be very useful in reducing the internal degree of freedom from the system.

Consider the guiding center atom in a strong magnetic field along z-direction. The pseudomomentum will be considered in zero external electric field. Total pseudomomentum is given by $\boldsymbol{K} = \boldsymbol{K}_i + \boldsymbol{K}_e$, where $\boldsymbol{K}_i$ and $\boldsymbol{K}_e$ are the pseudomomentum for ion and electron respectively:

$$\boldsymbol{K} = m_i\dot{\boldsymbol{r}}_i + m_e\dot{\boldsymbol{r}}_e - \frac{e}{c}\boldsymbol{B} \times \boldsymbol{r}, \tag{4.31}$$

where the last term, for the constant magnetic field along z-direction, can be expressed by

$$-\frac{e}{c}\boldsymbol{B} \times \boldsymbol{r} = -\frac{eB}{c}y\,\hat{x} + \frac{eB}{c}x\,\hat{y} \tag{4.32}$$

where $\boldsymbol{r}$ $(= \boldsymbol{r}_e - \boldsymbol{r}_i)$ is the relative coordinates between the electron and ion. Canonical

momenta for the ion and the electron are given by

$$p_{xi} = m_i \dot{x}_i, \quad p_{yi} = m_i \dot{y}_i + \frac{eB}{c} x_i, \quad p_{zi} = m_i \dot{z}_i, \tag{4.33}$$

for the ion, and

$$p_{xe} = 0, \quad p_{ye} = -\frac{eB}{c} x_e, \quad p_{ze} = p_{ze}, \tag{4.34}$$

for the electron. Now, the pseudomomentum can be represented by the canonical momenta and coordinates given above by inserting the relations into the equation (4.31). Two constants of motion (P_ξ, P_η) are derived. They are defined by

$$\begin{aligned} \boldsymbol{K} &\equiv P_\xi \, \hat{x} + P_\eta \, \hat{y} \\ &= (p_{xi} + \frac{eB}{c} y) \, \hat{x} + (p_{yi} + p_{ye}) \, \hat{y}. \end{aligned} \tag{4.35}$$

where $y = y_e - y_i$.

Another constant of motion can be found from the motion along the field direction (z-direction), which is independent of other canonical variables perpendicular to the field, and it can be expressed by the motion of center of mass and reduced mass. The Hamiltonian is given by

$$H_{cm} = \frac{P_\zeta^2}{2M} + \frac{p_z^2}{2\mu}, \tag{4.36}$$

where

$$\begin{aligned} M &= m_i + m_e, \qquad \mu = \frac{m_i \, m_e}{m_i + m_e} \\ P_\zeta &= p_{zi} + p_{ze}, \qquad \zeta = \frac{m_i z_i + m_e z_e}{m_i + m_e} \\ p_z &= \frac{m_i p_{ze} - m_e p_{zi}}{m_i + m_e}, \quad z = z_e - z_i. \end{aligned} \tag{4.37}$$

Canonical transformation using the these new constants of motion and relative coordinates can be found as follows [113]:

$$\begin{aligned} P_\xi &= p_{xi} + \frac{eB}{c} y, \quad \xi = \frac{c}{eB}(p_{yi} + p_{ye}) + x_i \\ P_\eta &= p_{yi} + p_{ye}, \qquad \eta = \frac{c}{eB} p_{xi} + y_e \\ P_\zeta &= p_{zi} + p_{ze}, \qquad \zeta = \frac{m_i z_i + m_e z_e}{m_i + m_e}, \end{aligned} \tag{4.38}$$

and

$$\begin{aligned} p_y &= p_{ye} + \frac{eB}{c}x_i, \qquad & y &= y_e - y_i \\ p_z &= \frac{m_i p_{ze} - m_e p_{zi}}{m_i + m_e}, \qquad & z &= z_e - z_i. \end{aligned} \tag{4.39}$$

Classically, this is a canonical transformation, as can be verified by observing that the Poisson brackets for the new coordinates and momenta have the canonical value of unity. The transformed Hamiltonian will be a function of newly defined canonical variables such as pseudomomentum, relative coordinates and their conjugate momenta:

$$H = H(P_\xi, P_\eta, P_\zeta, p_y, p_z, y, z). \tag{4.40}$$

With the new canonical variables, the transformed Hamiltonian is given by

$$\begin{aligned} H &= I_{ce}\Omega_{ce} + \frac{1}{2m_i}\left(P_\xi - \frac{eB}{c}y\right)^2 + \frac{1}{2m_i}\left(P_\eta - p_y\right)^2 + \frac{P_\zeta^2}{2M} + \frac{p_z^2}{2\mu} \\ &\quad - \frac{e^2}{\sqrt{\left(\frac{c}{eB}p_y\right)^2 + y^2 + z^2}} \end{aligned} \tag{4.41}$$

where P_ξ and P_η are pseudomomentum. In summary, new canonical variables and constants of motion are

$$\begin{aligned} Canonical\ Variables &: P_\xi,\ P_\eta,\ P_\zeta,\ p_y,\ p_z,\ y,\ z, \\ Constants\ of\ motion &: I_{ce},\ P_\xi,\ P_\eta,\ P_\zeta. \end{aligned} \tag{4.42}$$

4.3 Integrability of the Hamiltonian in the Limit of the Guiding Center Motion

Action-angle variables have been generally used to find the constants of motion. Not only do they reduces the degrees of freedom, but make it also possible to discuss the atomic dynamics as a function of the constants of motion. In addition, constants of motion provide simplified equations of motion, thereby, analytic solutions are possible

in some cases. Analytic solutions are not always possible, however, action-angle variables lead to more compact form of the Hamiltonian and allow easy analysis of the system. The constant of motion can also be found by other ways (like the pseudomomentum in a specific condition presented at previous section).

The scaled Hamiltonian (4.47) has only one constant of motion, P_η. Obtaining and solving the equations of motion are important part of the analysis of the guiding center atom. Solving them, in general, is a question of integration. A system of n degree of freedom will have n differential equations that are second order in time. The solution of each equation will require two integrations resulting in $2n$ constants of integration. In a specific case, these constants will be determined by the initial conditions. However, majority of problems are not completely integrable. Even when complete solutions cannot be obtained, it is often possible to extract a large amount of information of the system motion. Finding the constant of motion is related to the conservation of a quantity and it leads to more compact equations of motion. Thus, the constants of motion are important to determine the integrability of the Hamiltonian.

4.3.1 Scaling

Working in the center of mass coordinates, the motion along ζ-axis will be ignored, and its conjugate momentum P_ζ will be zero. It is possible without losing generality to put $P_\xi = 0$, also, by orienting the coordinates so that P_ξ is zero. This will be done simultaneously as we choose the orientation at the CM frame. Thus the Hamiltonian is given by

$$H = I_{ce}\Omega_{ce} + \frac{1}{2m_i}\left(\frac{eB}{c}y\right)^2 + \frac{1}{2m_i}\left(P_\eta - p_y\right)^2 + \frac{p_z^2}{2\mu} - \frac{e^2}{\sqrt{\left(\frac{c}{eB}p_y\right)^2 + y^2 + z^2}} \quad (4.43)$$

Using scaled value eliminates the need for carrying along undesirable constants or makes numerical constants amenable to numerical calculation. Scaling of the

Hamiltonian (4.43) is done as follows:

$$\begin{aligned}
&\text{scaled time } \rightarrow \frac{m_i c}{eB} \simeq 2.58610 \times 10^{-9}\, sec \\
&\text{scaled length } \rightarrow \left(\frac{m_i c^2}{B^2}\right)^{1/3} \simeq 9.75774 \times 10^{-7}\, m \\
&\text{scaled mass } \rightarrow m_i \simeq 1.66054 \times 10^{-27}\, kg.
\end{aligned} \tag{4.44}$$

where the charge uses a unit of "statcoulomb", "Gauss" for the magnetic field and "gram" for the mass. The magnetic field used is 40081.4 Gauss. Replacing the initial coordinates and momenta using scaled variables given by

$$\begin{aligned}
y \rightarrow y' \left(\frac{m_i c^2}{B^2}\right)^{1/3}, \qquad & p_y \rightarrow p'_y \left(\frac{e^3 m_i B}{c}\right)^{1/3} \\
z \rightarrow z' \left(\frac{m_i c^2}{B^2}\right)^{1/3}, \qquad & p_z \rightarrow p'_z \left(\frac{e^3 m_i B}{c}\right)^{1/3} \\
P_\eta \rightarrow P'_\eta \left(\frac{e^3 m_i B}{c}\right)^{1/3}, &
\end{aligned} \tag{4.45}$$

for the coordinates and momenta, and

$$\begin{aligned}
&\mu \rightarrow \mu' m_i \\
&I_{ce} \rightarrow I'_{ce} e^2 \left(\frac{B^2}{m_i c^2}\right)^{1/3} \\
&H \rightarrow H' e^2 \left(\frac{B^2}{m_i c^2}\right)^{1/3},
\end{aligned} \tag{4.46}$$

for the reduced mass, constant of motion and energy. Therefore, the Hamiltonian (4.43) can be rewritten (after dropping the primes)

$$H = \nu I_{ce} + \frac{1}{2}(P_\eta - p_y)^2 + \frac{1}{2}y^2 + \frac{1}{2\mu_e}p_z^2 - \frac{1}{\sqrt{p_y^2 + y^2 + z^2}} \tag{4.47}$$

where ν is a mass ratio (m_i/m_e) and $\mu_e = m_e/M$. For large mass of M, $M \gg m_e$, μ_e can be approximated m_e/m_i. Scaled Hamiltonian (4.47) can be separated into three different motions:

$$H = H_{ce} + H_y + H_z. \tag{4.48}$$

where, the first term H_{ce} is the transverse motion of the electron represented by I_{ce}, the second Hamiltonian describes harmonic oscillation in y-motion, and the third term indicates the motion along field direction. In case of H_y, the momentum appears shifted by P_η. This harmonic oscillation can be reduced to a product of corresponding action and angle variables. The remaining z-motion, H_z, includes a momentum in its potential term leading to indistinct shape of the potential. In guiding center motion, however, the orbit of the transverse motion of a electron is a circular motion with radius r which is considered to be a constant.

The reduction of dimensionality for the guiding center Hamiltonian could be performed by the proper orientation of the frame of reference. Action-angle variable also are a useful tool to find constants of motion. Determination of the coordinates at the center of mass made possible to eliminate another degree of freedom, the pseudomomentum. The scaled Hamiltonian could be separated into three different parts describing the motion along y, z-direction and rapid gyromotion of the electron. Following sections describe details about each Hamiltonian at the center of mass frame.

4.3.2 Integrability of the System for $P_\eta = 0$

P_η is the only constant of motion in (4.47). The dynamics of the system will be investigated for both zero and non zero values. This section starts by letting $P_\eta = 0$. When the constant is zero, it provides a limitation of the motion such as onset of ionization. The following calculation will show the conditions for the onset of ionization. Moreover it gives a good basic form of Hamiltonian to investigate the system containing the nonzero pseudomomentum, $P_\eta \neq 0$. The Hamiltonian for $P_\eta = 0$ is given by

$$H_0 = \frac{1}{2}(p_y^2 + y^2) + \frac{1}{2\mu_e}p_z^2 - \frac{1}{\sqrt{p_y^2 + y^2 + z^2}}, \tag{4.49}$$

where the action from the rapid gyromotion of a electron, νI_{ce}, was eliminated because it did not affect the dynamics at all. The first term of (4.49) is the Hamiltonian of a harmonic oscillation of y-motion and the second term is about z-motion.

To find the constant of motion for the y-motion, consider equations of motion for y and p_y given by

$$\begin{aligned} \dot{p}_y &= -y - \frac{y}{(p_y^2 + y^2 + z^2)^{3/2}} \\ \dot{y} &= p_y + \frac{p_y}{(p_y^2 + y^2 + z^2)^{3/2}}. \end{aligned} \tag{4.50}$$

Adding two equations after multiplying another variable at each equation such as $y\dot{p}_y + p_y\dot{y}$, leads to

$$p_y^2 + y^2 = 2C \tag{4.51}$$

where C is a constant. An action variable with respect to y can be defined and calculated from a general expression:

$$I_y = \frac{1}{2\pi} \oint p_y dy, \tag{4.52}$$

which leads to $I_y = C$ and shows that I_y is also a constant. Thus, the action turns out to be

$$I_y = \frac{1}{2}(p_y^2 + y^2) = \textit{constant}, \tag{4.53}$$

One more degree of freedom can be eliminated by above relation and the Hamiltonian (4.49) can be described by

$$H_0(I_y, p_z, z) = \frac{1}{2\mu_e} p_z^2 + I_y - \frac{1}{\sqrt{2I_y + z^2}}, \tag{4.54}$$

and the effective potential of the Hamiltonian is given by

$$V_{I_y}(z) = I_y - \frac{1}{\sqrt{2I_y + z^2}}. \tag{4.55}$$

Figure (9) shows the shape of the potential for several values of I_y. The effective potential has its minimum at $z = 0$ and no maxima but it tends to a constant as z is

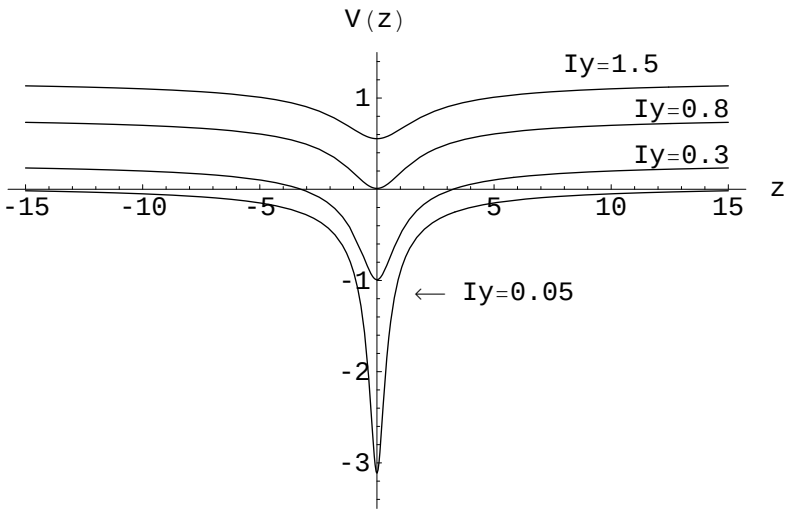

Figure 9: Graph of the potential $V_{I_y}(I_y, z)$ for $I_y = 0.05$, 0.3, 0.8 and 1.5 in scaled units.

becoming larger. The minimum of each potential is gradually shifting upward as the constant I_y increases.

A conjugate angle variable with respect to the action, I_y, will be found from following equations of motion:

$$\begin{aligned} \dot{\theta}_y &= \frac{\partial H}{\partial I_y} = 1 + \frac{1}{(2I_y + z^2)^{3/2}} \\ \dot{z} &= \frac{p_z}{\mu_e} \\ \dot{p}_z &= -\frac{z}{(2I_y + z^2)^{3/2}}. \end{aligned} \tag{4.56}$$

Instead of solving the equations of motion directly, consider the motion at a extremum and the shape of the equations. Details will be discussed following sections. The equation for the angle variable, θ_y, shows that $\dot{\theta}_y$ can not be zero, therefore the angle variable can not have any stationary point and there is no bound motion with respect to the frequency of the angle variable. Suppose $p_z = 0$ at a minimum point ($z = 0$).

The equations of motion are given by

$$\begin{aligned} z &= 0 \\ p_z &= 0 \\ \dot{\theta}_y &= 1 + \frac{1}{(2I_y)^{3/2}} \end{aligned} \tag{4.57}$$

At this time, the motion is stable and the energy is given by

$$H_0 = E_{I_y} = I_y - \frac{1}{\sqrt{2I_y}}. \tag{4.58}$$

If $p_z = 0$ as $z \to \infty$, the equations of motion are

$$\begin{aligned} p_z &= 0 \\ \dot{\theta}_y &= 1, \end{aligned} \tag{4.59}$$

the motion is also stable and the energy is given by

$$H_0 = E_{I_y} = V_{I_y} = I_y. \tag{4.60}$$

When $E_{I_y} = 0$, this is the onset of ionization because the larger z with $p_z = 0$ corresponds to a no interactive system, which is completely ionized. z was defined as the separation of the electron and ion along field direction at (4.37).

4.3.3 Integrability of the System for $P_\eta \neq 0$

The Hamiltonian for nonzero pseudomomentum in scaled unit is given by

$$H(P_\eta, p_y, p_z, y, z) = \frac{1}{2}\left[(P_\eta - p_y)^2 + y^2\right] + \frac{1}{2\mu_e}p_z^2 - \frac{1}{\sqrt{p_y^2 + y^2 + z^2}} \tag{4.61}$$

where $\mu_e = m_e/M$. When it is compared to the Hamiltonian (4.49), this Hamiltonian has a shifted momentum for its y-motion. An action and conjugate angle variable can be found from the general definitions. The following calculations are intended to find constants of motion and thereby make the system integrable.

The Hamiltonian can be separated into two parts, y-motion and z-motion as treated from the previous section. However, this section will consider the original expression for the Hamiltonian without separation. Equations of motion for the Hamiltonian are given by

$$\begin{aligned}
\dot{z} &= \frac{p_z}{\mu_e} \\
\dot{p_z} &= -\frac{z}{(p_y^2 + y^2 + z^2)^{3/2}} \\
\dot{y} &= -(P_\eta - p_y) + \frac{p_y}{(p_y^2 + y^2 + z^2)^{3/2}} \\
\dot{p}_y &= -y - \frac{y}{(p_y^2 + y^2 + z^2)^{3/2}}.
\end{aligned} \tag{4.62}$$

Consider the equations of motion about y and p_y. The exact treatment about z and p_z will be dealt with at following section. The derivatives of variables are performed with respect to the scaled time. The equations can be handled to produce following relation,

$$y\dot{y} + p_y\dot{p}_y = -P_\eta y. \tag{4.63}$$

This relation drives to solutions with trigonometric functions:

$$\begin{aligned}
y &= C\sin\theta_y \\
p_y &= P_\eta + C\cos\theta_y,
\end{aligned} \tag{4.64}$$

where the angle variable θ_y came from a solution for second order differential equation with respect to y or p_y. The constant C will be determined by defining a action variable I_y, and integrating the action after replacement by eq. (4.64). It should be notified that I_y can not be called a conjugate action about the angle θ_y and constant of motion at this time.

$$\begin{aligned}
I_y &= \oint p_y dy \\
&= \oint (C^2\cos^2\theta_y + CP_\eta\cos\theta_y)d\theta_y
\end{aligned} \tag{4.65}$$

results in

$$I_y = \frac{1}{2}C^2. \tag{4.66}$$

Thus, the I_y turns out to be a constant of motion. Conjugate angle variable can be found by a canonical transformation which transforms y and p_y into a angle variable and I_y, respectively. Suppose that the angle variable is θ_y. The relations (4.64) are canonical, which can be easily verified by checking the Poisson brackets are equal to unity. Transformation of the y-mode into harmonic oscillator action-angle variables can be done by rewriting the transformation in terms of θ_y and I_y as follows,

$$\begin{aligned} y &= \sqrt{2I_y}\sin\theta_y \\ p_y &= P_\eta + \sqrt{2I_y}\cos\theta_y. \end{aligned} \tag{4.67}$$

Using (4.64) and (4.66), the action variable can be written as

$$I_y = \frac{1}{2}\left((P_\eta - p_y)^2 + y^2\right). \tag{4.68}$$

The Hamiltonian of y-motion can be represented by the action I_y. θ_y can be derived from eq. (4.67) as

$$\theta_y = \tan^{-1}\left(\frac{y}{P_\eta - p_y}\right). \tag{4.69}$$

Thus, the Hamiltonian is described by

$$H(I_y, \theta_y, p_z, z) = I_y + \frac{1}{2\mu_e}p_z^2 - \frac{1}{\sqrt{2I_y + P_\eta^2 + z^2 + 2P_\eta\sqrt{2I_y}\cos\theta_y}}. \tag{4.70}$$

In the general case, the action I_y is not a constant of the motion as its conjugate angle θ_y appears in the Hamiltonian. To the contrary, the I_y is constant at this Hamiltonian, which was shown from eq. (4.66). Before looking at the dynamics it is instructive to rewrite the Hamiltonian to more closely resemble the special case of $P_\eta = 0$. Remembering the Hamiltonian for $P_\eta = 0$,

$$H_0 = \frac{1}{2}(p_y^2 + y^2) + \frac{1}{2\mu_e}p_z^2 - \frac{1}{\sqrt{p_y^2 + y^2 + z^2}},$$

the Hamiltonian can be rewritten to resemble H_0:

$$H(I_y, \theta_y, p_z, z) = I_y + \frac{1}{2\mu_e} p_z^2 - \frac{1}{\sqrt{2I_y + P_\eta^2 + z^2}} \left[1 + 2P_\eta \frac{\sqrt{2I_y}}{2I_y + P_\eta^2 + z^2} \cos\theta_y \right]^{-1/2}. \tag{4.71}$$

Clearly, in the limit $P_\eta \to 0$ the Hamiltonian reduces to H_0 studied in the previous section. Define a value $\Delta \equiv \Delta(I_y, p_y, z)$ as,

$$\Delta(I_y, p_y, z) = \frac{\sqrt{2I_y}}{2I_y + P_\eta^2 + z^2}. \tag{4.72}$$

If the Δ is small, as it would be if z is large, then Δ will approach unity and the dynamics will locally be integrable. Here, the large z can be achieved by very weak coupling. The integrability of the system for the large z was shown at previous section. However, otherwise the system becomes strongly coupled for very small z and the Δ is not negligible. This strong coupling leads to the system nonintegrable.

To illustrate the behavior as $\Delta \ll 1$ in detail, approximate the system by the Taylor expansion:

$$(1+x)^{-1/2} = 1 - \frac{x}{2} + \frac{3x^2}{8} + O[x^3], \tag{4.73}$$

where the terms with higher order of square were neglected by approximation. The Hamiltonian can be approximated as follow,

$$H(I_y, \theta_y, p_z, z) \simeq I_y + \frac{1}{2\mu_e} p_z^2 - \frac{1}{\left(2I_y + P_\eta^2 + z^2\right)^{1/2}} - \frac{P_\eta \sqrt{2I_y} \cos\theta_y}{\left(2I_y + P_\eta^2 + z^2\right)^{3/2}}. \tag{4.74}$$

and the equations of motion are given by

$$\begin{aligned}
\dot{z} &= \frac{1}{\mu_e} p_z \\
\dot{p}_z &= -\frac{z}{\left(2I_y - P_\eta^2 + z^2\right)^{3/2}} + f(I_y, P_\eta, z)\, P_\eta \cos\theta_y \\
\dot{\theta}_y &= 1 + \frac{1}{\left(2I_y - P_\eta^2 + z^2\right)^{3/2}} - g(I_y, P_\eta, z)\, P_\eta \cos\theta_y \\
\dot{I}_y &= h(I_y, P_\eta, z)\, P_\eta \sin\theta_y,
\end{aligned} \tag{4.75}$$

where

$$
\begin{aligned}
f(I_y, P_\eta, z) &= \frac{3z\sqrt{2I_y}}{\left(2I_y + P_\eta^2 + x^2\right)^{5/2}} \\
g(I_y, P_\eta, z) &= \frac{P_\eta^2 + z^2 - I_y}{\sqrt{2I_y}\left(2I_y + P_\eta^2 + z^2\right)^{5/2}} \\
h(I_y, P_\eta, z) &= -\frac{\sqrt{2I_y}}{\left(2I_y + P_\eta^2 + z^2\right)^{3/2}}.
\end{aligned} \tag{4.76}
$$

Note that in the limit of $\Delta \ll 1$, or large value of z, the representations f, g and h will come close to zero and the system will be integrable. The motion of guiding center of weak binding can be explained through this analysis in a phase space. Integrability of the system depends on the type of binding, weak binding or strong coupling. For the large z, the dynamics of the system is integrable. However, as the z comes close to zero, eventually it will pass through zero, the system experiences a strong coupling and suffers a kick. Following this kick, z again becomes large and the system returns to the region of phase space characterized by integrable behavior [112, 113].

4.4 The Governing Motion of the Guiding Center Atom in Various Limits

The Hamiltonian of guiding center atom has been transformed so as to be a function of constants of motion by canonical transformations. The Hamiltonian represented by constants of motion has few number of variables and its equations of motion have compact forms to solve. In addition, the scaling introduces great simplification in the analysis of the system. The scaled units eliminates the system's dependence on parameters such as mass, charge or magnitude of the applied field. Without loss of generality, the values of the constants of motion can be chosen arbitrarily but reasonably. The guiding center atom with weak binding in a strong magnetic field generated limitations on the motion of the atom in specific directions and, thereby, on the constants of motion. For the properly chosen constants of motion, the system

will show various kinds of motion. The motion of the guiding center Hamiltonian by various conditions will be investigated through this section.

4.4.1 Motion along the Field Direction

In the Hamiltonian (4.47), the sum of the last two terms that govern the z motion are the binding energy

$$H_z(p_z, z) = \frac{1}{2\mu_e} p_z^2 - \frac{1}{\sqrt{r^2 + z^2}}, \tag{4.77}$$

where $p_y^2 + y^2$ of (4.47) was substituted by a constant r^2 for future analysis. The r indicates a radius at a transverse plane to the magnetic field and it can be treated by a constant by eq. (4.53) and (4.68). From the "unscaled" Hamiltonian (4.43), r^2 is given by

$$\begin{aligned} r &= (x_e - x_i)^2 + (y_e - y_i)^2 \\ &= \left(\frac{c}{eB} p_y\right)^2 + y^2 \\ &= p_y^2 + y^2. \quad \text{(in scaled unit)} \end{aligned} \tag{4.78}$$

The electron kinetic energy associated with velocity components transverse to the magnetic field is bound up in the cyclotron action, I_{ce}. For a bound electron-ion pair, H_z is negative. Another constant of motion is given by the bounce action for the z motion.

$$I_z = \frac{1}{2\pi} \oint p_z dz$$

For the negative H_z, p_z can be expressed as follows:

$$p_z = \sqrt{2\mu_e} \left(-(-rH_z) + \frac{1}{\sqrt{r^2 + z^2}} \right)^{1/2}. \tag{4.79}$$

where a negative sign in $-rH_z$ was added because of negative H_z. Defining a new integration variable, $q \equiv H_z \sqrt{r^2 + z^2}$, with a constant $\gamma = -rH_z$, the action variable

can be carried out using complete elliptic integral while H_z and r are constants [113], The constant of motion for the z motion is given by

$$I_z = \sqrt{\mu_e r}\,\Phi(\gamma) \tag{4.80}$$

where,

$$\begin{aligned}\Phi(\gamma) &= \frac{2\sqrt{2}}{\pi\sqrt{\gamma}}\int_{\gamma}^{1}\sqrt{\frac{q-q^2}{q^2-\gamma^2}}dq \\ &= \frac{2\sqrt{2}}{\pi\gamma\sqrt{1+\gamma}}\left[\gamma\,K\left(\frac{\gamma-1}{\gamma+1}\right)-\gamma(\gamma+1)\,E\left(\frac{\gamma-1}{\gamma+1}\right)\right. \\ &\qquad \left.+\Pi\left(\frac{\gamma-1}{\gamma+1},\frac{\gamma-1}{\gamma+1}\right)\right]\end{aligned} \tag{4.81}$$

where K, E and Π are complete elliptic integrals of the first, second and third kind elliptic integrals given by (A.4), (A.5) and (A.6) from appendix B, respectively. Figure 10 illustrates the function Φ as a function of γ on the interval $\gamma = 0$ and $\gamma = 1$. Also, it shows a graphical inversion to obtain H_z as a function of I_z and r as follows

$$H_z(r, I_z) = -\frac{1}{r}\Phi^{-1}\left(\frac{I_z}{\sqrt{\mu_e r}}\right). \tag{4.82}$$

When γ goes to 1, Φ has a very small value. The action I_z comes close to zero unless r goes to infinity. To investigate the limit, approximate the function around $\gamma = 1$. For $\gamma \simeq 1$,

$$\gamma = -rH_z \simeq 1. \tag{4.83}$$

so,

$$H_z \simeq -\frac{1}{r}. \tag{4.84}$$

H_z has the shape of Coulomb potential and the amplitude of electron oscillations in the Coulomb well is small compared to r, and the potential is approximately harmonic. In this case $\Phi(\gamma)$ can be approximated by linear dependence:

$$\Phi(\gamma) \simeq 1 - \gamma \tag{4.85}$$

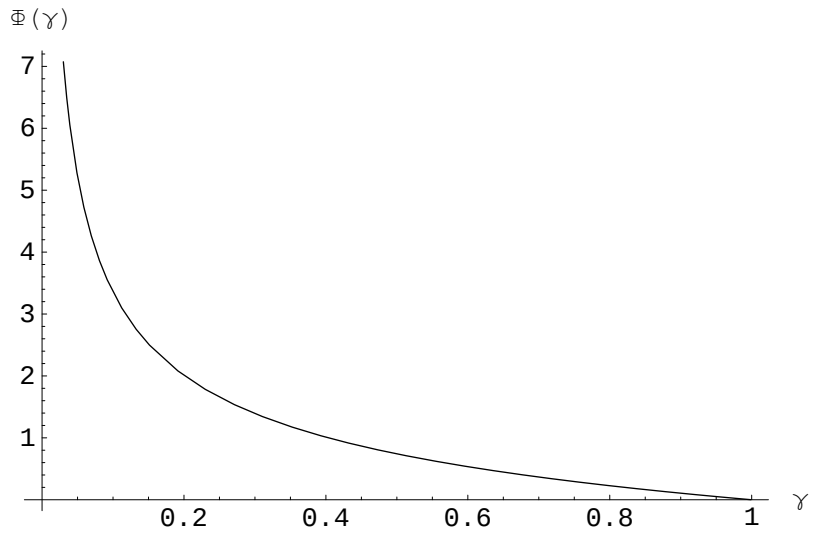

Figure 10: Graph of Φ (γ) in the interval [0,1]. When γ increases to *1*, the function Φ decreases to zero. For γ=1, the Φ becomes zero.

and

$$I_z \simeq \sqrt{r\mu_e}(1-\gamma). \tag{4.86}$$

Therefore, the H_z related with I_z can be found by replacing the γ by $-rH_z$,

$$H_z = -\frac{1}{r} + I_z\omega_z \tag{4.87}$$

where the angle variable $\omega_z = 1/\sqrt{\mu_e r^3}$. A correction term of an oscillation energy, $I_z\omega_z$, was added to the Coulomb potential. Thus the limit, $\gamma \simeq 1$, implies that the total binding energy is the sum of Coulomb potential between two particles at a transverse plane to the magnetic field and a small oscillation energy along the field direction. A pair of electron-ion moves along the magnetic field with a small internal bounce motion of frequency, ω_z. Thus, another constant of motion could be obtained for the bounce motion using the elliptic integral. Motion at the transverse plane resulted in pseudomomentum. Using the pseudomomentum leads to a possibility of investigation of the motion at the transverse plane. Following section is intended to the analysis of guiding center motion using phase trajectories.

4.4.2 The Motion of Electron-Ion pair when I_z=0

$I_z = 0$ corresponds to $\gamma = 1$ from the previous section. At this limit, the only potential governing the motion along the field direction is the Coulomb potential and the internal small oscillation along the magnetic field can be ignored, The magnitude of z at the center of mass frame will be considered to be a small value. Transformed Hamiltonian contains several constants of motion in guiding center limit and it can be more simplified by proper approximation. Considering a Hamiltonian including the z motion (4.47),

$$H = \nu I_{ce} + \frac{1}{2}(P_\eta - p_y)^2 + \frac{1}{2}y^2 - \frac{1}{r}\Phi^{-1}\left(\frac{I_z}{\sqrt{\mu_e r}}\right). \tag{4.88}$$

The mass μ_e can be approximated to m_e/m_i for larger m_i. The action I_{ce} for a rapid gyromotion of a electron can be eliminated from the Hamiltonian. Without loss of generality the Hamiltonian can be written as,

$$H = \frac{1}{2}(P_\eta - p_y)^2 + \frac{1}{2}y^2 - \frac{1}{\sqrt{p_y^2 + y^2}} + I_z\omega_z, \tag{4.89}$$

with $\omega_z = 1/\sqrt{\mu_e r^3}$. For a simple case, consider $I_z = 0$. As shown from the Figure 10, when $\gamma = 1$ the elliptic function has zero as its value. Thus the inversion of the function will have a value of unity for $I_z = 0$ and lead to a reduced Hamiltonian given by

$$H = \frac{1}{2}(P_\eta - p_y)^2 + \frac{1}{2}y^2 - \frac{1}{\sqrt{p_y^2 + y^2}}, \tag{4.90}$$

where r was replaced by $p_y^2 + y^2$ for analysis. The r was driven at eq. (4.78) in detail. So the phase space (y, p_y) depends on only two parameters, H and P_η. The following analysis is based on the Hamiltonian above. Figure 11 shows a three-dimensional plot of the energy surface for $P_\eta = 2.5$ and its contour plot. Figure 12(a) is a plot for $y = 0$ of the Hamiltonian when $P_\eta = 2.5$. This graph shows clearly two minima and a saddle. The first minimum exists at $(p_y = 0, H \to \infty)$ and the second at $(p_y = p_{yo}, H = H(p_{yo}))$. Figure 12(b) shows that the second minimum disappears for

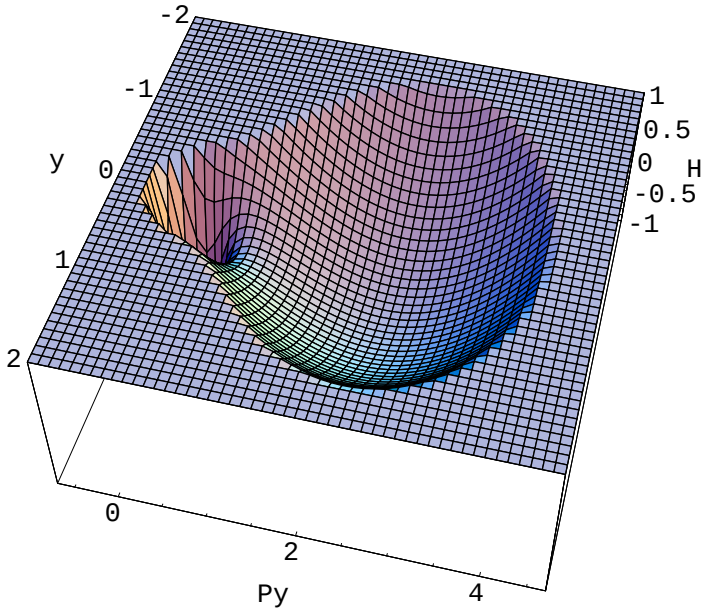

(a)

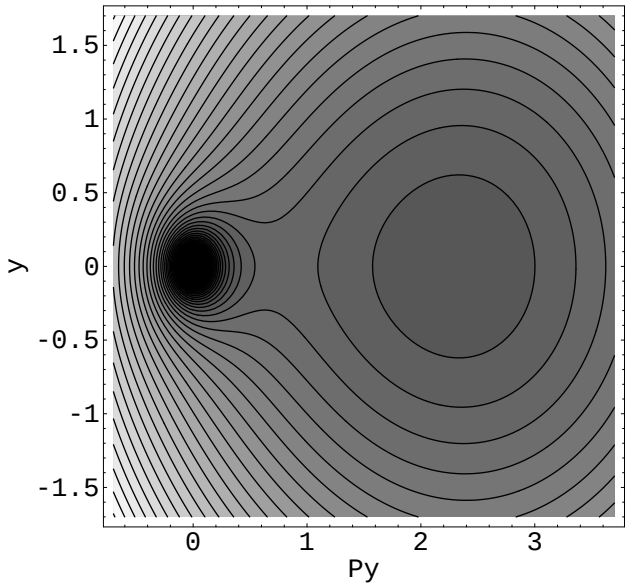

(b)

Figure 11: (a). Three-dimensional plot of the Hamiltonian for $P_\eta = 2.5$ and (b) contour plot of the energy surface at $P_\eta = 2.5$.

a smaller P_η less than 1.88988. The Figure 12(b) show plots for various P_η, 0.5, 1.0, 1.88988 and 2.5. With the smaller values of P_η (smaller than a critical value), the graph shows no minimum. The critical value is calculated as $P_\eta = 3/2^{2/3}$. Contour plots for $P_\eta = 1.0$ and $P_\eta = 3/2^{2/3}$ are followed.

The motion at the saddle point will be a complicated mix of the motion at the minimum and the saddle. When the motion happens at near ($y = 0$, $p_y = 0$), the radius of transverse motion given by $r = \sqrt{p_y^2 + y^2}$ will be small resulting in which electron $\mathbf{E}\times\mathbf{B}$ drifts around the ion (see the Figure 7). Rewrite the equations of motion for ion in unscaled unit using eq. (4.33):

$$\begin{aligned} \dot{x}_i &= \frac{p_{xi}}{m_i} \\ \dot{y}_i &= \frac{p_{yi}}{m_i} - \frac{eB}{m_i c} x_i. \end{aligned} \tag{4.91}$$

The terms of RHS can be replaced by other canonical variables using (4.37) and (4.38). Using scaled units, the equations are described by

$$\begin{aligned} \dot{x}_i &= -y \\ \dot{y}_i &= P_\eta - p_y. \end{aligned} \tag{4.92}$$

Thus, the velocity of the ion in the transverse plane is given by

$$v_i = \sqrt{y^2 + (P_\eta - p_y)^2} \simeq P_\eta. \tag{4.93}$$

The transverse velocity of ion is nearly constant. This velocity also can be calculated by taking the average of each velocity:

$$< \dot{x}_i >= 0, \quad < \dot{y}_i >= P_\eta. \tag{4.94}$$

These results shows that the bound electron-ion pair moves across the magnetic field with velocity P_η. If p_y is smaller than P_η initially, the crossing velocity will be similar to the initial velocity of the ion.

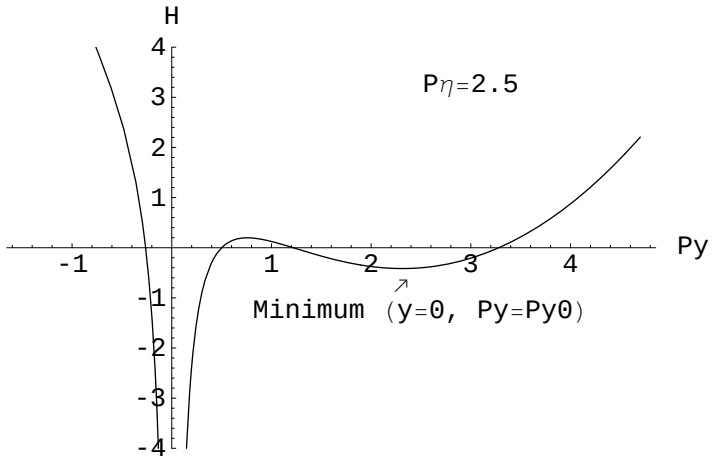

(a)

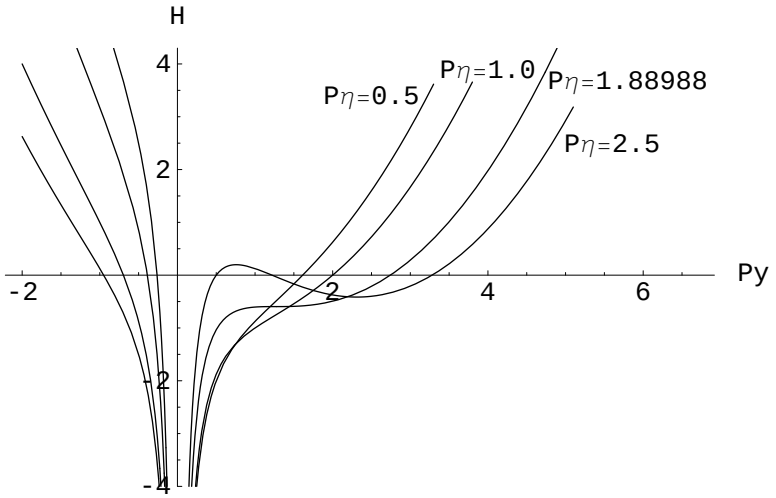

(b)

Figure 12: Graphs for $y = 0$. (a) is a plot for $P_\eta = 2.5$. Clearly, one minimum ($p_y \simeq 2.31310$) and a saddle ($p_y \simeq 0.75756$) are shown. (b) shows that how the minimum disappears as P_η decreases. The critical value for no minimum is $P_\eta = 3/2^{2/3} \simeq 1.88988$.

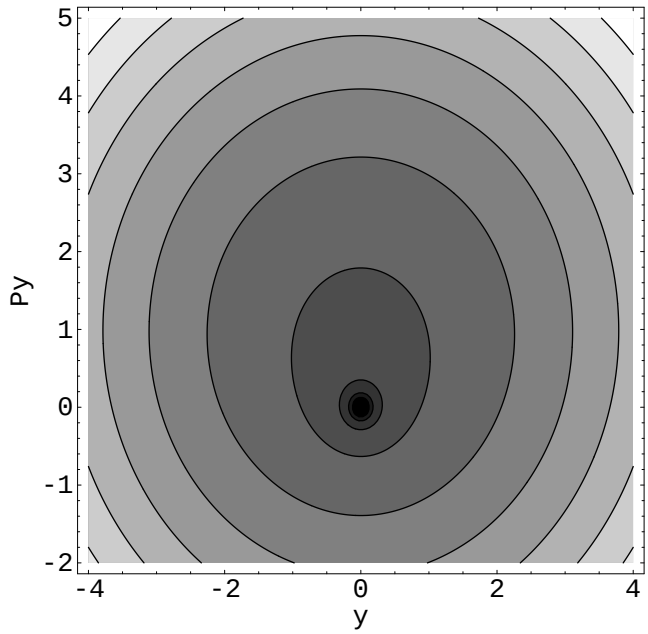

(a)

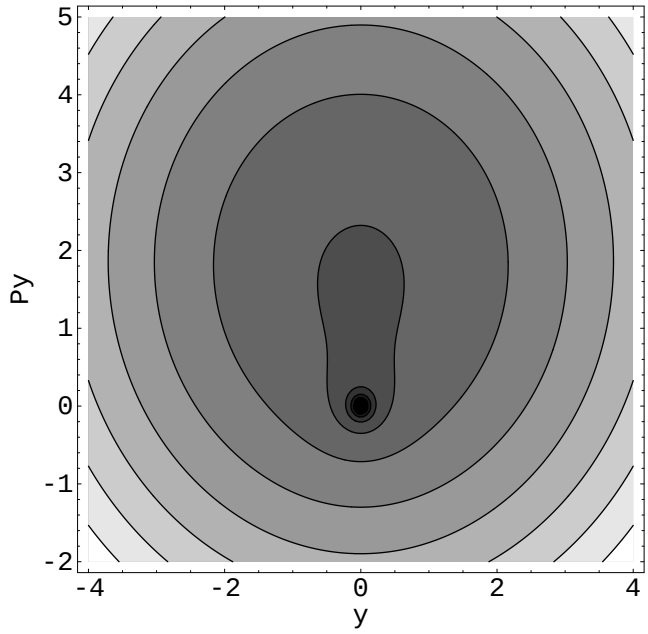

(b)

Figure 13: Contour plots for (a) $P_\eta = 1.0$ and (b) $P_\eta = 3/2^{2/3} \simeq 1.88988$.

The electron velocity also can be found from eq. (4.25) and (4.39) as follows,

$$\begin{aligned} x_e &= -\frac{c}{eB}p_{ye} = x_i - \frac{c}{eB}p_y \quad \text{(in unscaled units)} \\ &= x_i - p_y \qquad\qquad\qquad\quad \text{(in scaled units)} \\ y_e &= y_e. \end{aligned} \tag{4.95}$$

Using the eq. (4.62), the derivatives of x_e and y_e with respect to time can be derived:

$$\begin{aligned} \dot{x}_e &= -\dot{p}_{ye} = \frac{y}{(p_y^2+y^2+z^2)^{3/2}} \\ \dot{y}_e &= \dot{y} + \dot{y}_i = \frac{p_y}{(p_y^2+y^2+z^2)^{3/2}}, \end{aligned} \tag{4.96}$$

so, the velocity of the electron in the transverse plane is given by

$$v_e = \frac{r}{(r^2+z^2)^{3/2}}, \tag{4.97}$$

where $r = \sqrt{p_y^2+y^2}$. This velocity can be expanded around $r = 0$ to result in

$$v_e \simeq \frac{1}{r^2}. \tag{4.98}$$

Thus, for small radius the velocity v_e will be large. If r, P_η are constant, their velocities are constant with a relation, $v_i{=}r^2 P_\eta\, v_e$. To keep the drifting motion, the electron drift velocity should be larger than the velocity of the ion, or drifting frequency should be larger than the cyclotron frequency of the ion,

$$\omega_D > \Omega_i, \tag{4.99}$$

where ω_D and Ω_i are electron drifting frequency and ion cyclotron frequency, respectively. This provides a condition for the electron $\mathbf{E}\times\mathbf{B}$ drifting. If the velocity of the ion is bigger than the velocity of the electron, the drifting electron can not keep up with the ion and the radius of the ion cyclotron motion will be larger than the radius of the electron cyclotron motion. If the binding is relatively weak, the ion will leave the electron eventually, while the electron is oscillating along the magnetic field.

The motion at another minimum ($p_y = p_{yo}$) shows another feature for weak binding. Same condition ($y = 0$) but ($p_y = p_{yo}$) is applied to the system. If $y = 0$ and p_y=fixed, than the radius r will be constant through the motion. Investigate the velocities of two particles. From the equation (4.92) and (4.96), the velocities at ($y = 0$, $p_y = p_{yo}$) can be written as

$$\begin{aligned} \dot{x}_i &= 0 \\ \dot{y}_i &= P_\eta - p_{yo}, \end{aligned} \tag{4.100}$$

and for small z the velocity of the electron is given by

$$\begin{aligned} \dot{x}_e &= 0 \\ \dot{y}_e &= \frac{p_{yo}}{(p_{yo}^2 + z^2)^{3/2}} \simeq \frac{p_{yo}}{|p_{yo}|^3}, \end{aligned} \tag{4.101}$$

where the $\dot{y}_e$ can be approximated for small z,

$$\dot{y}_e = \frac{p_{yo}}{|p_{yo}|^3}. \tag{4.102}$$

In addition, the minimum position was found by

$$\frac{\mathrm{d}H}{\mathrm{d}p_y} = -(P_\eta - p_y) + \frac{p_y}{|p_y|^3} = 0, \tag{4.103}$$

where $H(y = 0, p_z = 0)$ from eq. (4.90) was used. The above relation leads to

$$P_\eta - p_y = \frac{p_y}{|p_y|^3}. \tag{4.104}$$

This proves that $\dot{y}_i \simeq \dot{y}_e$. Thus, the electron and ion form a pair and move together with same velocity,

$$v = \sqrt{2}(P_\eta - p_{yo}). \tag{4.105}$$

The electron and ion $\mathbf{E}\times\mathbf{B}$ drift under the field from each other. This pair forms a "drifting-pair" [113]. Figure 14 shows a motion of the drifting-pair.

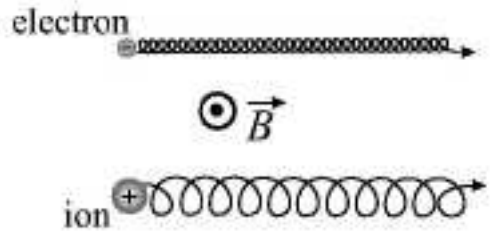

Figure 14: Schematic plot of a motion that occurs when electron and ion form a drifting pair [113].

For nonzero but small I_z, the important difference is the binding energy, which is a correction term. The binding energy is given in Eq.(4.87). Rewrite the binding energy as a function of the radius r

$$H_z = \frac{1}{r} + \frac{I_z}{\mu_e r^3} \tag{4.106}$$

The binding energy is still proportional to r^{-1}. However, the phase space of the Hamiltonian (4.89) depends on three parameters, P_η, H and I_z, rather than two parameters for the case of $I_z = 0$. When $I_z = 0$, the critical value was $P_\eta = 3/2^{2/3}$ and the second minimum existed at p_{yo}. When $I_z \neq 0$, however, the critical value changes. Figure 15(a) shows plots for different values of k $(=I_z/\sqrt{\mu_e})$. As the k increases, the slopes at $p_y = p_{yo}$ increase slightly. Thus the critical value will decrease as the value k increases. Figure 15(b) shows the critical value P_c as a function of k ranging from 0 to 1.

4.4.3 Coherent States for an Electron-ion Pair

The three dimensional plot of Figure 11 indicates the possibility for the construction of the coherent states. The energy H is a function of P_η, p_y and y. If the pseudo-momentum P_η is bigger than the critical value, $P_\eta = 3/2^{2/3}$, an energy minimum point exists along $y = 0$. Using the Taylor expansion around a minimum point of

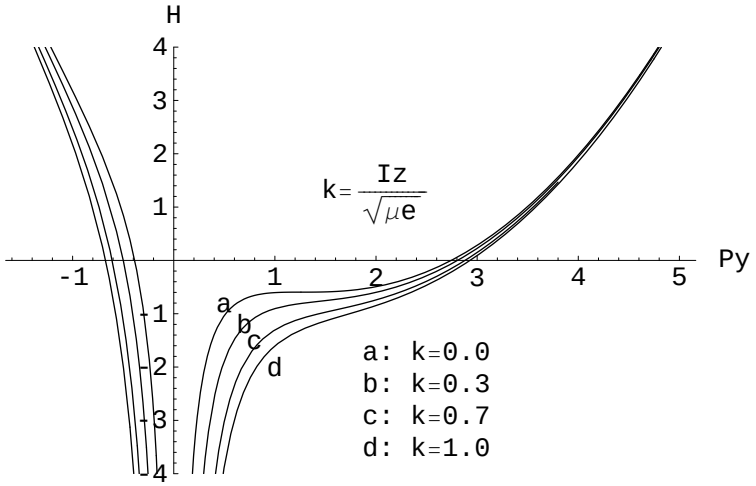

(a)

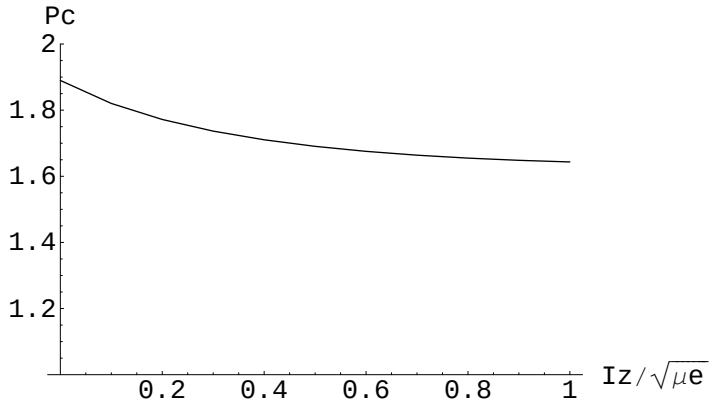

(b)

Figure 15: (a) Plots of energy surfaces for different k's for fixed $P_\eta = 3/2^{2/3}$, the critical value for $I_z = 0$. (b) the critical value (P_c) decreases as $k = I_z/\sqrt{\mu_e}$ increases.

the system after the canonical transformation of the Hamiltonian (4.90) around the minimum point shifts the center from the origin to the equilibrium point. Coherent states can be built up at the equilibrium point which is a minimum. Rewrite the Hamiltonian

$$H = \frac{1}{2}\left[(P_\eta - p_y)^2 + y^2\right] + \frac{1}{2\mu_e}p_z^2 - \frac{1}{\sqrt{p_y^2 + y^2 + z^2}}. \tag{4.107}$$

where $\mu_e = m_e/M$. The equilibrium point can be calculated by setting the equations of motion equal to zero

$$\begin{aligned}
\dot{y} &= -(P_\eta - p_y) + \frac{p_y}{(p_y^2 + y^2 + z^2)^{3/2}} = 0 \\
\dot{z} &= \frac{p_z}{\mu_e} = 0 \\
\dot{p}_y &= -y - \frac{y}{(p_y^2 + y^2 + z^2)^{3/2}} = 0 \\
\dot{p}_z &= -\frac{z}{(p_y^2 + y^2 + z^2)^{3/2}} = 0
\end{aligned} \tag{4.108}$$

Solving the equations results in the equilibrium points

$$\begin{aligned}
y_0 &= z_0 = p_{zo} = 0 \\
p_{y_0} &= \frac{P_\eta r_0^3}{r_0^3 + 1}
\end{aligned} \tag{4.109}$$

where $r_0 = (p_{y_0}^2 + y_0^2 + z_0^2)^{1/2}$. Thus the solutions shows that the equilibrium point exists when $z = p_z = 0$, $y = 0$ and $p_y = p_{yo}$ in the phase space. Consider a canonical transformation

$$\begin{aligned}
y = y', \qquad p_y = p_{yo} + p_y' \\
z = z', \qquad p_z = p_z'.
\end{aligned} \tag{4.110}$$

Expanding the Hamiltonian in the neighborhood of the minimum $(y, p_y, z, p_z) = (0, p_{y0}, 0, 0)$ to the second-order transforms the Hamiltonian (4.90) into a harmonic oscillator (dropping the primes)

$$H = \frac{p_y^2}{2\mu_y} + \frac{p_z^2}{2\mu_e} + \frac{1}{2}ay^2 + \frac{1}{2}bz^2 + \Theta_0 \tag{4.111}$$

where

$$\begin{aligned} a &= \frac{1}{2} + \frac{1}{2p_{yo}^3} \\ b &= \frac{1}{p_{yo}^3} \\ \mu_y &= \frac{p_{yo}^3}{p_{yo^3} - 2} \\ \mu_e &= \frac{m_e}{m_e + m_i}, \end{aligned} \tag{4.112}$$

and

$$\Theta_0 = \frac{1}{2p_{yo}^4} - \frac{1}{p_{yo}}. \tag{4.113}$$

The Hamiltonian eq.(4.111) is a two dimensional harmonic oscillator. Figure 16 is the graph of the energy surface for $y = z = 0$ showing plots of (a) the approximated harmonic Hamiltonian of (4.111) and (b) the Hamiltonian (4.90) together. It shows that the system can be locally harmonic at the minimum point. The z-motion can be decoupled from the Hamiltonian. The nondispersive wavepacket for the Hamiltonian will have exactly same form with the displaced ground state wave function of a harmonic oscillator:

$$\Psi(y) = \frac{1}{\sqrt{b}\pi^{1/4}} \exp[-(y - y_{cl})^2/2b^2], \tag{4.114}$$

where $b = \sqrt{\hbar/m\omega}$ for a classical harmonic oscillator with a frequency ω. y_{cl} is the classical trajectory. The variable of the above coherent state, y, is the relative distance between the two particles. The constructed coherent state with respect to the variable y will correspond to the separation of the two particles. Thus the coherent state can be used to explain the $\mathbf{E}\times\mathbf{B}$ drifting pair of the Figure 14 because the coherent state will be a non-spreading wave packet as long as the separation of the electron-ion pair remains constant or changes harmonically.

4.5 Conclusions

The integrability of the $electron - ion$ pair system has been investigated by finding constants of motion and applying the limit for guiding center motion in a magnetic field. Constants of motion were found by various properties of the system:

(1) Because the rapid gyromotion of the electron in the uniform magnetic field, the action I_{ce} was a good adiabatic invariant and Ω_{ce} was a constant. The product $I_{ce}\Omega_{ce}$ was constant and did not influence the dynamics of the remaining variables.

$$I_{ce}\Omega_{ce} = \text{ constant} \tag{4.115}$$

(2) Rapid cyclotron motion could be averaged out in the limit of which the electron cyclotron frequency was the largest of the dynamical frequencies and the cyclotron radius was the smallest of the length scales. Because the electronic motion influenced the Hamiltonian dynamics only along z-axis, the position of the electron in a transverse plane to the magnetic field was specified by

$$(x_e,\, y_e) \to (-\frac{c}{eB}p_{ye},\, y_e), \tag{4.116}$$

(3) Moving along the magnetic field direction generated constants of motion illustrating transverse motion to the field. The pseudomomentum was the constant of the motion which was important in separating the center of mass and internal degrees of freedom. For this guiding center atom, the pseudomomentum, P_ξ and P_η, were given by

$$\begin{aligned} \boldsymbol{K} &\equiv P_\xi\,\hat{x} + P_\eta\,\hat{y} \\ &= (p_{xi} + \frac{eB}{c}y)\,\hat{x} + (p_{yi} + p_{ye})\,\hat{y}. \end{aligned}$$

(4) Working in the center of mass coordinates, the motion along ζ-axis was ignored, and its conjugate momentum P_ζ could be chosen to be zero. P_ζ and ζ were given by

$$P_\zeta = p_{zi} + p_{ze}, \qquad \zeta = \frac{m_i z_i + m_e z_e}{m_i + m_e}. \tag{4.117}$$

One of the pseudomomentum (for instance, P_ξ) could be eliminated by orienting the coordinates at the center of mass frame.

(5) For the condition $I_z = 0$, the only governing potential was the Coulomb potential and the small internal oscillation along the field direction could be ignored. Because the mass of the ion was much larger than the mass of the electron, the motion along z-axis could be eliminated from the Hamiltonian without loss of generality. The total binding energy was the sum of Coulomb potential between two particles at a transverse plane to the magnetic field and a small oscillation energy along the field direction. Thus the pair of electron-ion moved along the magnetic field with a small internal bounce motion of frequency, ω_z. Another constant of motion could be obtained for the bounce motion using the elliptic integral. Even though another constant of motion was found, the Hamiltonian could not be separated into kinetic and potential parts.

(6) Rather than finding the potential function to investigate the system, the Hamiltonian could be expanded at its minimum point and the expansion produced harmonic oscillator Hamiltonian, thereby constructing the coherent state. The coherent state constructed at the minimum point could explain the $\mathbf{E}\times\mathbf{B}$ drifting pair because the relative distance between the particles was used to construct the coherent state as a function of y.

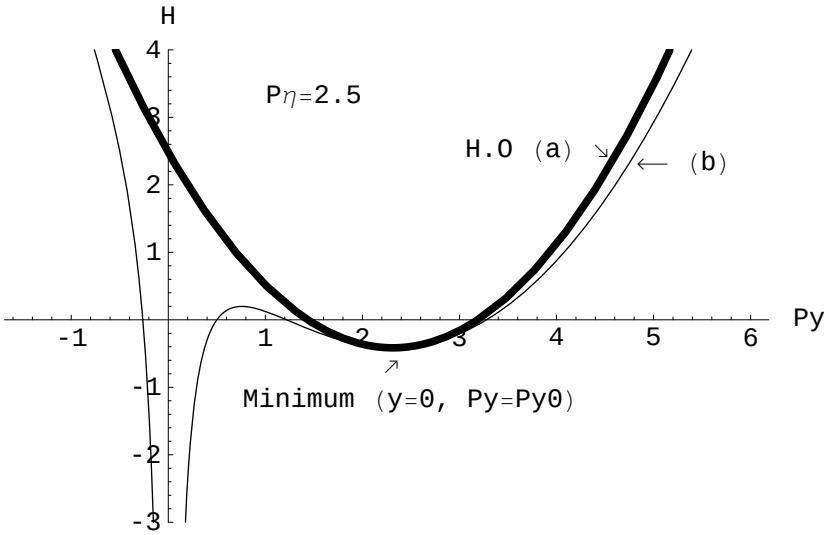

Figure 16: Plots of energy surface of (a) approximated harmonic Hamiltonian (denoted "H.O.") and (b) energy surface for $y = 0$, $I_z = 0$. The minimum is located at $p_{yo} = 2.3131$ when $P_\eta = 2.5$.

CHAPTER V

STABILITY ANALYSIS OF THE ION-PAIR "RYDBERG" CONFIGURATIONS

5.1 Introduction

In the previous chapter, we have discussed the electron-ion pair with a large mass difference. Many of the properties of the electron-ion pair have been derived from the large difference in mass between the ion and the electron. An ion pair, the subject of this chapter, is essentially a heavy particle system interacting by means of a Coulombic potential [133]. These states bear much similarity to high-lying Rydberg states of atoms and molecules. They can be formed by exciting a complex mixture of zeroth-order states in the Franck-Condon region at short intermediate distances, and this prepared state can evolve, with small probability, to a long-range charge-separated state, which in the ion pair [134, 135, 136]. As an another heavy particle system, antihydrogen atoms were analyzed theoretically and experimentally in Ref. [137] which showed how the internal orbits of antihydrogen atoms depend on the external magnetic field.

In this chapter, we show that it is possible to form stable coherent wavepackets [61, 138] which correspond to very long living ion-pair states. This ion pair can be compared to a hydrogen atom possessing a rather heavy electron. Investigation will rely on classical mechanics, which has proven its utility in various recent investigation of Rydberg state phenomena, e.g., the role of collisions with ions in ZEKE spectroscopy [139, 140, 141, 142, 143, 144].

This section will focus on the production of non-spreading wavepackets by exploiting mechanisms analogous to those which, in celestial mechanics, stabilize the Trojan

asteroids.

5.2 Hamiltonians Involving the Mass Ratio

An excellent description of the procedure for treating both neutral and charged N-particle systems in constant electric and magnetic fields is given by Johnson *et al.* [120]. In case of a two-body Coulombic system (masses m_1 and m_2, charges $-e$ and Ze) interacting with constant electric and magnetic fields, after separation of the center of mass the Hamiltonian may be written

$$H = \frac{1}{2M}(\boldsymbol{K} - e\boldsymbol{B} \times \boldsymbol{r})^2 + \frac{1}{2\mu}(\boldsymbol{p} - e\beta\boldsymbol{B} \times \boldsymbol{r})^2 + \boldsymbol{E} \cdot \boldsymbol{r} - \frac{Ze^2}{r}. \tag{5.1}$$

where $r = |\boldsymbol{r}|$, μ is the reduced mass, and β=$(m_2 - m_1)/2M$. The pseudomomentum $\boldsymbol{K}$ is a constant of motion as was shown through the section 4.2.2 and 4.2.3. The differences of this system with previous system are the existence of the electric field and comparable masses. Atomic units are adopted for analysis: the unit of length is the Bohr radius a_0 for a two body system of reduced mass μ and "nuclear" charge Ze, i.e., a_0=$\hbar^2/\mu Ze^2$ - the particle of mass m_2 is taken to be the nucleus. If the system is composed of H^+ and H^- ions (Z=1), the units are

$$\begin{aligned} \mu &\simeq \frac{1}{2}m_H \\ a_0 &= \frac{\hbar^2}{\mu e^2} \end{aligned}$$

In these units μ=$\hbar$=a_0=e=1. Suitable measures of the electric and magnetic field strengths are

$$E_0 = \frac{eZ}{a_0^2}\,,\ B_0 = \frac{\hbar c}{e a_0^2} \tag{5.2}$$

and it is convenient to work with the dimensionless electric and magnetic fields, F=$\boldsymbol{E}/E_0$ and $\omega_c = \boldsymbol{B}/B_0$. The fields are measured in units that depend explicitly on the masses. The coupling between the internal and CM motion , i.e., the motional

Stark term is given by

$$\frac{1}{M}(\boldsymbol{B}\times\boldsymbol{r})\cdot\boldsymbol{r}. \tag{5.3}$$

Without loss of generality, $\boldsymbol{K}$ and $\boldsymbol{F}$ may be taken to lie along arbitrary directions in the $x-y$ plane so that it simplifies the discussion to assume that they point along orthogonal axes. Assuming that the magnetic field lies along the z-axis and setting Z=1 leads to the effective internal Hamiltonian [120]

$$H = E = \frac{1}{2}(p_x^2+p_y^2+p_z^2) - \frac{1}{r} - \frac{\omega_c}{2}\left(\frac{1-\delta}{1+\delta}\right)(xp_y - yp_x) + \frac{\omega_c^2}{8}(x^2+y^2) + \left(F+\frac{\omega_c K}{M}\right)x \tag{5.4}$$

where mass ratio is δ=m_1/m_2. The Hamiltonian with $\delta = 0$ is equivalent to the two dimensional $\boldsymbol{E}\times\boldsymbol{B}$ Hamiltonian for the hydrogen atom with an effective electric field term $(F+\omega_c K/M)x$ [150, 151, 152]. Even when this system is in a circular polarized field (CP) and a static electric field, moving in a rotating frame (rotating frequency ω_f) results in the same form of Hamiltonian with (5.4) but with differing magnitude of coefficients. Assuming the pseudomomentum $K = 0$,

$$H = \frac{1}{2}(p_x^2+p_y^2+p_z^2) - \frac{1}{r} - \left(\omega_f + \frac{\omega_c}{2}\frac{1-\delta}{1+\delta}\right)(xp_y - yp_x) + Fx + \frac{\omega_c^2}{8}(x^2+y^2) \tag{5.5}$$

The Coriolis-like paramagnetic term $(xp_y - yp_x)$ mixes coordinates and momenta and so prevents the construction of a potential energy surface. As mentioned before, this difficulty can be treated using the method of ZVS. If $\delta = 1$, then the Hamiltonian is completely separable into purely kinetic term and coordinate dependent potential term. For intermediate values of δ the dynamics is sufficiently similar to $\delta = 0$ not to require a separate discussion. Consider the two mass ratios, $\delta \neq 1$ and $\delta = 1$. The following discussions are intended to find nondispersive states for each cases.

5.3 Scaling Properties and Coherent States at a Minimum

If $\delta \neq 1$, the Coriolis-like paramagnetic term $(xp_y - yp_x)$ strictly prevents the construction of a potential energy surface. Following Chapter 2, the ZVS can be constructed as follows

$$\begin{aligned} \Upsilon &= H(\dot{x}, \dot{y}, x, y) - \frac{\dot{x}^2 + \dot{y}^2}{2} \\ &= -\frac{1}{r} + Fx - \frac{\omega_f \left(\omega_f + \omega_c \frac{1-\delta}{1+\delta}\right)}{2}(x^2 + y^2). \end{aligned} \tag{5.6}$$

The equilibrium points of the ZVS are found to lie long the x-axis at $y = 0$ and $z = 0$ by simultaneously solving the following set of equations:

$$\dot{q} = \frac{\partial H}{\partial p_q} = 0, \;\; \dot{p_q} = -\frac{\partial H}{\partial q} = 0. \tag{5.7}$$

where $q = x, y, z$. The ZVS (5.6) has a same form as the ZVS of the maximum configuration of the hydrogen atom in CP field and magnetic field. The maximum configuration is important because it raises the possibility of forming an coherent state. Recall that the ZVS is not a potential energy surface even though it may share some properties with it: A ZVS can support stable motion at its maximum. The existence of equilibria that can support non-spreading coherent wavepackets [58, 61, 138] has been shown in detail at Chapter 2. The equation (5.7) is a generalization of that work to ion-pairs in which the masses are variable. For the case H^+-H^- pair, the masses are almost same and the paramagnetic term Coriolis term of eq.(5.5) becomes negligible.

If $\delta = 1$, the Hamiltonian (5.5) reduces to

$$H = \frac{1}{2}(p_x^2 + p_y^2 + p_z^2) - \frac{1}{r} + \frac{\omega_c^2}{8}(x^2 + y^2) + Fx. \tag{5.8}$$

This Hamiltonian can be separated into kinetic energy and ordinary potential energy surface:

$$V = -\frac{1}{r} + \frac{\omega_c^2}{8}(x^2 + y^2) + Fx. \tag{5.9}$$

The equilibrium points lie along the x-axis. The potential can be rewritten as a function of x for future investigation.

5.3.1 Scaling Properties of the External-field Induced Minimum

We will concentrate on the scaling with magnetic fields because strong magnetic fields are more difficult to include in experiments than electric field.

The potential in question is

$$V(x) = -\frac{1}{|x|} + \frac{\omega_c^2}{8}x^2 + Fx \tag{5.10}$$

Denoting the minimum and the maximum as $x_1(F,\omega_c)$ and $x_2(F,\omega_c)$ respectively, the scaling is derived as follows: Since both the minimum and maximum will occur for $x < 0$,

$$\begin{aligned} \frac{\mathrm{d}V}{\mathrm{d}x} &= \frac{\mathrm{d}}{\mathrm{d}x}\left(x^{-1} + \frac{\omega_c^2}{8}x^2 + Fx\right) = 0 \quad (\mathrm{x} < 0) \\ &= -\frac{1}{x^2} + \frac{\omega_c^2}{4}x + F = 0. \end{aligned} \tag{5.11}$$

The scaling

$$x_j(F,\omega_c) = \omega_c^{-2/3} x_j^{(s)}(F\omega_c^{-4/3}, 1) \tag{5.12}$$

converts the above equation

$$-\left(\frac{1}{x_j^{(s)}}\right)^2 + \frac{1}{4}x_j^{(s)} + F\omega_c^{-4/3} = 0, \tag{5.13}$$

and therefore corresponds to the appropriate parameters of unit magnetic fields and electric fields $F\omega_c^{-4/3}$. Similarly, the depth of the outer minimum is

$$\begin{aligned} \Delta(F,\omega_c) &= V(x_2) - V(x_1) \\ &= \omega^{2/3}\Delta^{(s)}(F\omega_c^{-4/3}, 1). \end{aligned} \tag{5.14}$$

The outer minimum disappears when

$$F \leq \frac{3}{4}\omega_c^{4/3}. \tag{5.15}$$

The numerical parameters for the $H^+ - H^-$ pair are:

$$\begin{aligned} \text{reduced mass } \mu &= 920\ electron\, mass \\ a_0 &= 5.76 \times 10^{-8}\, \mu m \\ E_0 &= 4.33 \times 10^{15}\, V cm^{-1} \\ B_0 &= 1.98 \times 10^{11}\, T, \end{aligned} \tag{5.16}$$

with these values, we find the following results for the potential minimum

Table 1: Numerical values of the scaled field variables and depth of the outer minimum for various intensities of the magnetic field.

B/T	$F/V(cm^{-1})$	$x_1/\mu m$	$x_2/\mu m$	$Well\,Depth\Delta/cm^{-1}$
1	3.5	-6.5	-2.5	1.4
	7.0	-14.3	-1.5	25.6
	10.4	-21.6	-1.2	72.0
	13.9	-28.9	-1.0	139.6
3	13.9	-2.8	-1.3	1.3
	17.4	-3.8	-1.1	7.2
	20.8	-4.7	-0.9	16.3
	24.3	-5.5	-0.8	28.1
	27.8	-6.3	-0.8	42.4
	31.2	-7.1	-0.7	59.3
	34.2	-8.0	-0.7	78.5
5	38.2	-3.1	-0.7	17.0
	41.6	-3.4	-0.7	24.0
	45.1	-3.7	-0.6	32.1
	48.6	-4.0	-0.6	41.0
	52.0	-4.3	-0.6	51.0
10	72.9	-1.4	-0.6	5.1
	76.3	-1.5	-0.5	7.5
	79.0	-1.5	-0.5	10.2
	83.3	-1.6	-0.5	13.2
	86.8	-1.7	-0.5	16.5

5.3.2 Coherent States at the Minimum

Figure 17 (a) is the energy surface at $y = z = 0$ for $\delta = 1$, electric field strength of $10\,V/cm$ and a magnetic field of 1 Tesla. Its three-dimensional plot is given by the Figure 17 (b). The graph shows a equilibrium point at $x_m \simeq -3.5817 \times 10^8$ in atomic units, which is almost 20μ (microns) in unscaled units. The symbol (H.O.) in the graph illustrates the harmonic oscillator. The expansion of the potential function in the neighborhood of the equilibrium point involves a canonical transformation from the original coordinates to the equilibrium configuration [38]. This shifts the center from the origin to the equilibrium point. The coherent state can be built up at the equilibrium point which is a minimum. Using following relation

$$\begin{aligned} x = x_m + \xi, \qquad & p_x = p_\xi \\ y = \eta, \qquad & p_y = p_\eta \\ z = \zeta, \qquad & p_z = p_\zeta \end{aligned} \tag{5.17}$$

leads to a new potential function :

$$V = -\frac{1}{r} + \frac{\omega_c^2}{8}(\xi^2 + \eta^2) + \left(F + \frac{\omega_c^2 x_m}{4}\right)\xi + F x_m. \tag{5.18}$$

with

$$x_m = -\frac{4r^3 F}{4 + r^3\omega_c^2} \tag{5.19}$$

where $r = (\xi^2+\eta^2+\zeta^2+2x_m\xi+x_m^2)^{1/2}$. Expanding the function to the second-order around (ξ, η, ζ) = (0,0,0) results in

$$H = \frac{1}{2}(p_\xi^2 + p_\eta^2 + p_\zeta^2) + \frac{1}{2}(a\xi^2 + b\eta^2 + c\zeta^2) + \Theta_0 \tag{5.20}$$

where

$$\begin{aligned} a &= \frac{\omega_c^2}{4} - \frac{2}{x_m^3} \\ b &= \frac{\omega_c^2}{4} + \frac{1}{x_m^3} \\ c &= \frac{1}{x_m^3} \end{aligned} \tag{5.21}$$

with

$$\Theta_0 = \frac{\omega_c^2 x_m^2}{8} + F x_m - \frac{1}{x_m}. \tag{5.22}$$

The transformed Hamiltonian is the three-dimensional harmonic oscillator function. Thus coherent states can be constructed at the minimum, explained in Chapter 2 in detail, and the frequencies along each axes are given by $\sqrt{a}$, $\sqrt{b}$ and $\sqrt{c}$. The motion along z (or ζ) axis is stable and separable from the Hamiltonian. Because the coherent state corresponding to the motion at $x-y$ plane was constructed with respect to the relative coordinates at the center of mass frame, the distance between the two particles will not diverge or converge as long as the wavepacket is not spreading.

5.4 Conclusions

The ion pair is essentially a heavy particle system interacting through a Coulombic potential. The difficulty of treating the the system by a potential function can be solved by the method of ZVS. The Hamiltonian involves a coefficient δ, mass ratio, this coefficient introduced two separate discussion about the system, $\delta \neq 1$ and $\delta = 1$. When $\delta \neq 1$ the Hamiltonian was completely of the same form as the Hamiltonian discussed before, which was transformed to harmonic oscillator by proper canonical transformation and thereby the coherent state could be built. When $\delta = 1$, the Hamiltonian was completely separable to purely kinetic term and coordinate dependent potential term. For intermediate values of δ the dynamics was similar to $\delta = 0$. Through a canonical transformation, the system was shifted to the minimum and the potential function was expanded around the point. It transformed the Hamiltonian the the three dimensional harmonic oscillator function and the coherent state could be constructed at the minimum. The distance between the two particles will not diverge or converge as long as the wavepacket is nondispersive. Thus it was possible

to prepare locally harmonic regimes in ion pair system thereby allowing the creation of almost completely non-dispersive coherent atomic states.

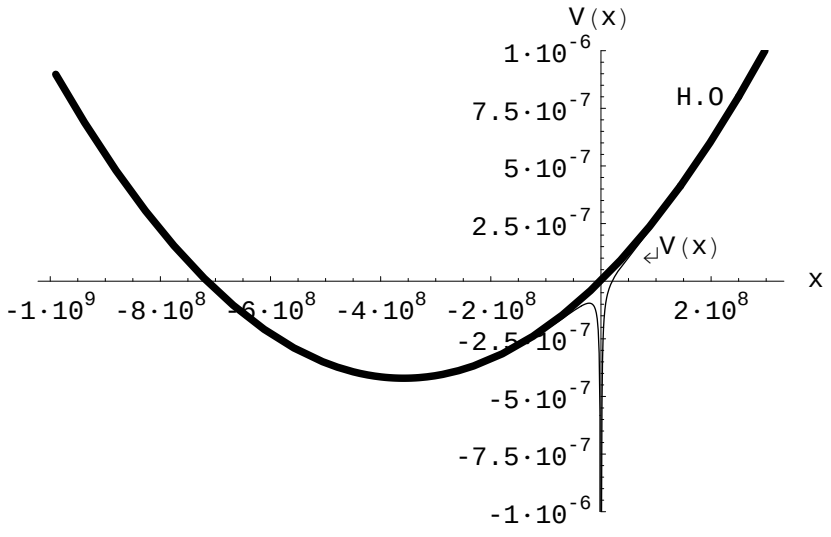

(a)

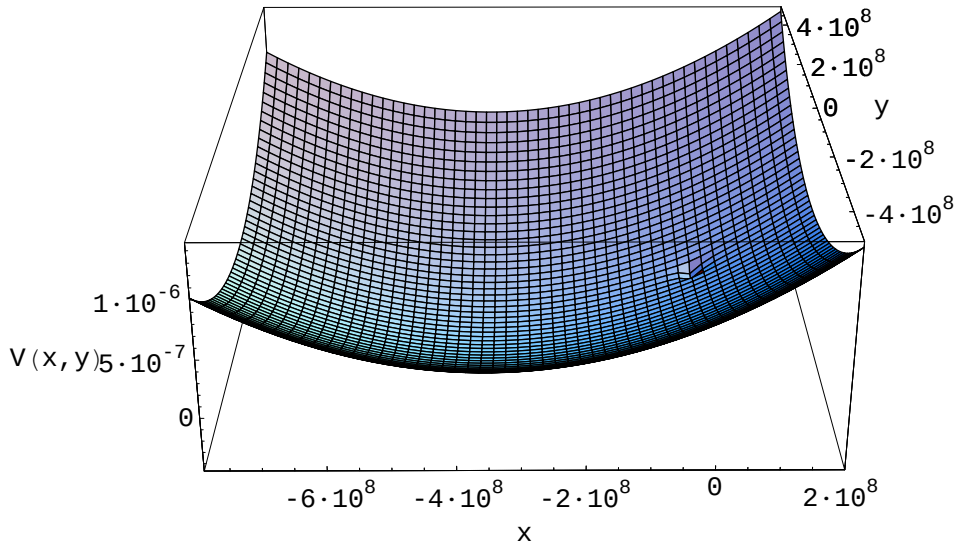

(b)

Figure 17: Plots of energy surface for $\delta = 1$ of (a) two-dimensinal and (b) three-dimensional. Energy surface has a minimum at $x_m \simeq -3.5817 \times 10^8$ a.u. for $B = 1T$ and $E = 10V/cm$. (H.O.) indicates the harmonic oscillator and it shows very good agreement.

CHAPTER VI

CLASSICAL ANALYSIS OF THE IONIZATION OF TWO ELECTRON ATOMS

6.1 Introduction

The three-body problem with Coulomb interactions is one of the most important examples of nonintegrable Hamiltonian systems [6]. The classical dynamics of collinear e^-Ze^- Coulomb three-body system (eZe configuration) was mainly motivated by the interest of applying semiclassical methods to chaotic systems. As an improvement on Wannier's pioneering work [155], its results are in excellent agreement with experiments [156, 157, 158, 159, 160]. Advances in a semiclassical treatment of the three-body Coulomb problem were possible only due to a better understanding of the classical dynamics of the system. For the eZe configuration, the special interest lies in chaotic scattering. In the case of classical chaotic scattering, the scattering functions have a fractal set of singularities [161]. This fractal set of singularities is the result of the interaction of the incoming electron asymptotes with the underlying chaotic invariant set. When the scattering electron trajectory starts exactly on the stable manifold of the chaotic set it stays on the chaotic set forever, resulting in a singularity of the scattering function. Furthermore, the structure of the set of singularities is the same as the structure of the chaotic invariant set [162]. Furthermore, the chaotic invariant set is usually represented by the construction of a Horseshoe Map [163] in an appropriate Poincaré surface of section. The stable and unstable manifolds for a fixed point should be clarified before the construction of a Horseshoe Map. However, we will show in this chapter that the map can not be obtained for the system of one-dimensional three-body Coulomb interaction. This will be discussed in the last

section.

6.2 Classical Dynamics of Three-Body Coulomb Problem

6.2.1 Scaling of the Hamiltonian

For a nucleus with charge Z and infinite mass, the nonrelativistic Hamiltonian configured by two Coulomb potential and a interaction term between two electrons, reads in atomic units ($e = m_e = 1$)

$$H = E = \frac{p_{r1}^2}{2} + \frac{p_{r2}^2}{2} - \frac{Z}{r_1} - \frac{Z}{r_2} + \frac{1}{r_{12}}, \tag{6.1}$$

where the electron-nucleus distances are given by $r_j\,(j = 1, 2)$ and the distance between the electrons is r_{12} ($=|r_1 \pm r_2|$). The "+" sign corresponds to eZe configuration and "–" sign to the Zee configuration. Z will be 2 for the helium atom. Whenever an interparticle distance vanishes (particle collision), the potential energy diverges. Figure 18 is a schematic plot of the coordinates.

The classical Three-Body system can be reduced to four degrees of freedom after eliminating the center of mass motion and incorporating the conservation of the total angular momentum. In the case of zero angular momentum, the equations of motion for the Hamiltonian reduce to three degrees of freedom because both electrons are confined to a common plane of the three-dimensional configuration space. This means that the total angular momentum of the electrons points perpendicular to the plane. Such a planar system describes the general motion for the case of zero angular momentum. Using infinite nuclear mass approximation, scaling properties are considered in the three body Coulomb problem in two different ways, (1) scaling the phase space coordinates with respect to energy and, (2) scaling out an overall size parameter considering only the shape dynamics of the system [164]. The energy dependence of the classical dynamics is equivalent to a scaling transformation of the classical motion in phase space, since the potential energy is a homogeneous function

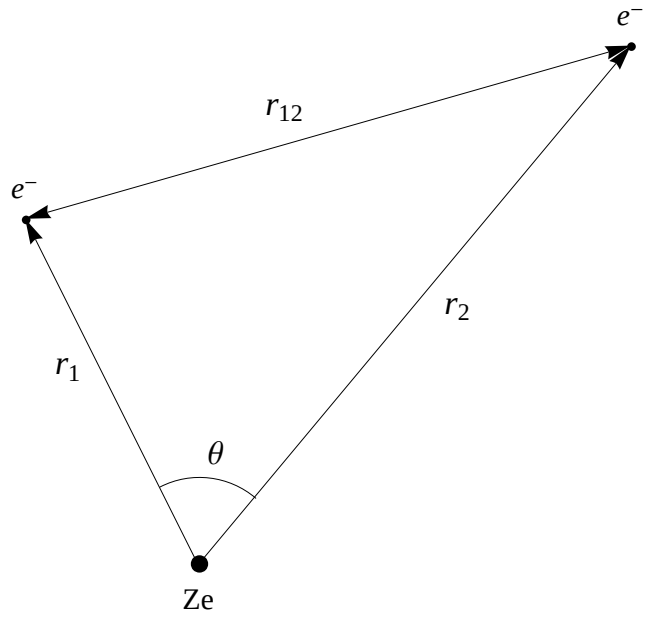

Figure 18: Schematic plot of the coordinates r_1, r_2 and r_{12}.

of the coordinates. Choosing the canonical transformation

$$\begin{aligned} r_i &= |E| r_i' \\ p_{ri} &= \frac{1}{\sqrt{|E|}} p_{ri}' \end{aligned} \tag{6.2}$$

and a time transformation

$$t = |E|^{3/2} t' \tag{6.3}$$

eliminates the energy dependence in the classical Hamiltonian. The dynamics for the classical system can be reduced to three district cases by the above transformations

$$H = \frac{p_{r1}^2}{2} + \frac{p_{r2}^2}{2} - \frac{Z}{r_1} - \frac{Z}{r_2} + \frac{1}{|r_1 + r_2|} = \begin{cases} +1 & \mathrm{E} > 0 \\ 0 & \mathrm{E} = 0 \\ -1 & \mathrm{E} < 0 \end{cases}$$

Briefly, $H = +1$ regime corresponds to the energy region in which three-body breakup is possible. There exist no periodic orbits of the electron and at least one electron escapes to infinity [6]. This region is linked to $E > 0$ and is important for studying

the energy dependence on the total quantum cross section for the three particle fragmentation by considering the breakup along Wannier orbit [155, 165]. At a ridge of the Wannier orbit, the conditions for introducing the orbit, $p_\alpha = 0$ and $\alpha = \pi/4$ is connected to $E = 0$ configuration. Detailed discussion of this energy regime can be found in Rost [166, 167].

The classical dynamics for $E < 0$ are linked to $E = -1$. In this regime, only one electron can escape classically and it will do for the most initial conditions. The phase space can be reduced to four dimensions. In this regime, only one electron can escape classically and it will do for the most initial conditions. The phase space can be reduced to four dimensions and the dynamics in the reduced space turns out to be relatively simple. A similar approach has been employed by Wannier [155] by extrapolating dynamical behavior at $E = 0$ to the dynamics for $E > 0$.

The dynamics for $E = 0$ can be reduced to four dimensional system using an additional scaling relation (6.2) following McGehee [168].

6.2.2 Fixed Points and Invariant Manifold of the eZe Configuration

The Hamiltonian (6.1) can be transformed to a representation in hyperspherical coordinates for zero angular momentum. Define a hyperradius and hyperangle as follows

$$\begin{aligned} R &= \sqrt{r_1^2 + r_2^2} \\ \tan\alpha &= \frac{r_2}{r_1} \end{aligned} \tag{6.4}$$

where $r_1 = R\cos\alpha$, $r_2 = R\sin\alpha$. Interelectronic angle will be defined by θ as a difference between two azimuthal angles of each electrons. Thus the Hamiltonian may be transformed to

$$H = \frac{1}{2}\left(P_R^2 + \frac{p_\alpha^2}{R^2} + \frac{p_\theta^2}{R^2\cos^2\alpha\sin^2\alpha}\right) + \frac{1}{R}V(\alpha,\theta) \tag{6.5}$$

where

$$V(\alpha,\theta) = -\frac{Z}{\cos\alpha} - \frac{Z}{\sin\alpha} + \frac{1}{\sqrt{1-2\cos\alpha\sin\alpha\cos\theta}}. \tag{6.6}$$

If (θ,p_θ) equals (0,0) or (π,0), then θ remains constant. The motion then reduces by one degree of freedom and resembles that of a collinear atom. If (α,p_α) equals (0,0), ($\pi/4$,0), or ($\pi/2$,0). For $\alpha = 0$ and $\alpha = \pi/2$ the motion is reduced to that of a single electron atom. The solution $\alpha = \pi/4$ defines the Wannier ridge of collective motion, where both electron-nucleus distances are the same for all times [170]. In the special case of zero angular momentum, the motion of the three particles is confined to a plane fixed in configuration space [153]; the Hamiltonian including finite nucleus mass terms and after elimination of the center of mass coordinates can be found in Richter *et al.* [154]. If one-dimensional configuration is considered, the interelectronic angle will be set to zero resulting in a reduced Hamiltonian

$$H = E = \frac{1}{2}\left(P_R^2 + \frac{p_\alpha^2}{R^2}\right) - \frac{1}{R}\left(\frac{Z}{\cos\alpha} + \frac{Z}{\sin\alpha} - \frac{1}{\cos\alpha+\sin\alpha}\right) \tag{6.7}$$

where ($2n\pi < \alpha < 2n\pi + \frac{\pi}{2}$). The equations of motion are given by

$$\begin{aligned}
\dot{R} &= P_R \\
\dot{\alpha} &= \frac{p_\alpha}{R^2} \\
\dot{P}_R &= \frac{p_\alpha^2}{R^3} - \frac{1}{R^2}\left(\frac{Z}{\sin\alpha} + \frac{Z}{\cos\alpha} - \frac{1}{\cos\alpha+\sin\alpha}\right) \\
\dot{p}_\alpha &= \frac{1}{R}\left(Z\frac{\sin\alpha}{\cos^2\alpha} - Z\frac{\cos\alpha}{\sin^2\alpha} + \frac{\cos\alpha-\sin\alpha}{(\cos\alpha+\sin\alpha)^2}\right).
\end{aligned} \tag{6.8}$$

Scaling may be performed to the variables with respect to the hyperradius (R). Scaling transformations by

$$\begin{aligned}
P_R &= \frac{1}{\sqrt{R}}\bar{P}_R \\
p_\alpha &= \sqrt{R}\bar{p}_\alpha \\
\alpha &= \bar{\alpha} \\
H &= \frac{1}{R}\bar{H}
\end{aligned} \tag{6.9}$$

and a transformation of the time

$$\mathrm{d}t = R\sqrt{R}\,\mathrm{d}\bar{t}. \tag{6.10}$$

result in new equations of motion (dropping the "bar" in the equations). However, $\bar{H}$ will be used for convenience.

$$\begin{aligned}
\dot{\alpha} &= p_\alpha, \qquad & \dot{p}_\alpha &= -\frac{1}{2}P_R p_\alpha - \frac{\partial}{\partial\alpha}V(\alpha) \\
\dot{R} &= RP_R, & \dot{P}_R &= \frac{1}{2}p_\alpha^2 + \bar{H} \\
\dot{\bar{H}} &= P_R\bar{H}. & &
\end{aligned} \tag{6.11}$$

Fixed points and invariant subspaces can be found from the equations of motion (6.11) as follows,

$$\begin{aligned}
p_\alpha &= 0 \\
\alpha &= \frac{\pi}{4} \\
P_R &= \pm P_0 = \pm\sqrt{\sqrt{2}(4Z-1)}.
\end{aligned} \tag{6.12}$$

From the second condition above,

$$\tan\alpha = r_2/r_1 = 1 \tag{6.13}$$

the distances between the nucleus and two electrons, r_1 and r_2, are equal. R denotes the hyperradius, the radius in hyperspace represented by r_1 and r_2, increases for a positive P_R and decrease for a negative P_R. When it decreases, $P_R = -P_0$, the two electrons will collide with the nucleus simultaneously. The point P_R will be called triple collision point (TCP). Its time reversal produces $P_R = +P_0$. Because overall dynamics is invariant under $p \to -p$ and $\mathrm{d}t \to -\mathrm{d}t$, the time reversal of TCP corresponds to double escape point. The triple collision point and double escape point (DEP) are thus equivalent and related by time reversal symmetry. From the Hamiltonian eq. (6.5) and scaling transformation (6.9), the Wannier ridge space is

described by

$$\bar{H} = \frac{1}{2}P_R^2 + 2p_\theta^2 - 2\sqrt{2}Z + \frac{1}{\sqrt{1-\cos\theta}} = 0, \tag{6.14}$$

and it is a compact space with the topology of a sphere where the fixed points form opposite poles [164]. Figure 19 shows a plot of the TCP and DEP. The interior of the sphere corresponds to the phase space of Wannier ridge for $E < 0$ and the Wannier ridge is connected to eZe configuration at the fixed points of $E = 0$ along Wanner orbit (WO), where satisfies following relations

$$\alpha = \pi/4,\ \theta = \pi,\ p_\alpha = 0, \quad \text{and } p_\theta = 0 \text{ for } E < 0. \tag{6.15}$$

The Hamiltonian along the Wannier orbit is given by

$$\bar{H} = \frac{P_R^2}{2} - 2\sqrt{2}Z + \frac{\sqrt{2}}{2} = 0, \tag{6.16}$$

resulting in

$$P_R = \pm P_0 = \pm\sqrt{\sqrt{2}(4Z-1)} \tag{6.17}$$

which is same as the value derived in eq. (6.12).

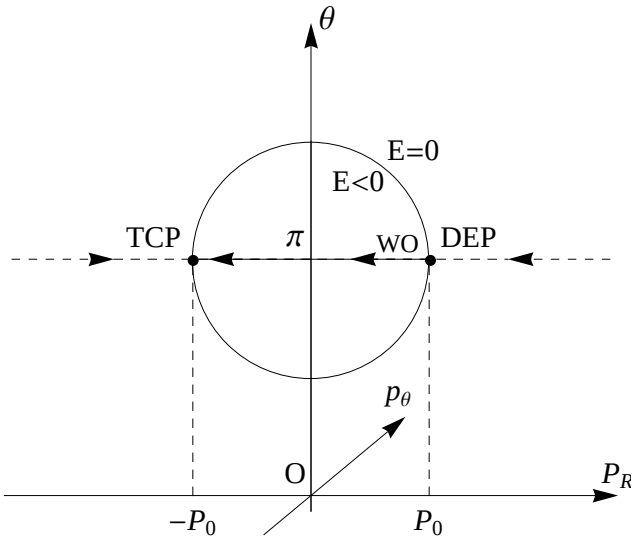

Figure 19: Wannier ridge manifold for $E = 0$. Along the Wannier orbit (WO) the subspaces are connected through TCP and DEP [164].

For the eZe configuration, the orbit coming from $P_R \ll -P_0$ close to triple collision orbit will approach the TCP point along the a triple collision orbit which ends in the TCP. After reaching to TCP, it will leave the triple collision region into one of the orbit of single ionization toward $P_R \gg P_0$ [164]. This single ionization will be considered in following section.

6.3 Analysis of the eZe configuration in Regularized Coordinates

An essential ingredient for the classical analysis of the Three Body Coulomb problem is the regularization of the motion. In analogy to the motion of the electron in the hydrogen atom, the motion can be regularized for binary collisions, where only one interparticle distance vanishes. However, the triple collision ($r_1 = r_2 = r_{12} = 0$) cannot be regularized, e.g. these solutions have branch points of infinite order [171]. Thus, it is very hard to access to information near the triple collision point. This is why asymptotic analysis is introduced to the three body chaotic scattering problem. Regularization deals with infinite or divergent expressions like $1/r$ as $r \to 0$. It introduces an auxiliary concept of a regulator, for example, the minimal distance r in space which is useful if the divergences arise from short-distance physical effects. The correct physical result is obtained in the limit in which the regulator goes away, however, the virtue of the regulator is that for its finite value, the result is finite. The regularization is the first step to obtain a completely finite and meaningful result.

6.3.1 Kustaanheimo-Stiefel Coordinates

To regularize the binary collisions a procedure of Aarseth and Zare [173] will be used, which is essentially a double Kustaanheimo-Stiefel (KS) transformation together with a modified Levi-Civita regularization. Levi-Civita's regularization of the plane motion

starts with introducing a parameter-plane $w = u_1 + iu_2$ mapped onto the physical $z - plane$ conformally by the transformation

$$\begin{aligned} z &= x_1 + ix_2 = w^2 \\ &= u_1^2 - u_2^2 + i(2u_1u_2). \end{aligned} \tag{6.18}$$

Accordingly parabolic coordinates are introduced in the physical plane. A conical section centered at the origin of the $w - plane$ is transformed into a conical section of the $z - plane$ having one focus at the origin; therefore the transformation is very practical method for the discussion of a Kepler or Coulomb potential problem [174]. For the one-dimensional eZe configuration, rewrite the Hamiltonian,

$$H = E_0 = \frac{p_{r1}^2}{2} + \frac{p_{r2}^2}{2} - \frac{Z}{r_1} - \frac{Z}{r_2} + \frac{1}{r_1 + r_2}. \tag{6.19}$$

The transformation to regularized coordinates (Q_i,P_i),

$$\begin{aligned} r_1 = Q_1^2, \qquad p_{r1} = \frac{P_1}{2Q_1} \\ r_2 = Q_2^2, \qquad p_{r2} = \frac{P_2}{2Q_2} \end{aligned} \tag{6.20}$$

and

$$\mathrm{d}t = Q_1^2 Q_2^2 \, \mathrm{d}\tau \tag{6.21}$$

lead to a new Hamiltonian

$$H_Q = \frac{P_1^2}{8Q_1^2} + \frac{P_1^2}{8Q_2^2} - \frac{Z}{Q_1^2} - \frac{Z}{Q_2^2} + \frac{1}{Q_1^2 + Q_2^2}. \tag{6.22}$$

where τ describes the scaled time. Thus, the regularized Hamiltonian is defined by

$$G = Q_1^2 Q_2^2 (H_Q - E_0), \tag{6.23}$$

and associated equations of motion are given by

$$\begin{aligned} \frac{\mathrm{d}Q_i}{\mathrm{d}\tau} &= \frac{\partial G}{\partial P_i} \\ \frac{\mathrm{d}P_i}{\mathrm{d}\tau} &= -\frac{\partial G}{\partial Q_i}. \end{aligned} \tag{6.24}$$

It is advantageous to employ McGehee scaling [168] by the hyperradius (R) in addition to the KS transformation:

$$\begin{aligned} Q_i &= \sqrt{R}\bar{Q}_i \\ P_i &= \bar{P}_i \\ \mathrm{d}\tau &= \frac{1}{\sqrt{R}}\,\mathrm{d}\bar{\tau} \end{aligned} \tag{6.25}$$

with $R = \sqrt{r_1^2 + r_2^2} = \sqrt{Q_1^4 + Q_2^4}$. The equations of motion in the scaled coordinates are given by

$$\begin{aligned} \frac{\mathrm{d}\bar{Q}_1}{\mathrm{d}\bar{\tau}} &= \frac{1}{4}\bar{Q}_2^2\bar{P}_1 - \frac{1}{4}\bar{Q}_1^3\bar{Q}_2^2(\bar{Q}_1\bar{P}_1 + \bar{Q}_2\bar{P}_2) \\ \frac{\mathrm{d}\bar{Q}_2}{\mathrm{d}\bar{\tau}} &= \frac{1}{4}\bar{Q}_1^2\bar{P}_2 - \frac{1}{4}\bar{Q}_1^2\bar{Q}_2^3(\bar{Q}_1\bar{P}_1 + \bar{Q}_2\bar{P}_2) \\ \frac{\mathrm{d}\bar{P}_1}{\mathrm{d}\bar{\tau}} &= -\frac{1}{4}\bar{Q}_1\bar{P}_2^2 + 2Z\bar{Q}_1 - 2\bar{Q}_1\bar{Q}_2^2 + \bar{Q}_1^5\bar{Q}_2^2 + 2R\bar{Q}_1\bar{Q}_2^2E_0 \\ \frac{\mathrm{d}\bar{P}_2}{\mathrm{d}\bar{\tau}} &= -\frac{1}{4}\bar{Q}_2\bar{P}_1^2 + 2Z\bar{Q}_2 - 2\bar{Q}_2\bar{Q}_1^2 + \bar{Q}_2^5\bar{Q}_1^2 + 2R\bar{Q}_2\bar{Q}_1^2E_0. \end{aligned} \tag{6.26}$$

The scaled energy $\bar{E}$ is given by $\bar{E} = RE$ and the equation of motion with respect to the scaled time is

$$\frac{\mathrm{d}\bar{E}}{\mathrm{d}\bar{\tau}} = \frac{1}{2}\bar{Q}_1^2\bar{Q}_2^2(\bar{Q}_1\bar{P}_1 + \bar{Q}_2\bar{P}_2)\bar{E}. \tag{6.27}$$

The derivatives of hyperradius and time with respect to the scaled time are given by

$$\begin{aligned} \frac{\mathrm{d}R}{\mathrm{d}\bar{\tau}} &= \frac{1}{2}R\bar{Q}_1^2\bar{Q}_2^2(\bar{Q}_1\bar{P}_1 + \bar{Q}_2\bar{P}_2) \\ \frac{\mathrm{d}t}{\mathrm{d}\bar{\tau}} &= R\sqrt{R}\bar{Q}_1^2\bar{Q}_2^2 \end{aligned} \tag{6.28}$$

Thus regularized equations without singularities are obtained.

6.3.2 Preparation of the Chaotic Invariant Set

The fixed points are found from the equations of motion for the Hamiltonian (6.1),

$$\begin{aligned} \dot{r_2} &= p_{r2} \\ \dot{p}_{r2} &= -\left(\frac{Z}{r_2^2} - \frac{1}{(r_1 + r_2)^2}\right) \end{aligned} \tag{6.29}$$

Equations for r_1 can be found by replacing the index by 1. The the fixed points are

$$\begin{aligned} p_2 &= 0 \\ r_2 &= \pm\infty. \end{aligned} \tag{6.30}$$

For a given value r_2 ($\neq 0$), the eigenvalues (λ) are given by

$$\lambda^2 = \frac{4}{r_2^3}(1 \pm \sqrt{2}) \tag{6.31}$$

where for $\lambda^2 > 0$ the system has hyperbolic fixed points. Thus the considered three-body Coulomb problem contains the hyperbolic fixed points and thereby the stable or unstable manifold may be constructed near the fixed points.

The Hamiltonian of the considering three-body Coulomb problem consists of 5 contributions:

1. The kinetic energy of electron 1 = $p_{r1}^2/2$
2. The kinetic energy of electron 2 = $p_{r2}^2/2$
3. The potential between electron 1 and the origin = - Z/r_1
4. The potential between electron 2 and the origin = - Z/r_2
5. The potential between the two electrons = + $1/(r_1 + r_2)$

At energy $E < 0$ two asymptotic arrangement channels are open:

(a) The channel 0 where both electrons go far away only opens for positive total energy.

(b) In channel 1, the electron 1 goes far away and electron 2 stays close to the origin. The corresponding asymptotic Hamiltonian is

$$H_{as1} = \frac{p_{r1}^2}{2} + \frac{p_{r2}^2}{2} - \frac{Z}{r_2} - \frac{Z-1}{r_1}. \tag{6.32}$$

From far away the electron 1 sees an effective charge $Z-1$ at the origin. The channel interaction W_1 is the difference between the complete Hamiltonian and the asymptotic

channel Hamiltonian

$$\begin{aligned} W_1 &= -\frac{Z}{r_1} + \frac{1}{r_1 + r_2} + \frac{Z-1}{r_1} \\ &= \frac{1}{r_1 + r_2} - \frac{1}{r_1} \\ H &= H_{as1} + W_1. \end{aligned} \tag{6.33}$$

First, the interaction which plays the role of some kind of scattering potential, is short range. When $r_1 \gg r_2$, W_1 can be approximated as follows

$$\begin{aligned} W_1 &= \frac{1}{r_1 + r_2} - \frac{1}{r_1} \\ &\simeq \frac{1}{r_1}\left(1 - \frac{r_2}{r_1} - 1 + O(r_1^{-2})\right) \\ &\simeq \frac{r_2}{r_1^2}. \end{aligned} \tag{6.34}$$

Thus it falls off like $1/r^2$ and avoids all problems with the asymptotic conditions which a Coulomb potential has.

Second, this interaction is always negative if the two electrons are placed on different sides of the origin, actually eZe configuration set the two electrons on different sides, *i.e.*, the potential is a strictly attractive scattering potential.

Following the contributions, Figure 20 shows the plot of the scattering time as an example of the scattering function. The graph illustrates the chaotic scattering region for negative energy ($E = -1$). Details will be explained in the next section. The scattering function is a quantity which can be used for the reconstruction of the internal dynamics [169]. Thus, initial conditions in a asymptotic regime, eventually, allow to understand the structure of singularities of the scattering function [172].

The phase angle of the Figure 20 can be calculated from action-angle variable for the motion of the bound electron. The time derivative of the angle variable may be calculated as

$$\dot{\phi} = \frac{(-2E_2)^{3/2}}{Z} \tag{6.35}$$

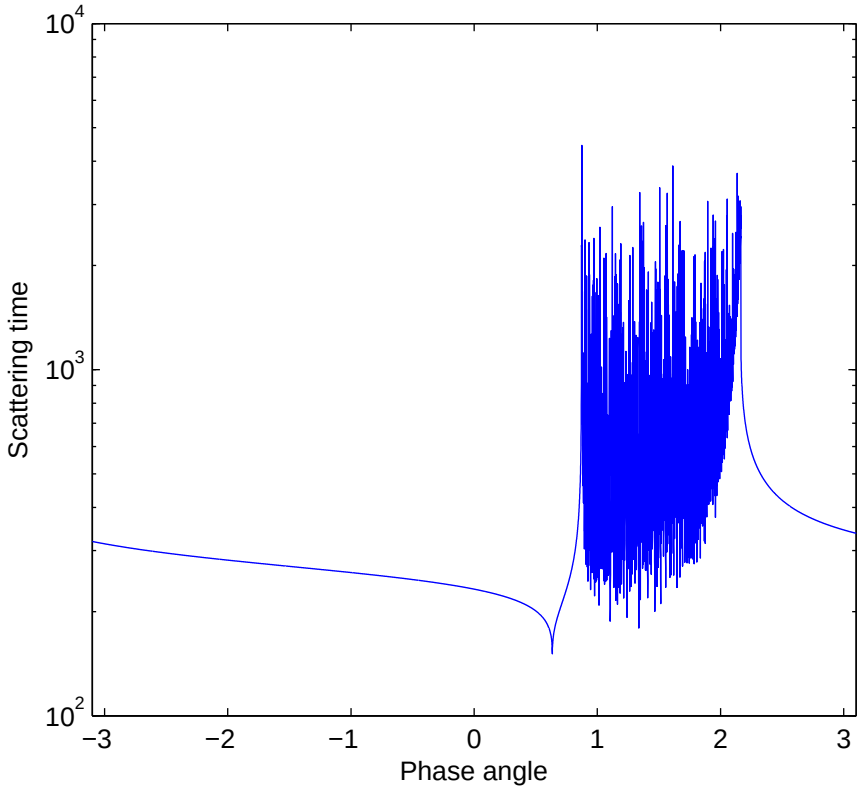

Figure 20: This plot shows the scattering time on a domain which covers all singularities over the phase angle $-\pi < \delta\phi < -\pi$.

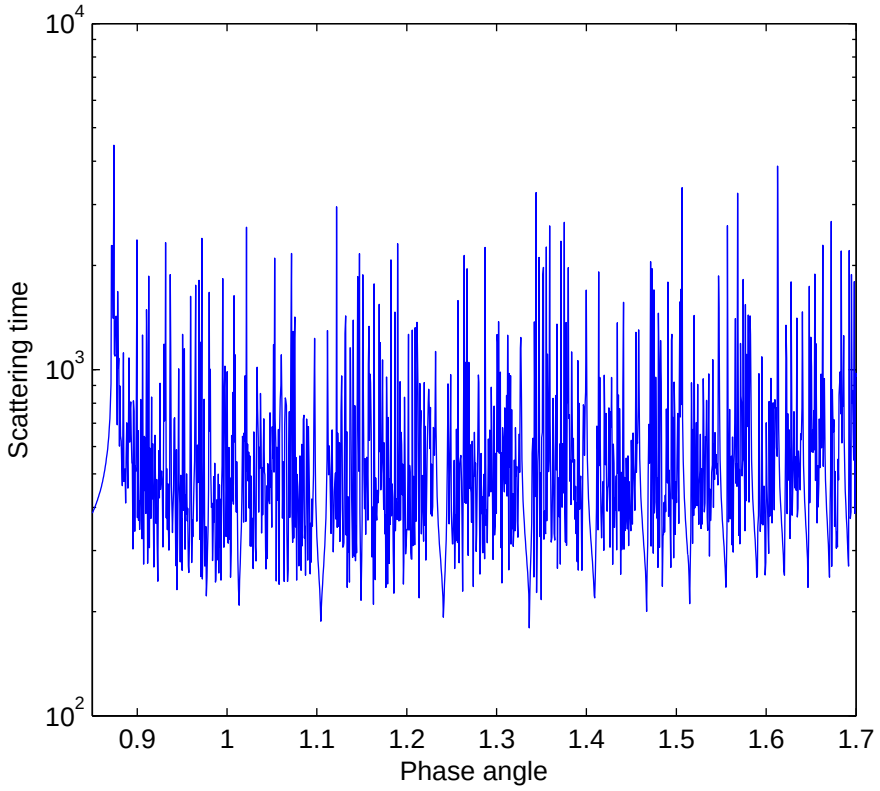

Figure 21: Magnification of subintervals of the scattering function. The intervals of continuity can be labeled by their level of hierarchy.

Thus the period of the motion is given by

$$T_2 = \frac{\pi a}{\sqrt{2|E_2|}}, \tag{6.36}$$

where a ($=-Z/E_2$) is the oscillation length of the bound electron, and E_1, E_2 correspond to the energy of outer and bound electron, respectively. A distance that the outer electron passes during a period of the motion of the bound electron, which is represented by δr_1 is defined from an approximation, initial location r_0 much larger than the oscillating length of the motion of a bound electron. If the outer electron is located far from the nucleus, the Hamiltonian of the electron is simply the free electron's Hamiltonian. Using the time derivative of the distance, the δr_1 is represented by

$$\delta r_1 = \pi a \sqrt{\left|\frac{E_1}{E_2}\right|}. \tag{6.37}$$

Using above two equations the phase angle is given by a function of δr_1

$$\delta\phi = -\frac{2E_2}{Z}\sqrt{\left|\frac{E_2}{E_1}\right|}\delta r_1. \tag{6.38}$$

(c). For channel 2, the Hamiltonian and associated equations of motion of the system can be defined in analogy by interchanging the indice.

When the negative energy $E = -1$ and channel 1 are considered, the Poincarée map will be chosen to the surface of intersection which is $p_{r2} = 0$. For channel 1, this is a good choice. Let's take as line of initial conditions a segment of the curve

$$p_{r1}(r_1) = \sqrt{\frac{2(Z-1)}{r_1}} \tag{6.39}$$

for r_1 sufficiently large so that the asymptotic Hamiltonian is a good approximation. The position of the other electron (2) must be kept constant at $r_2 = Z$ for these initial conditions. Then on this line electron 2 provides all the energy -1 and electron 1 has energy 0. Therefore, far out this line is a very good approximation to the separatrix between going off to infinity and returning. i.e. it is a very good approximation to the

stable manifold of the point at infinity. With negative momentum, i.e. the negative branch of the square root in the above equation, the unstable manifold is obtained, or it is in reverse depending on which side the electron 1 is placed. Remaining calculation to get invariant manifold is to iterate the initial line segments forward or backward many times to generate the homoclinic tangle. Note that the initial errors go to zero exponentially in the iteration process because the initial errors are transverse to the initial line segment, i.e. they point in the unstable/stable direction which shrinks exponentially in the iteration process.

6.4 The Scattering Time and Horseshoe Map

One of the two electrons is located at an asymptotic location which is far enough so that the interaction is negligible. When it comes close to interaction region, the interaction should be considered. For very small distances, it is very difficult to do numerical calculations and analyze the scattering process. However, there is a indirect method to analyze the system without considering the small range interaction. Scattering functions give properties of the final electron asymptotes as a function of the incoming electron asymptotes. The investigation of the scattering functions is a variety of indirect study. The intersection of the incoming electron asymptotes with the invariant manifolds of the chaotic invariant set in the asymptotic region produces singularities [176]. The chaotic invariant set underlies the structure of the classical phase space in the sense that its properties determine the quantities that characterize the scattering process.

The Horseshoe Map is mainly intended for the structural understanding of the dynamics in chaotic system. In chaotic systems, we always have homoclinic and/or heteroclinic interactions of invariant manifolds [175], and this pair is always connected with a Horseshoe construction [175]. The Smale Horseshoe construction proceeds

stretching a so-called fundamental region [172]. The structural understanding of the chaotic scattering means some knowledge of the structure of the chaotic invariant set, so-called chaotic saddle, its partition and its thermodynamic quantities [177]. The matter of obtaining scattering functions directly from the system is complicated. This complication, however, can be avoided assuming that the scattering functions are directly available as asymptotic data [162]. We restrict our attentions to a simple case, eZe configuration. The goal of this section is to extract from asymptotic data information about the chaotic invariant set, represented by a Horseshoe construction in an appropriate Poincaré section [169, 161].

6.4.1 The Scattering Function

If the motion in the interaction region can be observed directly, the construction of the Horseshoe Map from this measurements is straightforward. We only consider the situation where the direct access to the interaction region is not possible and only the asymptotic preparation of initial states and asymptotic measurements of the final states are possible.

As mentioned earlier, the scattering function is a quantity which can be used for the reconstruction of the internal dynamics [169]. The time delay function, for instance, can be a good scattering function for the problem of eZe configuration because the data it contains give the properties of the final asymptote as a function of the properties of the initial asympototte. The scattering time signals, as a time delay function of this system, in the Figure 20 were scanned numerically with respect to the phase angle. Total energy was set to $E = -1$ and initial location of the outer electron to $r_1 = 100$ in atomic units. The regularized equations of motion in the previous section were used for numerical calculations. For each launched trajectories of a outer electron, the scattering time was measured until one of the electrons reached the

outgoing asymptotic region ($r_i = 100\,a.u.$, $i = 1\,or\,2$ same as the initial distance). The scattering time indicates the duration of which the electrons stayed in the interaction region.

The Figure 21, the magnification of the Figure 20, shows clearly the intervals of continuity, small gaps between two group of chaotic oscillating signals. The interval is the characteristic figure of the chaotic scattering which the construction of the Horseshoe Map is possible [178]. Each interval has a number of hierarchy level number and the number is the number of times which a scattering trajectory steps into the fundamental region. The number is a constant in any interval of continuity of the scattering functions. Thus the construction of the Horseshoe Map for the considering system, one-dimensional eZe configuration, may be possible.

6.4.2 Construction of the Horseshoe Map

Let the two fixed points be P_s and P_u. The stable manifold theorem states that for a smooth map, near a hyperbolic fixed point[1], the stable manifold, points whose forward orbit converges to the fixed point, and the unstable manifold, points with backward orbit converging to the fixed manifold, are both smooth manifolds. In this thesis, the stable and unstable manifold were searched over the phase space (r_1,$\dot{p}_1$) using an idea that if a point was on the stable manifold, the time evolution of the point forward in time would lead to the fixed point. To obtain the unstable manifold, the integration was performed backward in time to test if the point reached to the fixed point. The integrations of the stable manifold backward in time and the unstable manifold forward in time produce the invariant manifolds, thereby stable and unstable tendrils.

The stable and unstable manifolds by time evolution of the fixed points generates

[1] Also it is called saddle point. The eigenvalues (λ_1, λ_2) for the stability matrix are real and have opposite sign. $\lambda_1 < 0 < \lambda_2$ and λ_1, $\lambda_2 \in \boldsymbol{R}$.

fundamental region which is closed space made by the first segments of intersection of the manifolds started from the fixed points. Call the time evolution of the segments "tendril". Repeating the integration for the tendrils eventually construct the hierarchical structure for the Horseshoe Map [175, 169]. The hierarchy level of the intervals of continuity for a part of the time delay function can be constructed as follows:

(a) The computation of the time delay function from proper initial conditions in the asymptotic regime that completely intersects one tendril of the stable manifold of a outer fixed point P_s.

(b) The iteration of the initial conditions using the regularized equations of motion until the initial conditions converge toward the boundary of the fundamental region which is defined by the local segment of the stable and unstable manifold of a fixed point P_u.

(c) The mapping of the intersections of the set of initial conditions with the stable manifold of the fixed point P_s onto the intersections of the iterates with the same stable manifold.

This process will show that the singularity structure of the scattering function is the same as the pattern resulting from the intersection of the stable manifolds with the local segment of the unstable manifold of the another fixed point P_u [172]. That implies that the intervals of continuity of the scattering function correspond to the gaps that the tendrils of the stable manifolds cut into the fundamental area of the Horseshoe Map construction.

6.4.3 Discussion

Contrary to our expectation, the Horseshoe Map for the one-dimensional three body Coulomb problem could not be obtained by our research. The time evolution of a trajectory at initial asymptotes was obtained by integration along the regularized

equations of motion. The unstable and stable manifold obtained by integration of the fixed point, a initial asymptote which was located far enough to be assumed as a infinite distance. The integration was performed backward in time for the stable manifold and forward in time for the unstable manifold.

However, these two lines never met each other, and therefore the fundamental region could not be constructed. Figure 22 shows Poincaré surface of section, which shows chaotic properties of this eZe configuration for the energy $E = -1$ and the Figure 23 is the plot of the stable and unstable manifolds. Initially, the bound electron was located at its outer turning point and the momentum of the electron was zero at that time and the outer electron was located at the initial asymptote, $r = 100$ a.u.. Whenever the momentum of the bound electron was zero, the outer electrons coordinate and momentum were recorded for the Poincaré surface of section. Because the motion of the bound electron is a oscillatary motion, if it is not scattered, the motion of the outer electron in the phase space follows two trajectories.

Figure 24 shows the possible two trajectories. As it can be seen from the Figure 23, the stable (upper) and unstable (lower) manifolds have not cross each other, and therefore the fundamental region could not be constructed. However, the Figure 24, magnified figure of the Figure 23, showed a possible candidate for the construction of hierarchy. The dots and circles illustrated in the Figure 24 were obtained after tracing the trajectories of both electrons. The dot indicates that the outer electron was scattered and the circle explains the bound electron was scattered. The scattering takes place along the two trajectories alternatively. Thus, if the position of the change can be expressed in terms of phase angle and initial asymptote with a possible quantity which corresponds to the interval of the time delay function, the hierarchy structure could possibly be constructed.

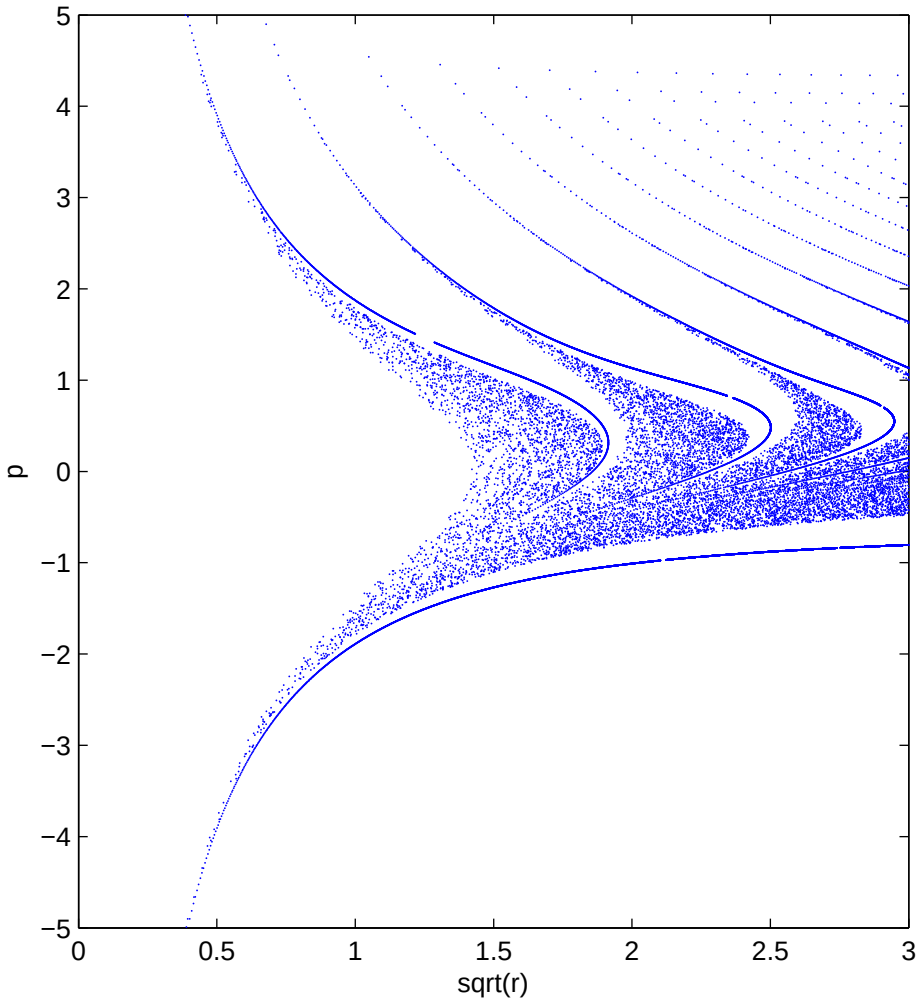

Figure 22: Poincaré surface of section of the outer electron for E=-1.

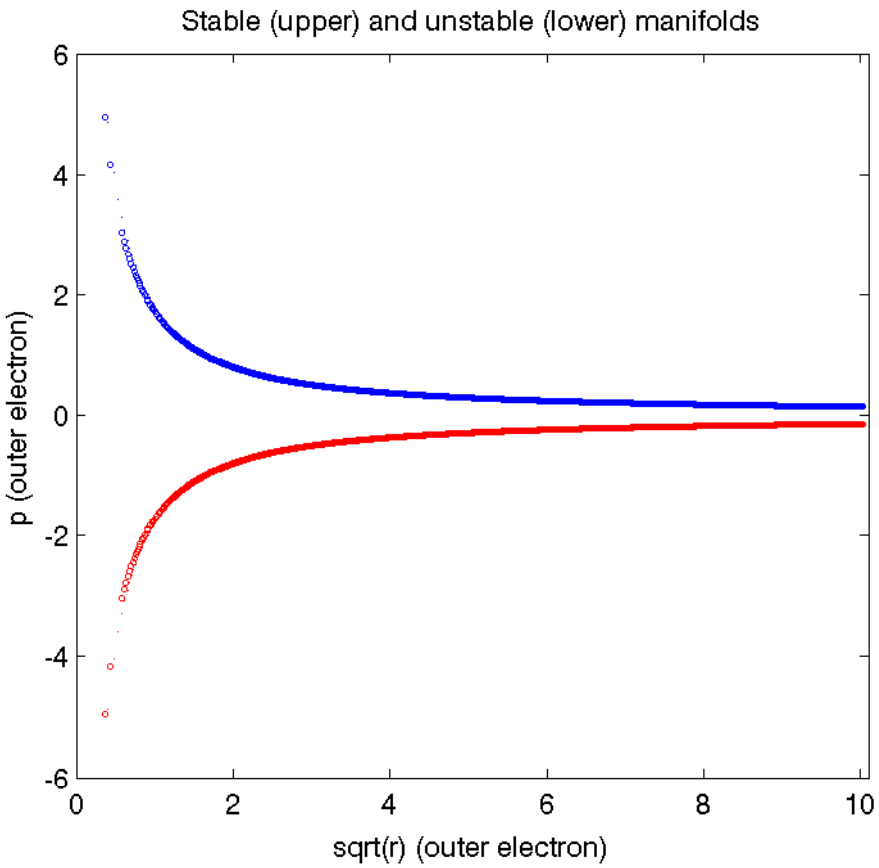

Figure 23: Stable ($p > 0$) and unstable ($p < 0$) manifolds.

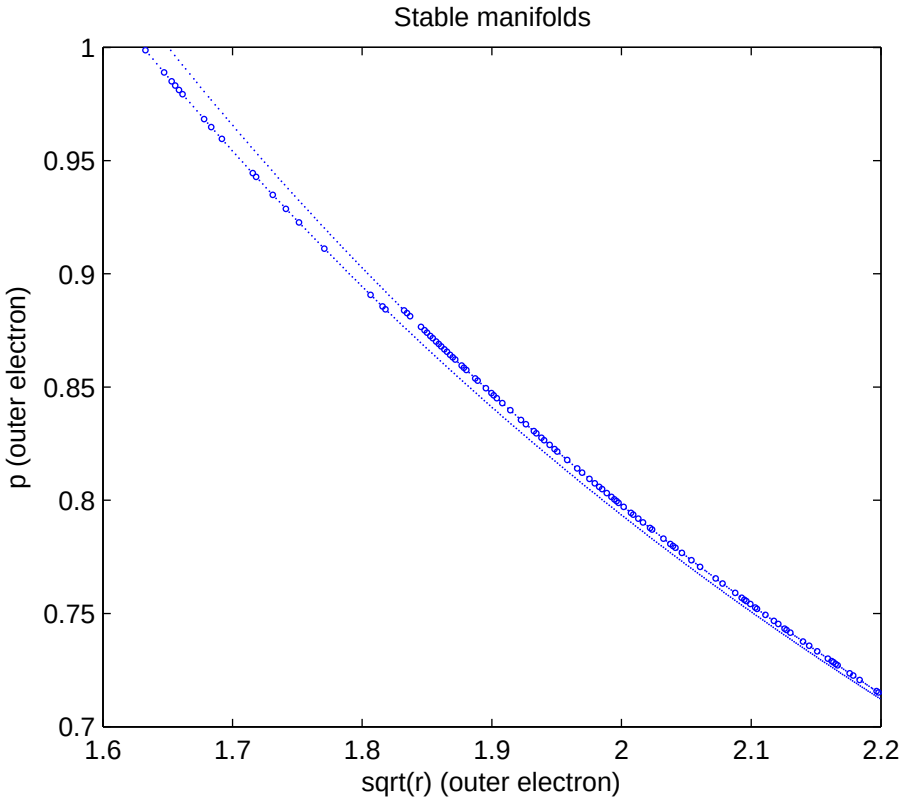

Figure 24: Magnified plot of the phase space of the Figure 23.

CHAPTER VII

CONCLUSIONS

In this thesis we investigated what modern nonlinear-dynamical methods could tell us about reducing the spreading of wavepackets in atomic physics. This thesis was devoted to atomic systems which contain large Coriolis-like interactions which were too large to be treated by perturbation theory and understanding the effect of Coriolis terms. These interaction terms might arise quite straightforwardly as a paramagnetic term for an atomic electron which interacted with a constant magnetic field, or more subtly, from viewing the atomic problem from a rotating frame.

The treatment of Coriolis terms by classical mechanics forced one to go beyond well-established notions of stability at a potential minimum. Indeed, by mixing coordinates and momenta in a bilinear fashion, the Coriolis term made the the definition of a conventional potential impossible. For, if the term were to be treated as part of the potential, that potential would become momentum dependent; whereas regarding it as a part of the kinetic energy could make the kinetic energy negative.

In Chapter 1, a well-established way of taking into account these subtleties was shown, transformation to a stable potential minimum. We went beyond the classical mechanics and explored the quantum mechanics of wave packets in such systems. We were guided by the work rotating systems known as under the name of "Cranked Oscillator" model. The model was summarized in the first chapter.

Chapter 2 showed the possibility of finding classical equilibrium points in the dynamics of the hydrogen atom in circularly polarized (CP) fields. These fields produced equilibrium points at which the coherent states could be constructed and the nature of the hydrogen atom was very similar to those of RTBP. The CP field created

the equilibrium points on the ZVS and the stable coherent wave packets could be launched at a equilibrium position and they were supported quantum mechanically.

In Chapter 3, we went one step further by asking if the motion of the electron, represented by a non-spreading (or slowly-spreading) wave packet could be controlled using external fields, such as a dipole field. The ultimate aim was to make wave packets move in a prescribed way before they could spread appreciably. As a first step, the behavior of cranked oscillator coherent states in a dipole field was presented, time independent and time dependent couplings: we found that they indeed could move in a way prescribed by the dipole field, constructing near-coherent states for specific atomic potentials. The properties in the field configuration were investigated by Glauber-type coherent states.

As an application of the construction of the coherent states by expanding the potential minimum, the guiding center atom was introduced at Chapter 4. The system of $electron - ion$ pair could not be separated into kinetic energy and potential nor a ZVS easily. Thus it needed to be manipulated into more separable form:

First, rapid cyclotron motion could be averaged out in the limit of which the electron cyclotron frequency was the largest of the dynamical frequencies. This cancellation was possible because of huge mass difference between the electron and ion, in addition to the strong magnetic field, which led to "guiding center" approximation.

Second, moving along the magnetic field direction generated constants of motion illustrating transverse motion to the field. The pseudomomentum played important role in separating the center of mass and reducing internal degrees of freedom.

Third, the motion along z-axis could be dealt with elliptic integral and the z-motion could be decoupled from the Hamiltonian.

Thus, the reduced Hamiltonian was obtained and the potential function indicated a two dimensional harmonic oscillator. The plot of the energy surface showed that the system could be locally harmonic at the minimum point. The coherent states

could be constructed at the minimum point as follows,

$$\Psi(y) = \frac{1}{\sqrt{b}\pi^{1/4}} \exp[-(y - y_{cl})^2/2b^2], \tag{7.1}$$

where $b = \sqrt{\hbar/m\omega}$ for a classical harmonic oscillator with a frequency ω. y_{cl} is the classical trajectory. The variable of the above coherent state, y, was the relative distance between the two particles, thus the constructed coherent state with respect to the variable y could be used to explain the $\mathbf{E}\times\mathbf{B}$ drafting pair of the Figure 14 because the coherent state would be a non-spreading wave packet as long as the separation of the electron-ion pair remained constant or changed harmonically.

In Chapter 5, as an extension of the guiding center atom, a ion pair in electromagnetic fields was treated. The ion pair is essentially a particle system interacting by means of a Coulombic potential. The Hamiltonian involved a coefficient δ, mass ratio. Because the ratio was almost equal to 1, the coefficient introduced two separate discussion about the system, $\delta \neq 1$ and $\delta = 1$. When $\delta \neq 1$ the behavior of Hamiltonian was quite similar to the Hamiltonian of the Chapter 4, guiding center atom, and the Hamiltonian could be transformed to harmonic oscillator by proper canonical transformation and thereby the coherent state could be built. When $\delta = 1$, the Hamiltonian was completely separable to purely kinetic term and coordinate dependent potential term. For intermediate values of δ the dynamics was similar to $\delta = 0$ not to require a separate discussion.

The canonically transformed system was shifted to the minimum and the potential function was expanded around the point. It transformed the Hamiltonian the the three dimensional harmonic oscillator function and the coherent state could be constructed at the minimum. The coherent states corresponding to the the distance between the two particles showed that the behavior of the states could be used to explain the motion of the ion pair such as drifting atom. Thus it was possible to prepare locally harmonic regimes in ion pair system thereby allowing the creation of almost completely non-dispersive coherent atomic states.

Chapter 6 showed a classical-mechanical investigation of the ionization of a highly excited atom. It involved the phenomenon of chaotic scattering which could be recognized by hierarchical structure of a scattering function. The singularity structure of the scattering function was the same as the pattern resulting from the intersection of the stable manifolds with the local segment of the unstable manifold. An essential ingredient for the classical analysis of the Three Body Coulomb problem was the regularization of the motion. The regularization was impossible near the triple collision point. The matter of obtaining scattering functions directly from the system was complicated. The complication, however, could be avoided by assuming that the scattering functions was directly available as asymptotic data and the asymptotic analysis.

The asymptotic analysis accompanies with the contruction of the Horseshoe Map which is mainly intended to the structural understanding of the dynamics in chaotic system. The goal of the analysis is to extract from asymptotic data information about the chaotic invariant set, represented by a horse construction in an appropriate Poincaré section.

Contrary to our expectation, the Horseshoe Map for the one-dimensional three body Coulomb problem could not be constructed. The time evolution of a trajectory at initial asymptotes was obtained by integration along the regularized equations of motion. The unstable and stable manifold obtained by integration of the fixed point, a initial asymptote which was located far enough to be assumed as a infinite distance, backward in time and forward in time for the stable manifold. The manifolds obtained these two lines never crossed each other, and the fundamental region could not be constructed. Without the fundamental region, the analysis could not be performed. However, a possible way of construction of the hierarchy structure was suggested from the Figure 24, where the two trajectories the scattering happened alternatively.

APPENDIX A

ELLIPTIC INTEGRALS

The incomplete elliptic integral of the first kind of Jacobi[132] is typical. It is

$$\int_0^x \frac{1}{\sqrt{(1-x^2)(1-k^2x^2)}}\mathrm{d}x. \tag{A.1}$$

Gradshteyn and Ryzhik[146] show a very complete collection of formulas. Concerned elliptic integral is the complete type of the elliptic integrals. Elliptic integrals occurs in physical problems and applications. For example, small amplitude oscillations of a pendulum has simple harmonic motion with a period T. For a maximum amplitude θ_M large enough so that $\sin\theta_M \neq \theta_M$, equation's motion leads to a nonlinear differential equation, so it is needed to turn to a different approach. Eqaution of motion for the angle variable from the conservation of energy for the oscillation is given by

$$\frac{\mathrm{d}\theta}{\mathrm{d}t} = \pm\left(\frac{2g}{l}\sqrt{\cos\theta - \cos\theta_M}\right)^{1/2} \tag{A.2}$$

where the mass of the pendulum m was canceled out and g is the gravitational constant. For a complete cycle, the period can be obtained by integration,

$$T = 4\sqrt{\frac{l}{g}}\int_0^{\pi/2} \frac{1}{\sqrt{1-k^2\sin^2\phi}}\mathrm{d}\phi \tag{A.3}$$

where $k = \sin(\theta_M/2)$. This defines the complete elliptic integral of the first kind $K(\gamma)$ [147, 148]. Generally used complete elliptic integrals of three kinds [147, 149] are defined as follows.

First kind complete elliptic integral $K(\gamma)$:

$$K(\gamma) = \int_0^1 \frac{1}{\sqrt{(1-x^2)(1-\gamma x^2)}}\mathrm{d}x, \tag{A.4}$$

where $0 \leq \gamma < 1$.

Second kind of complete elliptic integral $E(\gamma)$:

$$E(\gamma) = \int_0^1 \sqrt{\frac{1-\gamma^2 x^2}{1-x^2}} \mathrm{d}x, \tag{A.5}$$

where $0 \leq \gamma \leq 1$.

Third kind of complete elliptic integral $\Pi(\gamma, k)$

$$\Pi(\gamma, k) = \int_0^1 \frac{1}{(1-\gamma x^2)\sqrt{(1-x^2)(1-k^2x^2)}} \mathrm{d}x, \tag{A.6}$$

where $0 < k < 1$.

REFERENCES

[1] T. Remetter, P. Johnsson, J. Mauritsson, K. Varju, Y. Ni, F. Lepine, E. Gustavson, M. Kling, J. Khan, R. Lopez-Martens, K. J. Schafer, M.J. J. Vrakking, and A. L'Huillier, Nature Physics **2**, 323 (2006).

[2] P. H. Bucksbaum, Physics Today **59**, 57 (2006).

[3] Committee on AMO 2010, National Research Council, *Controlling the Quantum World of Atoms, Molecules and Photons: An Interim Report*, National Academies Press, Washington, DC (2005). Also available at *http://www.nap.edu/catalog/11482.html*.

[4] T.F. Gallagher, *Rydberg Atoms*, (Cambridge University Press, Cambridge, 1994).

[5] J.-P. Connerade, *Highly Excited Atoms*, (Cambridge University Press, Cambridge, 1998).

[6] G. Tanner, K. Richter, and J.M. Rost, Rev. Mod. Phys. **72**, 496)(2000).

[7] A. Bohr, Phys. Rev. **81**, 134, 331 (1951).

[8] D. Papousek and M.R. Aliev, *Molecular Vibrational-Rotational Spectra*, (Elsevier, Amsterdam, 1982).

[9] N. Bohr, and J. Wheeler, Phys. Rev. **56**, 426 (1939).

[10] D.R. Inglis, Phys. Rev. **96**, 1059 (1954).

[11] M.G. Mayer, Phys. Rev. **75**, 1969 (1949); **78**, 16, 22 (1950).

[12] O. Haxel, J.H. Jensen, and H.E. Suess, Phys. Rev. **75**, 1766 (1949); Naturwiss, **36**, 155 (1949).

[13] J. Rainwater, Phys. Rev. **79**, 432 (1950).

[14] A. Bohr and B.R. Mottelson, *Nuclear Structure, Vol. II*, (W.A Benjamin, Reading, MA, 1975), pp.84-88.

[15] B. Mottelson and J.G. Valatin, Phys. Rev. Lett. **5**, 511 (1960).

[16] T. Udagawa and R.K. Sheline, Phys. Rev. **147**, 671 (1966).

[17] K.Y. Chan and J.G. Valatin, Nucl. Phys. **82**, 222 (1966); *ibid.* **85**, 261 (1966).

[18] D.R. Bes, S. Landowne, and M.A.J. Mariscotti, Phys. Rev. **166**, 1045 (1968).

[19] J. Krumlinde, Nucl. Phys. **A121**, 306 (1968).

[20] E.R. Marshalek, Phys. Rev. **139**, B770 (1965); **158**, 993 (1967).

[21] B. Banerjee, H.J. Mang, P. Ring, Nucl. Phys. A **215**, 366 (1973); H.J. Mang, Phys. Reports **18** C, no. 6 (1975).

[22] D.R. Inglis, Phys. Rev. **97**, 701 (1955).

[23] V.G. Zelevinskii, Sov. J. Nucl. Phys. **22**, 565 (1975).

[24] J.G. Valatin, Proc. R. Soc. **238**, 132 (1956).

[25] G. Ripka, J.P. Blaizot and N. Kassis, *Heavy-ion, High-Spin states and Nuclear Structure* vol1 (Vienna:IAEA, 1975).

[26] D. Glas, U. Mosel and P.G. Zint, Z. Physik A, **285**, 83 (1978).

[27] Schrödinger E., Naturwissenschaften, **14**, 664 (1926).

[28] R.J. Glauber. Phys. Rev. **131**, 2766 (1963).

[29] M. Lax, W.H.Louisell, IEEE J. Quantum Electron, **QE-3**, 47 (1967).

[30] F.W. Cumming and J.R. Johnston, Phys. Rev. **151**, 105, 183 (1968).

[31] P.C. Marin, *Proc. 9th Int. Conf. Low-Temp. Phys., Colombus, Ohio* ed. J.G. Daunt *et al* (New York, Plenum, 1965).

[32] P. Carruthers and K.S. Dy, Phys. Rev. **147**, 214 (1966).

[33] D.J. Rowe and R. Bassermann, Can. J. Phys. **54**, 1941 (1976).

[34] G.Ghosh, B.Dutta-Roy and M.Dey, J. Phys. G:Nucl. Phys. **3**, 1077 (1977).

[35] J.M. Danby, *Fundamentals of Celestial Mechanics*, (Macmillan, New York, 1962).

[36] G.W. Hill, Am. J. Math. **1**, 5 (1878).

[37] P. Kappertz and M. Nauenberg, Phys. Rev. A **47**, 4749 (1993).

[38] A. Deprit, Astron. J. **71**, 77 (1966).

[39] A. Deprit, and A. Deprit-Bartholomé, Astron. J. **72**, 173 (1967).

[40] I. Bialynicki-Birula, M. Kalińsky, and J.H.Eberly. Phys. Rev. Letts. **73**, 1777 (1994).

[41] D. Farrelly and T. Uzer, Phys. Rev. Lett. **74**, 1720 (1995).

[42] M. J. Rakovic, T. Uzer, and D. Farrelly, Phys. Rev. A **57**, 2814 (1998).

[43] W. Petrich, M.H. Anderson, J.R. Ensher, and E.A. Cornell, Phys. Rev. Lett. **74**, 3352 (1995).

[44] M.H. Anderson, J.R. Ensher, M.R. Matthews, C.E. Wieman, and E.A. Cornell, Science **269**, 198 (1995).

[45] M. Nauenberg, C.Stroud, and J. Yeazell. Sci. Am. **270**, 44 (1994).

[46] G. Raithel, M. Fauth, H. Walther, Phys. Rev. A **47**, 419 (1991).

[47] J.A. Yeazell, C.R. Stroud, Phys. Rev. A **43**, 5153 (1991).

[48] D. Farrelly, Phys. Lett. A **191**, 265 (1994).

[49] J.C. Gay, L.R. Pendrill, and B. Cagnac, Phys. Lett. A **72**, 315 (1979).

[50] L.A. Burkova, I.E. Dzyaloshinskii, G.F. Drukarev, and B.S. Monozon, Zh. Eksp. Teor. Fiz. **71**, 526 (1976) [Sov. Phys. JETP **44**, 276 (1976)].

[51] S.K. Bhattacharya and A.R.P. Rau, Phys. Rev. A **26**, 2315 (1982).

[52] L.I. Gorkov and I.E. Dzyaloshinski, Zh. Eksp. Teor. Fiz. **53**. 717 (1967) [Sov. Phys. JETP **26**, 449 (1968).

[53] O. Dippel, P. Schmelcher, and L.S. Cederbaum, Phys. Rev. A **49**, 4415 (1994).

[54] E. Lee, A.F. Brunello, and D. Farrelly. Phys. Rev. Letts. **75**, 3641 (1995).

[55] V. Szebehely, *Theory of Orbits: The Restricted Problem of Three Bodies*, (Academic, New York, 1967).

[56] A. Deprit in *The Big Band and George Lemaitre*, edt. A Berger (Reidel, Dordrecht, 1984) pp. 151-180.

[57] A. Deprit, Bull. Soc. Math. Belg. **14**, 46 (1962).

[58] A.F. Brunello, T. Uzer, and D. Farrelly. Phys. Rev. Letts. **76**, 2874 (1996).

[59] K. Weierstrass, in *Weierstrass: Mathematische Werke*, reprinted (Olm, and Johnson, Hildesheim, 1967), Vol. 1, pp.233-246; R.S.Mackay, in *Nonlinear Phenomena and Chaos*, edited by S.Sarkar (Hilger, Bristol, 1986), pp.254-270.

[60] V.I. Arnold, *Ordinary Differential Equations*, (MIT Press, Cambridge, 1985).

[61] C. Cerjan, E. Lee, D. Farrelly, and T. Uzer. Phys. Rev. A **55**, 2222 (1997).

[62] M.A.Z. Habeeb, J. Phys. G **13**, 651 (1987).

[63] K.F. Liu and G. Ripka, Nucl. Phys. A **293**, 333 (1977).

[64] D. Farrelly, T. Uzer, P.E. Raines, J.P. Skelton, and J.A. Milligan, Phys. Rev. A **45**, 4738 (1992).

[65] N.N. Bogoliubov, *Lectures on Quantum Systems, vol. I, Quantum Statistics* (Gordon and Breach, New York, 1967).

[66] S.V. Tyablikov, *Methods in the Quantum Theory of Magnetism* (Plenum, New York, 1967).

[67] M.S. Krishnan and T. Carrington, Jr., J. Chem. Phys. **94**, 461 (1991).

[68] W. M. Zhang, D. H. Feng and R. Gilmore, Rev. Mod. Phys. **62**, 867 (1990).

[69] G. Alber, P. Zoller, Phys. Rep. **199**, 231 (1991).

[70] L. Marmet, H. Held, G. Raithel, J.A Yeazell and H. Walther, Phys. Rev. Letts. **72**, 3779 (1994).

[71] J. Wals, H.H Fielding, J.F. Christian, L.C. Snoek, W.J. van der Zande and H.B. van Linden van den Heuvell, Phys. Rev. Letts. **72**, 3783 (1994).

[72] P.Gulshani, Can. J. Phys. **57**, 998 (1979).

[73] V.P.Gutschick, M.M.Nieto, Phys. Rev. D **22**, 403 (1980).

[74] J.G. Hartly, J.R.Ray, Phys. Rev. D **25**, 382 (1982).

[75] R. F. Fox, Phys. Rev. A **59**, 3241 (1999).

[76] E. Schrödinger. In K. Prizibram, editor, *Letters in Wave Mechanics*, (Philos. Library, New York, 1967), pp. 189.

[77] Christopher C.Gerry, *Coherent states and the Kepler-Coulomb problem*, Phys. Rev. A **33**, 6 (1986).

[78] M. Nauenberg, Phys. Rev. A **40**, 1133 (1989).

[79] J.C. Gay, D. Delande, and A. Bommier, Phys. Rev. A **39**, 6587 (1989).

[80] John R. Kaluder. J. Phys. A **29** , L293 (1996).

[81] P. Majumdar, H.S. Sharatchandra, Phys. Rev. A **56**, R3322 (1997).

[82] R.R. Jones, D. You, and P.H. Bucksbaum, Phys. Rev. Letts. **70**, 1236 (1993).

[83] J.A. Yeazell and C.R. Stroud, Phys. Rev. Letts., **60**, 1494 (1988).

[84] R.J. Brecha, G. Raithel, C. Wagner, and H. Walther, Opt. Commun. **102**, 257 (1993).

[85] P. Nussenzveig, F. Bernardot, M. Brune, J. Hare, J.M. Raimond, S. Haroche, and W. Gavlik, Phys. Rev. A **48**, 3991 (1993).

[86] L. Chen, M. Cheret, F. Roussel, and G. Spiess, J. Phys. B **28**, L437 (1993).

[87] L. Marmet, H. Held, G. Raithel, J.A Yeazell and H. Walther, Phys. Rev. Letts. **72**, 3779 (1994).

[88] M. Kalińsky, J.H. Eberly. and I. Bialynicki-Birula, Phys. Rev. A **52**, 2460 (1995).

[89] M. Kalińsky, and J.H. Eberly, Phys. Rev. A **53**, 1715 (1996).

[90] M. Kalińsky, and J.H. Eberly, Phys. Rev. Letts. **77**, 2420 (1996).

[91] M. Mallalieu and C. R. Stroud, in *Coherent States: Past, Present and Future*, edited by D.H. Feng, J.R.Klauder, and M.R. Strayer (World Scientific, Singapore, 1994), pp. 301-314.

[92] A. Buchleitner, D. Delande, and J. Zakrzewski, Phys. Repts. **368**, 409 (2002).

[93] H. Maeda and T. F. Gallagher. Phys. Rev. Letts. **92**, 133004 (2004).

[94] T. Uzer, E. Lee, D. Farrelly, and A. F. Brunello, Contemporary Physics **41**, 1 (2000).

[95] E. Lee, A.F. Brunello, C. Cerjan, T. Uzer, and D. Farrelly. From Asteroids to Atoms: Quantum Wave Packets and the Restricted Three-Body Problem of Celestial Mechanics. In J.A. Yeazell and T. Uzer, editors, *The Physics and Chemistry of Wave Packets*, page 95 (2000).

[96] E. Lee, D. Farrelly, and T. Uzer, Optics Express **1**, 221 (1997).

[97] E.C.G. Sudarshan, Phys. Rev. Lett. **10**, 277 (1963).

[98] H. Weyl, *Gruppentheorie und Quantenmechanik*, (Hirzel, Leipzig) (1928).

[99] J.R. Klauder and E.C.G. Sudarshan, *Coherent States* (World Scientific, Singapore, 1985).

[100] R. Feynman, Phys. Rev. **84**, 108 (1951).

[101] E. Lee, A. Puzder, M.Y. Chou, T. Uzer, D. Farrelly, Phys. Rev. B **57**, 12281 (1998).

[102] M. Nauenberg. in *Coherent States: Past, Present and Future* (Ref. [91]), pp. 345-360.

[103] H. Goldstein, *Classical Mechanics* 2nd ed. (Addison-Wesley, Reading, MA, 1981), pp.383.

[104] A.M Perelomov, Commun. Math. Phys. **26**, 222 (1972).

[105] R. Gilmore, Ann. Phys., (NY) **74**, 391 (1972).

[106] R. Gilmore, Rev. Mev. de Fisica, **23**, 142 (1974).

[107] R. Gilmore, *Lie Groups, Lie Algebras and Some of Their Applications*, (Wiley, New York. 1974).

[108] R. Gilmore, J. Math. Phys. **15**, 2090 (1974).

[109] R.A. Fisher, M.M. Nieto and V.D. Sandberg, Phys. Rev. D **29**, 1107 (1984)

[110] A.I. Morozov, and L.S. Solev'ev, *Motion of charged particles in electromagnetic fields*, Reviews of Plasma Physics, Vol. **2** (Consultants Bureau, New York NY, 1966).

[111] D.H.E. Dubin, Phys. Rev. Lett. **92**, 195002 (2004).

[112] M.E. Glinsky and T.M. O'Neil, Phys. Fluids B **3**, 1279 (1991).

[113] S.G. Kuzmin and T.M. O'Neil, Physics of Plasmas, Vol. **11**, 2382 (2004).

[114] S.G. Kuzmin and T.M. O'Neil, Physics of Plasmas, Vol. **12**, 012101 (2005).

[115] J.E. Avron, I.W. Herbst, and B. Simon, Ann. Phys. (N.Y.) **114**, 431 (1978).

[116] J. Shertzer, J. Ackermann, and P. Schmelcher, Phys. Rev. A **58** 1129 (1998).

[117] A. Grossman, *Statistical Mechanics and Field Theory* (R.N.Sen and C.Weil, Eds., Halstead, 1972).

[118] M.H. Johnson, and M.A. Lippmann, Phys. Rev. **76**, 828 (1949).

[119] H.J. de Blank, Fusion Science and Technology, Vol. **45**, 47 (2004).

[120] B.R. Johnson, J.O. Hirschfelder, and K.H. Yang, Rev. of Mod. Phys. Vol.**55**, 109 (1983).

[121] H. Bacry, Ph. Combe, and J.L. Richard, Nuovo Cimento A **67**, 267 (1970)

[122] H. Bacry, Ph. Combe, and J.L. Richard, Nuovo Cimento A **70**, 267 (1970)

[123] J.E. Avron, I.W. Herbst, and B. Simon, Phys. Rev. A. **20**, 2287 (1979).

[124] E. Breitenberger, J. Opt. Soc. Am. **58**, 1315 (1968).

[125] B.P. Carter, J. Math. Phys. **10**, 788 (1969a).

[126] R.J. Elliott, and R. Loudon, J. Phys. Chem. Solids **15**, 196 (1960).

[127] H. Grotch, R.A. Hegstrom, Phys. Rev. A **4**, 59 (1971).

[128] H. Herold, H. Ruder, and G. Wunner, J. Phys. B **14**, 751 (1981).

[129] R.F. O'Connell, Phys. Lett., A **70**, 389 (1979).

[130] G. Wunner, H. Ruder, H. Herold, Phys. Lett. A **79**, 159 (1980).

[131] W. Opechowski and W.G. Tam, Phys. (Utr.) **42**, 525 (1969).

[132] C.G. Jacobi, *Fundamenta nova theoriae functionarum ellipticarum*, vol **1** (Gesammelte Werke, Bornträger, Königsberg, 1829).

[133] S. Pan and F.H. Mies, J. Chem. Phys. **89**, 3096 (1988).

[134] J.D.D. Martin and J.W. Hepburn, Phys. Rev. Lett. **79**, 3154 (1997).

[135] J.D.D. Martin and J.W. Hepburn, J. Chem. Phys. **109**, 8139 (1998).

[136] Q.J. Hu, Q. Zhang, and J.W. Hepburn, J. Chem. Phys. **124**, 124 (2006).

[137] D. Vrinceanu, B.E. Granger, R. Parrott, H.R. Sadeghpour, L. Cederbaum, A. Mody, J. Tan, and Gabrielse, Phys. Rev. Lett. **92**, 133402 (2004).

[138] E. Lee, A. Brunello and D. Farrelly, Phys. Rev. A **55**, 2202 (1997).

[139] D. Vrinceanu and M.R. Flannery, Phys. Rev. Lett. **82**, 3412 (1999).

[140] M.R. Flannery and D. Vrinceanu, Phys. Rev. Lett. **85**, 1 (2000).

[141] D. Vrinceanu and M.R. Flannery, Phys. Rev. Lett. **85**, 4880 (2000).

[142] D. Vrinceanu and M.R. Flannery, J. Phys. B, **33**, L721 (2000).

[143] M.R. Flannery and D. Vrinceanu, Phys. Rev. A **65**, 022703 (2002).

[144] P. Bellomo, D. Farrelly, and T. Uzer, J. Chem. Phys. **107**, 2499 (1997); *ibid.* **108**, 402 (1998); *ibid.* **108**, 5295 (1998).

[145] J.R. Klauder, J. Math. Phys. **4**, 1055 (Part I); 1058 (Part II) (1963).

[146] I.S. Gradshteyn, I.M. Ryzhik, *Tables of Ingegrals, Sums, and Products*, 5th ed. (Academic Press, New York, 1994).

[147] M. Abramowitz, and I.A. Stegun, in *Handbook of Mathematical Functions with Formulas, Graphs, and Mathematical Tables*, 9th printing (Dover, New York, 1972), pp. 587-607.

[148] G.B. Arfken, H.J. Weber, *Mathematical Methods for Physicists*, 5th. ed. (Academic Press, CA, 2001), pp.354-358.

[149] M. Henry, M. Victor, *Elliptic curves: function theory, geometry, arithmetic*, (Cambridge University Press, New York, 1997), pp.54-77.

[150] F. Penent, D. Delande and J.C. Gay, Phys. Rev. A **37**, 4707 (1988).

[151] G. Raithel, M. Fauth, H. Walther, Phys. Rev. A **44**, 1898 (1991).

[152] M.J. Gourlay, T.Uzer and D. Farrelly, Phys. Rev. A **47**, 3113 (1993)

[153] L.A. Pars, *A Treatise on Analytical Dynamics*, (London, Heinemann, 1965).

[154] K. Richter, G. Tanner, and D. Wintgen, Phys. Rev. A **48**, 4182 (1993).

[155] G. Wannier, Phys. Rev. **90**, 817 (1953).

[156] G.S. Ezra, K. Richter, G. Tanner, D. Wintgen, J. Phys. B **24**, L413 (1991).

[157] D. Wintgen, K. Richter, G. Tanner, Chaos **2**, 19 (1992).

[158] R. Blümel, W.P. Reinhardt, D.H. Feng, J.M. Yuan (Eds.), in: Direction in Chaos, Vol. 4, *Direction in Chaos, Quantum Nonintegrability*, (World Scientific, Singapore, 1992).

[159] P. Gaspard, S.A. Rice, Phys. Rev. A **48**, 54 (1993).

[160] K. Richter, D. Wintgen, J. Phys. B **23**, L197 (1990); Phys. Rev. Lett. **65**, 1965 (1990); J. Phys. B **24**, L413 (1991).

[161] C. Jung and A. Emmanouilidou, Chaos **15**, 023101 (2005).

[162] C. Jung, C. Lipp, and T.H. Seligman, Ann. Phys. (N.Y.) **275**, 151 (1999).

[163] P. Holmes, Phys. Rep. **193**, 137 (1990).

[164] M.H Lee, G. Tanner, and N.N. Choi, Phys. Rev. E **71**, 056208 (2005).

[165] B. Eckhardt, Habilitationsschrift (Universität Marburg, Marburg, 1991).

[166] J.M. Rost, J. Phys. B **28**, 3003 (1995).

[167] J.M. Rost, Phys. rep. **297**, 271 (1998).

[168] R. McGehee, Invent. Math. **27**, 191 (1974).

[169] E. Ott, *Chaos in Dynamical Systems*, (Cambridge University Press, Cambridge, U.K., 1993).

[170] U. Fano, Phys. Rep. **46**, 97 (1983).

[171] C.L. Siegel, Ann. Math. **42**, 127 (1941).

[172] A. Emmanouilidou, C. Jung, and L.E. Reichl, Phys. Rev. E **68**, 046207 (2003).

[173] S.J. Aarseth and K. Zare, Celest. Mech. **10**, 185 (1974).

[174] P. Kustaanheimo, E. Stiefel, C.R. Hebd. Seances Acad. Sci. **260**, 805 (1965).

[175] S. Smale, Bull. Am. Math. Soc. **73**, 747 (1967).

[176] C. Jung, H.J. Schulz, J. Phys. A **20**, 3607 (1987); t. T*acute*el, Phys. Rev. A **36**, 1502 (1987).

[177] C. Jung and T.H. Seligman, Phys. Rep. **285**, 77 (1997).

[178] B. Rückerl and C. Jung, J. Phys. A **27**, 55 (1994); *ibid*, 6741 (1994).